Title

Examining roles for Myb-like transcription factor function within the Arabidopsis circadian oscillator and in regulation of growth

Author

Baker, Cassandra

Publication Date

2023

Peer reviewed|Thesis/dissertation

Examining roles for Myb-like transcription factor function within the Arabidopsis circadian oscillator and in regulation of growth

By

CASSANDRA BAKER

DISSERTATION

Submitted in partial satisfaction of the requirements for the degree of

DOCTOR OF PHILOSOPHY

in

Integrative Genetics and Genomics

in the

OFFICE OF GRADUATE STUDIES

of the

UNIVERSITY OF CALIFORNIA

DAVIS

Approved:

Stacey Harmer, Ph.D.

Joanna Chiu, Ph.D.

Siobhan Brady, Ph.D.

Committee in Charge

2023

Table of Contents

Abstract iii

Chapter 1: Introduction 1

Chapter 2: Myb-like transcription factors have epistatic effects on circadian clock function but additive effects on plant growth 4

Chapter 3: Light quality-dependent roles of RVE proteins in the circadian system 34

Chapter 4: Conclusions and Future Directions 75

Acknowledgements 78

References 79

Appendix I: Generation of a *cca1 lhy rve34568* septuple mutant 88

Appendix II: Mutant allele sequences 89

Appendix III: CRISPR guide sequences 95

Appendix IV: Plasmid and Glycerol Stocks 96

Appendix V: Primer Stocks 98

Appendix VI: Seed Stocks 102

Abstract

Eukaryotic circadian clocks, or oscillators, are composed of transcriptional-translational feedback loops that generate biological rhythms with an approximate twenty-four hour period. These circadian rhythms continue in the absence of environmental cues, which helps organisms adapt to their environment. A family of Myb-like transcription factors act as components of the circadian oscillator in *Arabidopsis thaliana* and includes a group of repressors and a group of activators that act antagonistically to each other. *CIRCADIAN CLOCK ASSOCIATED 1* (*CCA1*) and *LATE ELONGATED HYPOCOTYL* (*LHY*) repress afternoon and evening-phased genes within the oscillator, while *REVEILLE 4* (*RVE4*), *REVEILLE 6* (*RVE6*), and *REVEILLE 8* (*RVE8*) activate these same targets.

In this study, I generated a *cca1 lhy rve468* quintuple mutant and assessed its circadian and growth phenotypes. Both *cca1 lhy* and *cca1 lhy rve468* mutants have poor circadian rhythms in a range of light conditions and low-amplitude rhythms of core clock gene expression. The *cca1 lhy rve468* mutant also flowers early, like *cca1 lhy*, which suggests that *CCA1* and *LHY* interact epistatically with *RVE4*, *RVE6*, and *RVE8* to regulate circadian phenotypes. However, hypocotyl elongation and leaf growth in *cca1 lhy rve468* mutants are similar to wild type, suggesting that *CCA1* and *LHY* interact additively with *RVE4*, *RVE6*, and *RVE8* to regulate growth phenotypes. These Myb-like factors therefore have separable functions in circadian regulation and growth.

I also generated *RVE4*, *RVE6*, and *RVE8* single, double, and triple mutants using CRISPR-Cas9 and characterized their growth and circadian phenotypes. My results suggest that the *RVEs* synergistically regulate flowering time, redundantly regulate leaf growth, and antagonistically regulate hypocotyl elongation. Using these *rve* mutants, I then investigated light quality-specific circadian regulation of the *RVEs* and found that blue light-specific enhancement of RVE target gene expression is reduced in *rve468* mutants. Additionally, the circadian period of *rve468* and *rve48* mutants lengthens as fluence rate increases specifically in blue but not red light conditions, while the period of wild type shortens as

fluence rate increases in all light qualities. RVE protein abundance and degradation rate are similar in monochromatic red and blue light and are therefore not responsible for the blue light-specific phenotypes of *rve* mutants. Furthermore, *ZEITLUPE* (*ZTL*) and *ELONGATED HYPOCOTYL 5* (*HY5*), which have blue light-specific circadian functions, interact additively with the *RVEs* to regulate circadian phenotypes. This suggests that the *RVEs* are involved in light quality-specific circadian regulation through a novel mechanism.

Chapter 1: Introduction

Many organisms have biological rhythms that match their changing environment. Perhaps the best understood are circadian rhythms, oscillations with an approximately twenty-four hour period that are produced by a cell autonomous circadian oscillator and are present in bacteria, plants, and mammals[1–3]. However, genetic evidence suggests that the circadian oscillator likely evolved independently in these diverse organisms[4,5].

Plants have long been a model system for the study of circadian rhythms; in fact, the first recorded circadian rhythm was observed in plants[2]. Since plants are sessile beings, their circadian clock is particularly important to help them predict environmental changes and respond appropriately. Clocks provide an adaptive advantage when the internal free-running period matches that of external day/night cycles[6]. Circadian clocks play an important role in plant responses to the environment, and clock genes have been targets of selection as humans have expanded crop species into new geographic regions[7]. A better understanding of the plant circadian clock and the specific roles of individual clock genes in oscillator function may therefore guide future efforts towards crop improvement.

As in other eukaryotes, the plant circadian oscillator is composed of a network of transcription factors that control each other's expression and that of thousands of output genes[8]. While oscillator function persists in the absence of environmental cues such as changes in light and temperature, these environmental factors can act as cues to change circadian clock phase. Light is particularly important for appropriate entrainment of the plant circadian clock, and multiple photoreceptors directly interact with core clock components[9].

Considerable effort has been expended on identifying clock components in the model plant *Arabidopsis thaliana*. Most of the more than twenty clock transcription factors currently identified act primarily as repressors of transcription[7]. Two such components are the Myb-like transcription factors *CIRCADIAN CLOCK ASSOCIATED 1* (*CCA1*) and *LATE ELONGATED HYPOCOTYL* (*LHY*), dawn-phased genes

that repress evening clock genes such as *TIMING OF CAB EXPRESSION1* (*TOC1*), *EARLY FLOWERING 4* (*ELF4*), and *LUX ARRHYTHMO* (*LUX*)[10]. The highly related *REVEILLE 4* (*RVE4*), *REVEILLE* (*RVE6*), and *REVEILLE* (*RVE8*) are midday-phased genes that act with members of the *NIGHT LIGHT-INDUCIBLE AND CLOCK-REGULATED* (*LNK*) family of transcriptional co-activators to activate the same evening targets[10]. Together, these two groups of Myb-like proteins act antagonistically to each other and promote robust circadian rhythms[11].

In addition to roles for RVE4, RVE6, and RVE8 within the core circadian machinery, connections between these *RVEs* and other biological processes continue to be discovered. In low temperatures, RVE4 and RVE8 proteins enhance freezing tolerance and activate expression of a master transcription factor involved in cold stress response[12]. RVE8 also promotes expression of anthocyanin biosynthesis genes[13], and anthocyanin is produced in response to abiotic stresses such as cold stress[14]. Interestingly, RVE4 and RVE8 both promote plant survival at high temperatures and activate expression of early heat shock-regulated genes[15]. More broadly, a recent multi-omics study of *RVE4*, *RVE6*, and *RVE8* found that these genes may be involved in abiotic stress responses, starch degradation, and proteasome activity[16]. While the mechanistic details of *RVE* involvement in these processes has yet to be discovered, circadian transcription factors often regulate physiological clock outputs in addition to their roles within the core clock network[8].

While *RVE4*, *RVE6*, and *RVE8* are known to act semi-redundantly within the circadian clock[17,18], the details of their roles within the oscillator are not well understood. Additionally, while *cca1 lhy rve468* partial loss-of-function mutants have been generated and shown to retain largely normal circadian clock function[11], potential interactions between the *RVEs* and *CCA1* and *LHY* have yet to be clarified. To further investigate these Myb-like transcription factors, I have generated likely null alleles of *RVE4*, *RVE6*, and *RVE8* using CRISPR-Cas9. I created a likely null *cca1 lhy rve468* quintuple mutant and found that these plants are only marginally rhythmic but have growth phenotypes similar to those of

wild-type plants. My data suggest that the Myb-like repressors and activators interact epistatically to regulate circadian rhythms and interact additively to regulate growth phenotypes. Additionally, I isolated all single and double *rve* mutant lines from a new *rve468* triple mutant and phenotypically characterized these CRISPR-Cas9-generated lines. Investigation of their light quality-specific phenotypes revealed that they have blue light-specific differences in circadian function. However, their blue light-specific phenotypes are not due to differences in RVE protein abundance, protein degradation rate, or interactions between the *RVEs* and two known blue light-factors. These new alleles will be useful for future studies, particularly as the *RVEs* continue to be examined for their functions beyond the core circadian clock.

Chapter 2: Myb-like transcription factors have epistatic effects on circadian clock function but additive effects on plant growth

Abstract

The functions of closely related Myb-like repressor and Myb-like activator proteins within the plant circadian oscillator have been well-studied as separate groups, but the genetic interactions between them are less clear. We hypothesized that these repressors and activators would interact additively to regulate both circadian and growth phenotypes. We used CRISPR-Cas9 to generate new mutant alleles and performed physiological and molecular characterization of plant mutants for five of these core Myb-like clock factors compared to a repressor mutant and an activator mutant. We first examined circadian clock function in plants likely null for both the repressor proteins, *CIRCADIAN CLOCK ASSOCIATED 1* (*CCA1*) and *LATE ELONGATED HYPOCOTYL* (*LHY*), and the activator proteins, *REVEILLE 4* (*RVE4*), *REVEILLE* (*RVE6*), and *REVEILLE* (*RVE8*). The *rve468* triple mutant has a long period and flowers late, while *cca1 lhy rve468* quintuple mutants, like *cca1 lhy* mutants, have poor circadian rhythms and flower early. This suggests that *CCA1* and *LHY* are epistatic to *RVE4*, *RVE6*, and *RVE8* for circadian clock and flowering time function. We next examined hypocotyl elongation and rosette leaf size in these mutants. The *cca1 lhy rve468* mutants have growth phenotypes intermediate between *cca1 lhy* and *rve468* mutants, suggesting that *CCA1*, *LHY*, *RVE4*, *RVE6*, and *RVE8* interact additively to regulate growth. Together, our data suggest that these five Myb-like factors interact differently in regulation of the circadian clock versus growth. More generally, the near-normal seedling phenotypes observed in the largely arrhythmic quintuple mutant demonstrate that circadian-regulated output processes, like hypocotyl elongation, do not always depend upon rhythmic oscillator function.

Keywords: *Arabidopsis thaliana*; *CCA1, LHY*; *RVE4*, *RVE6*, *RVE8*; flowering time; hypocotyl elongation

Introduction

The circadian clock is a biological timekeeper that allows organisms to anticipate predictable daily changes in the environment and regulate their responses to stimuli depending on the time of day.

This helps an organism synchronize with its surroundings, which provides a fitness advantage[6,19,20]. The importance of circadian clocks is further supported by their presence in diverse eukaryotes and some prokaryotes. Although specific circadian clock components are not conserved across higher taxa, clocks in eukaryotes are composed of interlocking transcriptional-translational feedback loops[5,10].

In plants, a family of Myb-like transcription factors is part of the core circadian clock and is highly conserved across land plants. Sub-clades in this family include one group of proteins that act primarily as repressors and one group of proteins that act primarily as activators. These factors bind to the same *cis*-element sequences and act antagonistically to each other[21–24]. In *Arabidopsis thaliana*, *CIRCADIAN CLOCK ASSOCIATED 1* (*CCA1*) and *LATE ELONGATED HYPOCOTYL* (*LHY*) are morning-phased Myb-like repressors that repress expression of *TIMING OF CAB EXPRESSION 1* (*TOC1*), *PSEUDO-RESPONSE REGULATOR 5* (*PRR5*), *PSEUDO-RESPONSE REGULATOR 7* (*PRR7*), and *PSEUDO-RESPONSE REGULATOR 9* (*PRR9*)[22,25]. These pseudo-response regulator proteins then reciprocally repress expression of *CCA1* and *LHY*[26–28]. CCA1 and LHY also repress expression of the evening complex genes *EARLY FLOWERING 3* (*ELF3*), *EARLY FLOWERING 4* (*ELF4*), and *LUX ARRHYTHMO* (*LUX*) [25,29–32]. *REVEILLE 4* (*RVE4*), *REVEILLE 6* (*RVE6*), and *REVEILLE 8* (*RVE8*) encode Myb-like transcription factors that act in opposition to CCA1 and LHY to activate expression of these same targets[23,24,33]. Considering these two groups of repressors and activators together, these atypical Myb-like factors are involved in all main transcription-translation feedback loops that compose the core clock[8,34].

Most of the core components of the plant circadian oscillator are transcription factors, which in addition to controlling each other's expression regulate genes involved in diverse physiological processes such as flowering time and growth. CCA1, LHY, PRR5, PRR7, and PRR9 indirectly regulate *CONSTANS* (*CO*) expression[35–37] and the CO protein activates expression of *FLOWERING LOCUS T* (*FT*) to promote flowering[38,39]. The evening complex (ELF3, ELF4, and LUX) directly represses expression of *PHYTOCHROME INTERACTING FACTOR 4* (*PIF4*) and *PHYTOCHROME INTERACTING FACTOR 5* (*PIF5*)[40],

genes that encode bHLH transcription factors that promote elongation of multiple plant organs. Adding another layer of regulation by the circadian clock, the activity of PIF proteins is modulated by their direct binding to TOC1 and the related proteins PRR5, PRR7, and PRR9[41–43]. PIF4 and PIF5 promote hypocotyl elongation at least in part by promoting expression of auxin biosynthesis genes[44–49]. As illustrated by these examples, circadian clock factors directly and indirectly regulate expression of genes that in turn control a wide range of important physiological processes. This complexity makes it difficult to determine whether the phenotypes of plants mutant for core clock genes are due to alterations in circadian rhythmicity *per se* or due to mis-regulation of downstream target genes.

As might be expected of factors with antagonistic effects on gene expression, *cca1 lhy* and *rve468* mutants have several opposite mutant phenotypes. Plants mutant for the repressors *CCA1* and *LHY* have short-period circadian rhythms, shorter hypocotyls and smaller leaves, and flower earlier than wild type[35,50–54]. Plants mutant for the *RVE4*, *RVE6*, and *RVE8* activators have long-period circadian rhythms, longer hypocotyls and larger leaves, and flower later than wild type[23,24,55]. *PIF4* and *PIF5* are required for the large rosette phenotype observed in *rve468* mutants[55].

Although *CCA1*, *LHY*, *RVE4*, *RVE6*, and *RVE8* mutants have been extensively characterized, the relationship between these repressors and activators both in the circadian clock and in regulation of plant growth remains unclear. The partial loss-of-function *cca1-1 lhy-20 rve4-1 rve6-1 rve8-1* mutants are highly rhythmic with an approximate twenty-four hour period in optimal growth conditions and are more phenotypically similar to wild-type plants than *cca1 lhy* or *rve4 rve6 rve8* mutants[11]. This is surprising given that *CCA1*, *LHY*, *RVE4*, *RVE6*, and *RVE8* are integral for normal clock function[23,24,33,50,52,56,57]. However, rhythmicity is greatly reduced in quintuple *cca1 lhy rve468* mutants maintained at non-optimal temperatures[11], suggesting that collectively the Myb-like factors act to increase circadian robustness and enhance adaptation to challenging growth conditions.

Since the previously studied *cca1 lhy rve468* mutant was not a null mutant[11], we wanted to determine if the clock remains robustly rhythmic in the absence of these five core factors. Here, we report the characterization of CRISPR-Cas9-generated alleles of *RVE4*, *RVE6*, and *RVE8* and their phenotypes alone and in combination with mutations in *CCA1* and *LHY*. We find that even in optimal growth conditions, these new quintuple mutants are only marginally rhythmic, with very low-amplitude rhythms. However, these plants have hypocotyl and rosette growth phenotypes comparable to wild-type plants, similar to the previously described phenotypes of the partial loss-of-function quintuple mutants[11]. We suggest that these activating and repressing core clock Myb-like factors interact epistatically in the control of circadian rhythms and flowering time, but additively in the control of several growth phenotypes.

Results

CCA1 and *LHY* are epistatic to *RVE4*, *RVE6*, and *RVE8* for circadian clock and flowering time function.

We generated a new *cca1 lhy rve468* mutant containing *lhy-100*[58], a nonsense mutation, rather than the hypomorphic *lhy-20* allele[59]. We also used CRISPR-Cas9 to create new frameshift mutations in *RVE4*, *RVE6*, and *RVE8*, all of which are predicted to cause premature stop codons and loss of function (Fig. 2.1A, Fig. S2.1). In *RVE4* this frameshift occurred in the first exon, upstream of the Myb-like DNA-binding domain (Fig. 2.1A, Fig. S2.1). In *RVE6* this frameshift occurred in the third exon, within the conserved proline-rich region just downstream of the Myb-like domain (Fig. 2.1A, Fig. S2.1). In *RVE8* this frameshift occurred in the fourth exon, upstream of the conserved C-terminal domain (Fig. 2.1A, Fig. S2.1). With these new alleles, the Cas9-negative *cca1-1 lhy-100 rve4-12 rve6-12 rve8-12* (hereafter referred to as *cca1 lhy rve468*) is likely a null mutant.

To investigate the rhythmicity of *cca1 lhy rve468*, we monitored circadian regulation of expression of a clock-regulated reporter gene, *CCR2::LUC2*, in a range of light qualities, light intensities, and temperatures. Rhythmicity of *cca1 lhy rve468* was compared to wild-type Col-0, *rve4-11 rve6-11*

rve8-11 (Fig. S2.1) (hereafter referred to as *rve468*), and *cca1-1 lhy-100* (hereafter referred to as *cca1 lhy*). The *rve4-11 rve6-11 rve8-11* alleles were generated using the same guide RNAs as the *rve4-12 rve6-12 rve8-12* alleles and have frameshift mutations in nearly identical locations, which are also predicted to cause premature stop codons and loss of function (Fig. S2.1, Appendix II). In constant darkness, both Col-0 and *rve468* have robust rhythmicity, while *cca1 lhy* and *cca1 lhy rve468* have generally poor rhythms with less than 25% of plants defined as rhythmic (Fig. 2.1B). Across a range of light intensities (from 1-200 µmol m^{-2} s^{-1}) of constant red plus blue, monochromatic red, or monochromatic blue light, Col-0 and *rve468* are similarly and highly rhythmic while *cca1 lhy* and *cca1 lhy rve468* both exhibit dampened rhythms (Fig. 2.1C – F, Fig. S2.2). This pattern is also observed at 30 °C, where *cca1 lhy* and *cca1 lhy rve468* have similarly dampened rhythms while Col-0 and *rve468* exhibit robust rhythms (Fig. 2.1G). In all tested conditions except 100 µmol m^{-2} s^{-1} monochromatic red and 100 µmol m^{-2} s^{-1} red plus blue light, the proportion of rhythmic plants in *cca1 lhy* and *cca1 lhy rve468* was not significantly different from each other but was significantly different from Col-0 (Pearson's Chi-squared and pairwise proportion test with Benjamin-Hochberg correction; $p < 0.05$). These data indicate that *cca1 lhy* and *cca1 lhy rve468* have similarly poor rhythmicity across a range of growth conditions.

To further compare the circadian phenotypes of *cca1 lhy* and *cca1 lhy rve468*, we examined the circadian periods of the small fraction of plants of these genotypes considered rhythmic (RAE < 0.6) in different light qualities. In constant darkness, 10 µmol m^{-2} s^{-1} red plus blue, and 10 µmol m^{-2} s^{-1} monochromatic blue light, the periods of *cca1 lhy* and *cca1 lhy rve468* seedlings are significantly different from those of *rve468* seedlings but not significantly different from each other (Fig. S2.3). In 10 µmol m^{-2} s^{-1} monochromatic red light, *cca1 lhy rve468* has a significantly longer period than *cca1 lhy* but is still significantly shorter than *rve468* (Fig. S2.3). Together, these data indicate that *cca1 lhy rve468* has similar circadian phenotypes to *cca1 lhy*.

Based on the dampened rhythms of *cca1 lhy rve468* mutants, we hypothesized that core clock gene expression would be arrhythmic in free-running conditions. To assess the expression patterns of core clock genes in these mutants, we next extracted RNA from plants grown in constant white light and carried out quantitative reverse-transcriptase polymerase chain reaction (qRT-PCR) assays. Expression of *TOC1*, *ELF4*, and *LUX* is rhythmic in Col-0 and *rve468* but has no amplitude in *cca1 lhy* and *cca1 lhy rve468* (Fig. 2.2), as expected based on our luciferase data (Fig. 2.1, Fig. S2.2). Mean expression of *LUX* and *PRR5* over the entire time course is significantly higher in both *cca1 lhy* and *cca1 lhy rve468* compared to wild type (one-way ANOVA and Tukey's post hoc test, $p < 1e^{-3}$). While mean expression of *TOC1* and *ELF4* across the time course is not significantly different in *cca1 lhy* and *cca1 lhy rve468* compared to Col-0, in both cases these transcripts are dampening towards the peak levels of expression in wild type (Fig. 2.2). For all clock genes examined, mean expression values are not significantly different between *cca1 lhy* and *cca1 lhy rve468* across the examined time points (one-way ANOVA and Tukey's post hoc test, $p > 0.05$). These data suggest that in constant conditions the loss of the repressive activity of CCA1 and LHY is epistatic to the loss of the activating function of the RVE proteins for these central clock genes.

We next investigated expression of a clock-regulated reporter gene, *CCR2::LUC2*, in *cca1 lhy rve468* and the parental mutants maintained in light-dark cycles to determine expression patterns in the presence of environmental cues. In seedlings subjected to long day (LD) photoperiods (16 hours light, 8 hours dark), the waveforms of *cca1 lhy rve468* are very similar to those of *cca1 lhy* but different from Col-0 and *rve468* (Fig. 2.3, Fig. S2.4). Furthermore, both *cca1 lhy* and *cca1 lhy rve468* have a sharp increase in luciferase activity shortly after dawn, suggesting decreased circadian regulation and increased responsiveness to environmental cues in these genotypes. In short day (SD) photoperiods (8 hours light, 16 hours dark), a similar pattern was observed in both *cca1 lhy* and *cca1 lhy rve468* (Fig. 2.3,

Fig. S2.4). This suggests that circadian function is similarly disrupted in *cca1 lhy* and *cca1 lhy rve468* mutants.

To further investigate the relationship between *CCA1*, *LHY*, *RVE4*, *RVE6*, and *RVE8*, we next examined the photoperiodic regulation of the transition from vegetative to reproductive growth as this response depends upon a functional circadian system[60,61]. In long days, *rve468* flowers significantly later than Col-0 when measured either by leaf number or days (Fig. 2.4), as previously observed[55]. In contrast, both *cca1 lhy* and *cca1 lhy rve468* flower significantly earlier than Col-0 in long days when measured by leaf number (Fig. 2.4). In short days, *rve468* flowers significantly later than Col-0 when measured by days but not when measured by leaf number (Fig. 2.4). As in long days, *cca1 lhy* and *cca1 lhy rve468* both flower significantly earlier than Col-0 in short days when measured either by leaf number or days. While *cca1 lhy rve468* flowers significantly later than *cca1 lhy* in short days, the flowering time is much closer to that of *cca1 lhy* than to *rve468* (Fig. 2.4). Overall, in both long and short days, flowering time for the *cca1 lhy rve468* mutant is similarly early as for *cca1 lhy*. Together, the gene expression and flowering time data suggest that *CCA1* and *LHY* are epistatic to *RVE4*, *RVE6*, and *RVE8* in circadian clock function and its coordination of flowering time.

***CCA1*, *LHY*, *RVE4*, *RVE6*, and *RVE8* are additive for growth.**

Given the similar circadian phenotypes of *cca1 lhy* and *cca1 lhy rve468*, we next wanted to compare the growth phenotypes of *cca1 lhy rve468* and *cca1 lhy*. Since hypocotyl elongation is regulated by the circadian clock[62], we hypothesized that *cca1 lhy rve468* mutants would have short hypocotyls like *cca1 lhy* mutants. We first grew seedlings in constant darkness or in constant light with intensities ranging from 0.1-30 µmol m^{-2} s^{-1} and measured their hypocotyl lengths. In all constant light conditions (monochromatic red, monochromatic blue, and red plus blue), *cca1 lhy* hypocotyls are shorter and *rve468* hypocotyls are longer than Col-0 (Fig. 2.5), consistent with previous reports[51,54,55]. Interestingly, *cca1 lhy rve468* has an intermediate hypocotyl length that is not significantly different

from Col-0 in most light conditions (one-way ANOVA and Tukey's post hoc test, $p > 0.05$) (Fig. 2.5). These data suggest that *CCA1*, *LHY*, *RVE4*, *RVE6*, and *RVE8* interact additively to regulate hypocotyl length in constant light conditions.

We next examined genetic interactions between *CCA1*, *LHY*, *RVE4*, *RVE6*, and *RVE8* on phenotypes of adult plants, measuring the petiole length and blade area of the fully expanded fifth rosette leaf of plants grown in long or short photoperiods. The overall appearance of *cca1 lhy rve468* plants is intermediate between that of the *cca1 lhy* and *rve468* mutants in both LD and SD conditions (Fig. 2.6A – B). In short days, *rve468* has a significantly longer median petiole length than Col-0 and *cca1 lhy* has a significantly shorter median petiole length than Col-0 (Fig. 2.6C), consistent with previous observations[55]. However, the median petiole length of *cca1 lhy rve468* is intermediate between that of *cca1 lhy* and Col-0 in both photoperiods (Fig. 2.6C), suggesting an additive genetic interaction between the positive and negative-acting Myb-like factors. The median blade area of *cca1 lhy* is significantly smaller than Col-0 in both long days and short days. Surprisingly, *rve468* has a significantly larger median blade area than Col-0 in long days[55] but a significantly smaller median blade area than Col-0 in short days (Fig. 2.6C). The median blade area of *cca1 lhy rve468* is larger than *cca1 lhy* in both photoperiods, although this is not significant in long days likely due to a high degree of variation in this condition (Fig. 2.6C). Together, these data suggest that *CCA1*, *LHY*, *RVE4*, *RVE6*, and *RVE8* interact additively to regulate elongation of hypocotyls in constant light and growth of leaves in long and short days.

Loss of the *RVE*s does not rescue *PIF4* and *PIF5* expression in *cca1 lhy* mutants.

PIF4 and *PIF5* are required for the large rosette size of *rve468* mutants and their expression is significantly increased in *rve468*[55]. We therefore hypothesized that expression of these genes might be elevated in *cca1 lhy rve468* compared to *cca1 lhy* and that this might contribute to their differences in size. We therefore examined *PIF* expression under constant white light using qRT-PCR. As expected based on the expression patterns of the core clock genes (Fig. 2.2), *PIF4* and *PIF5* expression is poorly

rhythmic in both *cca1 lhy* and in *cca1 lhy rve468* (Fig. 2.7). To our surprise, however, we found that expression levels of *PIF4* and *PIF5* in the double *cca1 lhy* and the quintuple *cca1 lhy rve468* plants are similarly low and not significantly different between these two genotypes (one-way ANOVA and Tukey's post hoc test, $p > 0.05$). Since other clock proteins are known to modulate PIF transcriptional regulatory activity[41–43], we next hypothesized that there might be differences in PIF4 and/or PIF5 activity in *cca1 lhy* and *cca1 lhy rve468* mutants. We therefore examined expression levels of known *PIF4* and *PIF5* targets implicated in auxin signaling and hypocotyl elongation, including *TRYPTOPHAN AMINOTRANSFERASE OF ARABIDOPSIS 1* (*TAA1*), *INDOLE-3-ACETIC ACID INDUCIBLE 29* (*IAA29*), *YUCCA 8* (*YUC8*), and *ARABIDOPSIS THALIANA HOMEOBOX PROTEIN 2* (*ATHB2*)[44–48,63,64]. Like the expression of *PIF4* and *PIF5* themselves, the overall expression patterns and mean levels of these genes are similar between *cca1 lhy* and *cca1 lhy rve468*, although mean expression levels of *TAA1* and *ATHB2* over the entire time course are slightly but significantly higher in *cca1 lhy* than in *cca1 lhy rve468* (one-way ANOVA and Tukey's post hoc test, $p < 0.05$) (Fig. 2.7). These data suggest that expression differences of *PIF4*, *PIF5*, and several of their targets involved in auxin biosynthesis or signaling are not likely responsible for observed differences in growth between *cca1 lhy* and *cca1 lhy rve468*.

Discussion

Here we present a likely null *cca1 lhy rve468* quintuple mutant and examine its clock and growth phenotypes compared to *cca1 lhy* and *rve468* mutants. We find that *CCA1* and *LHY* are epistatic to *RVE4*, *RVE6*, and *RVE8* in the regulation of the circadian clock and flowering time. However, *CCA1* and *LHY* are additive to *RVE4*, *RVE6*, and *RVE8* in the regulation of growth phenotypes. Interestingly, *cca1 lhy rve468* quintuple mutants grow similarly to wild-type plants despite being largely arrhythmic, suggesting that a functional oscillator is not required for near-normal phenotypes of circadian-regulated outputs.

Mutants with T-DNAs integrated into introns can be unstable.

There are conflicting reports in the literature regarding the overall rhythmicity of *cca1 lhy* mutants. In the Col-0 background, the *cca1-1* and *lhy-20* alleles are both T-DNA insertion mutants[57,59] and the double mutant has been described as either arrhythmic or rhythmic with a short-period[11,65–68]. A similar trend is observed with the *cca1-11 lhy-21* mutant in the Wassilewskija (Ws) background, which has been reported to be either arrhythmic or rhythmic with a short-period[53,54,69]. Some of these differences in reported rhythmicity may well be attributed to differences in growth conditions and the types of assays used to assess rhythmicity. However, we propose that some of these reported phenotypic differences may be due to instability of mutant alleles in which a T-DNA insertion has occurred within a non-coding portion of the gene (as is true for *cca1-1*, *cca1-11,* and *lhy-20*).

There are multiple reports of T-DNA suppression of the phenotypes of mutants with a T-DNA insertion within an intron[70–73]. This phenomenon is analogous to paramutation in that introduction of a second T-DNA locus induces the genetically stable upregulated expression of a previously silenced locus. The mechanism depends upon the RNA-dependent DNA methylation pathway and hypermethylation of intronic T-DNA sequences in the suppressed allele[70,71,73]. This process may have caused partial suppression of the *lhy-20* allele in the *cca1-1 lhy-20* double mutant as we observe considerable *LHY* expression in these plants[11].

In the *cca1-1 lhy-20 rve4-1 rve6-1 rve8-1* mutant, all alleles contain homologous T-DNA sequences inserted within introns which could potentially allow T-DNA suppression to occur. This possibility is supported by our observation that although we did not detect *RVE4* or *RVE8* expression when we first isolated the *rve4-1 rve6-1 rve8-1* mutants[11,24], after further generations of propagation we now detect expression of *RVE4* and *RVE8* in these plants (Fig. S2.5). We therefore expect that the new CRISPR-edited frameshift mutants of *RVE4*, *RVE6*, and *RVE8* that we report in this paper will, as stable alleles, prove very useful to the plant science community.

Improper circadian regulation does not guarantee altered growth phenotypes.

Mutant circadian phenotypes are often correlated with abnormal growth phenotypes, such as *rve468* mutants having a long period[24] as well as long hypocotyls and large rosettes[55]. Often such phenotypes are attributed to the malfunctioning of the circadian clockwork. However, most clock components are connected to many other pathways, such as the regulation of growth through control of *PIF4* and *PIF5* expression by the evening complex[40]. Many clock proteins are not only components of the circadian clock itself but also transcription factors that can directly control expression of hundreds of clock-controlled genes. This makes it difficult to determine if mutant phenotypes are due to disrupted clock function or due to altered expression levels of clock output genes. Here we show that *cca1 lhy rve468* is a mutant with highly reduced clock function but with similar hypocotyl (Fig. 2.5) and rosette growth phenotypes (Fig. 2.6) as wild-type plants. Especially in the constant-light conditions used to assess hypocotyl elongation, these data show that robust rhythmicity *per se* is not an important determinant of normal growth responses.

Plants mutant for all five Myb-like factors are photoperiodic.

Although rhythmicity of free-running gene expression is greatly reduced in *cca1 lhy rve468* mutants (Fig. 2.1 – 2.2), these plants retain photoperiodic responsiveness. The quintuple mutants flower later in short days than in long days as measured either by days to flowering or number of leaves produced before flowering (one-way ANOVA, $p < 1e^{-10}$ for both comparisons) (Fig. 2.4). This suggests that some clock function is retained even in these quintuple mutants. This is supported by our detection of some rhythmic *cca1 lhy rve468* plants in luciferase assays (Fig. 2.1, Fig. S2.2). This is most noticeable in constant red plus blue light conditions, where up to half of the *cca1 lhy rve468* seedlings had an RAE < 0.6 in at least one experiment (Fig. S2.2). qRT-PCR analysis also suggested some genes, like *LUX*, may have low-amplitude rhythms of gene expression in the quintuple mutant in constant conditions (Fig. 2.2).

It is surprising that *cca1 lhy rve468* retains some level of clock function given that these five core clock genes are involved in the main feedback loops within the core circadian clock[8,34]. However, in addition to these feedback loops, the evening complex can regulate itself, with *LUX* binding to its own promoter[74], and the evening complex and PRRs reciprocally repress each other's expression[27,74,75]. It may be that these remaining loops are sufficient to sustain the slight circadian function observed in these Myb-like quintuple mutants. Additional feedback loops likely allow the clock to better synchronize with the environment and cycle more robustly, but do not appear necessary for a low level of basal rhythmicity.

Materials and Methods

Plant Materials

All plants used are in the Columbia (Col-0) wild-type background. The *cca1-1* allele originally in the Wassilewskija (Ws) background[57] was backcrossed to Col-0 for six generations, then crossed to *lhy-100*[58] to generate *cca1-1 lhy-100*. This mutant was then transformed via floral dip[76] with the pC2L2 construct containing *CCR2::LUC2* to generate the *cca1-1 lhy-100 CCR2::LUC2* line used here. Col *CCR2::LUC2* was generated by crossing *cca1-1 lhy-100 CCR2::LUC2* to Col-0. The *rve4-11 rve6-11 rve8-11 CCR2::LUC2* mutant was generated by transforming Col *CCR2::LUC2* with the 8X-*RVE*_pMR333 Cas9-containing construct via floral dip[76]. The *cca1-1 lhy-100 rve4-12 rve6-12 rve8-12 CCR2::LUC2* mutant was generated by transforming *cca1-1 lhy-100 CCR2::LUC2* with the 8X-*RVE*_pMR333 Cas9-containing construct via floral dip[76]. Transgenic plants were initially selected on media containing 30 mg/L Basta and Cas9-negative lines were later selected for study. For Fig. S2.5, Col *CCR2::LUC+*, *rve4-1 CCR2::LUC+*, *rve8-1 CCR2::LUC+*, and *rve4-1 rve6-1 rve8-1 CCR2::LUC+* are as previously described[23,24].

Plasmids

The pC2L2 plasmid was created through traditional cloning methods by replacing *LUC+* within the previously described *CCR2::LUC+* plasmid[77] with *LUC2* from pGL4.10 (Promega, Madison, WI). The 8X-

*RVE*_pMR333 plasmid was created through Gateway cloning[78] between 8X-*RVE*_pEn-Chimera and pMR333 (generously donated by Dr. Mily Ron). CRISPR-Cas9 guides targeting *RVE3*, *RVE4*, *RVE6*, and *RVE8* were designed using the CRISPOR algorithm[79,80], multiplexed by interspersing tRNA and gRNA sequences as previously described[81], and synthesized by Genewiz (Genewiz, South Plainfield, NJ). Guide sequences are included in Appendix III. The synthesized guide fragment was incorporated into pEn-Chimera[82] through traditional cloning methods to create 8X-*RVE*_pEn-Chimera.

Genotyping

New CRISPR-Cas9 alleles were identified through PCR amplification followed by Sanger sequencing, mutant sequences included in Appendix II. Homozygous mutants of all alleles used in this research were identified through PCR amplification of genomic DNA. Primers used for genotyping are included in Appendix V.

Growth Conditions

Seeds were surface sterilized with chlorine gas and stratified in the dark for 2-4 days at 4°C. For luciferase imaging and qRT-PCR, seeds were plated on 1X Murashige and Skoog, 0.7% agar, 3% sucrose. Seedlings were entrained in light-dark cycles (12h light, 12h dark) under 50-60 µmol m^{-2} s^{-1} white light at 22°C for 6 days. For hypocotyl length assays, seeds were plated on 0.5X Murashige and Skoog, 0.7% agar and exposed to a 4-hour pulse of 50-60 µmol m^{-2} s^{-1} white light at 22°C to induce germination. Seedlings were then grown in the specified light conditions using monochromatic red and/or blue LEDs (XtremeLUX, Santa Clara, CA) at 22°C for 6 days. For flowering time and rosette growth assays, seeds were sown directly on soil and grown in light-dark cycles of the specified photoperiod under 150-200 µmol m^{-2} s^{-1} white light at 22°C.

***CCR2::LUC2* luciferase imaging**

Seedlings were sprayed with 3 mM D-luciferin, moved to the specified light conditions using red and/or blue LEDs (XtremeLUX, Santa Clara, CA), and imaged for 5-6 days under a cooled CCD camera (DU434-

BV, Andor Technology, or iKon M-934, Andor Technology). Neutral density filters (Rosco Laboratories or LEE Filters) were used to generate the specified light intensities of monochromatic red, monochromatic blue, or red plus blue light (Fig. 2.1C – E, Fig. S2.2, Fig. S2.3). Quantification of bioluminescence was performed using MetaMorph software (Molecular Devices) and circadian rhythms were analyzed with Biological Rhythm Analysis Software System (BRASS)[53].

qRT-PCR analysis

After entrainment, seedlings were moved to constant 50-60 µmol m^{-2} s^{-1} white light at 22°C at dawn (ZT0) and collected every 4 hours from ZT36 to ZT72. Sample preparation and qRT-PCR were performed as previously described[11] using a BioRad CFX96 thermocycler (Bio-Rad Laboratories, Hercules, CA). Relative expression and SEM values were obtained from the BioRad CFX96 software package. Primers used for qRT-PCR are included in Appendix V.

Hypocotyl length assays

After 6 days of growth, seedlings were transferred to transparent sheets and scanned at 600 dpi. Hypocotyls were individually measured using ImageJ[83].

Flowering time analysis

Date of flowering was recorded as the day the inflorescence stem reached 1 cm long. At that time, rosette leaves were counted to determine flowering time by leaf number. Cauline leaves were not included.

Rosette leaf measurements

After 30 days of growth, rosette leaf 5 was transferred to transparent sheets and scanned at 600 dpi. Blade area and petiole length were measured using LeafJ[84].

Statistical Analysis and Data Visualization

All statistical analyses and data visualization were performed using R[85]. Figures were generated using the tidyverse[86], RColorBrewer[87], cowplot[88], gridExtra[89], glue[90], and ggtext[91] packages. Gene models were

created using the genemodel package[92]. Statistical differences in fractions of rhythmic plants between genotypes were determined by Pearson's Chi-Squared test, followed by pairwise proportion tests with Benjamin-Hochberg correction for multiple testing using the rstatix package[93]. Rhythmicity of qRT-PCR expression was determined by the circacompare package[94]. Linear mixed-effect models were used in one-way ANOVA and Tukey's post hoc tests. To compare mean expression level between genotypes for qRT-PCR analysis, used model "expression ~ genotype + (1|plate)". To compare period phenotype differences between genotypes, used model "period ~ genotype + (1|rep)". To compare flowering time and rosette growth differences between genotypes within each condition (LD or SD), used model "growth phenotype ~ genotype + (1|rep) + (1|flat)". To compare hypocotyl length differences between genotypes at each fluence rate, used model "length ~ genotype + (1|rep)". Modeling was done with the lme4[95] and lmerTest[96] packages, tests were performed using the lattice[97], broom[98], and emmeans[99] packages. Results were visualized with the multcomp[100] and multcompView[101] packages.

Accession Numbers

Accession numbers for *Arabidopsis thaliana* genes referenced here:

ATHB2	AT4G16780
CCA1	AT4G16780
CO	AT5G15840
ELF3	AT2G25930
ELF4	AT2G40080
FT	AT1G65480
IAA29	AT1G65480
LHY	AT1G01060
LUX	AT3G46640
PIF4	AT2G43010
PIF5	AT3G59060
PRR5	AT3G59060
PRR7	AT5G02810

PRR9	AT2G46790
RVE4	AT5G02840
RVE6	AT5G52660
RVE8	AT3G09600
TAA1	AT1G70560
TOC1	AT5G61380
YUC8	AT4G28720

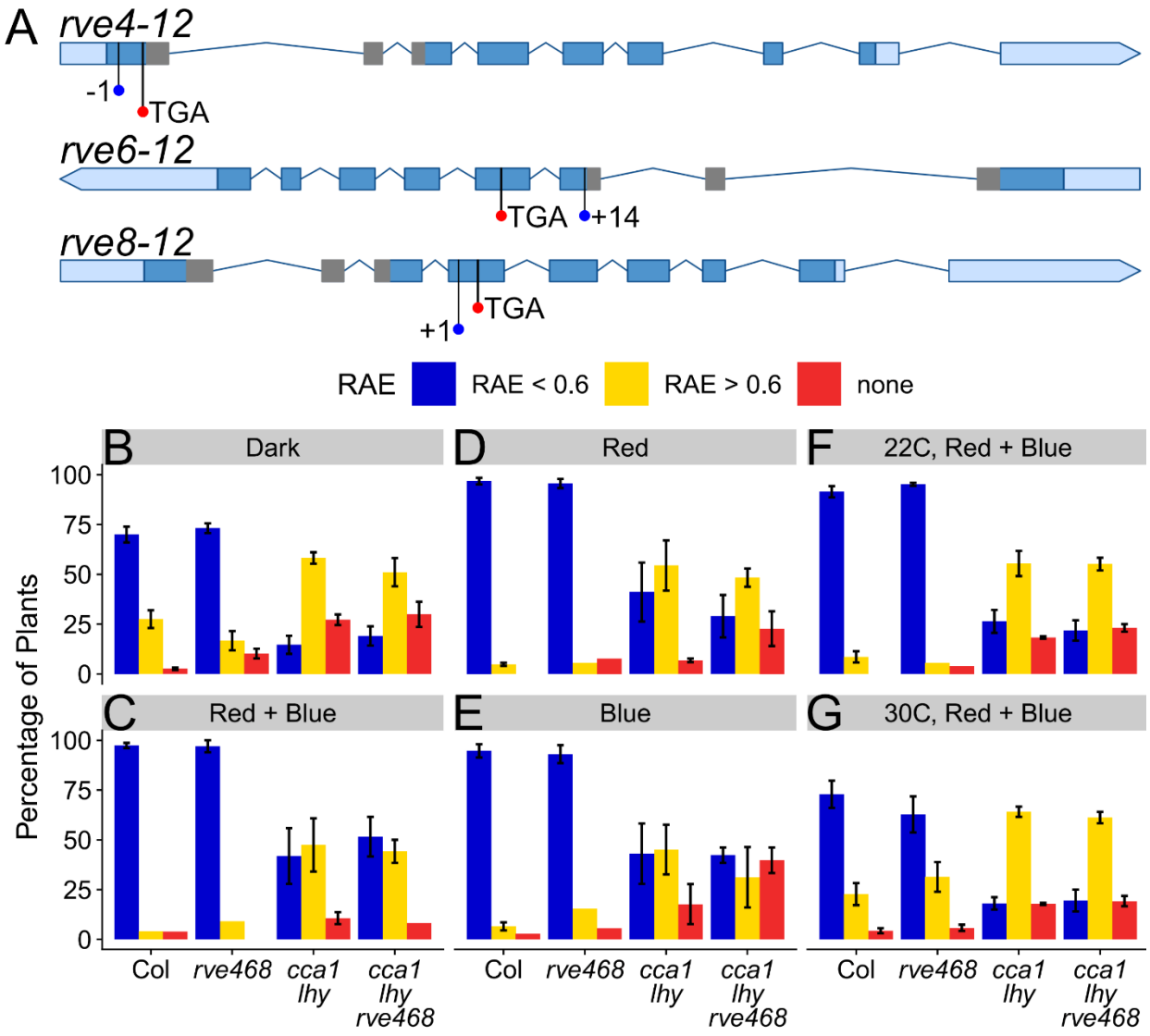

Figure 2.1: *cca1 lhy rve468* mutants have poor rhythms in all conditions tested. (A) Gene models of CRISPR-Cas9-generated *rve4-12*, *rve6-12*, and *rve8-12* alleles. Positions of insertions or deletions are shown by blue circles and positions of resulting premature stop codons are shown by red circles. Light blue represents untranslated regions while dark blue represents coding regions. Gray shading represents the coding regions of the Myb-like DNA-binding domains. (B – G) Rhythmicity as measured by relative amplitude error (RAE) across light qualities and temperatures, where RAE < 0.6 is defined as rhythmic and RAE > 0.6 defined as arrhythmic. Seedlings with luciferase activity that could not be fit to any cosine curve did not return an RAE. Error bars indicate ± SEM. (B) After entrainment at 22°C, seedlings were

transferred to constant darkness at 22°C. Data from three trials, n = 33-106 per trial. (C – E) After entrainment at 22°C, seedlings were transferred to constant 10 µmol m^{-2} s^{-1} light of the specified quality at 22°C. Data from three trials, n = 11-36 per trials. (F – G) After entrainment at 22°C, seedlings were transferred to 35 µmol m^{-2} s^{-1} red plus 35 µmol m^{-2} s^{-1} blue light at the specified temperature. Data from two trials, n = 34-71 per trial.

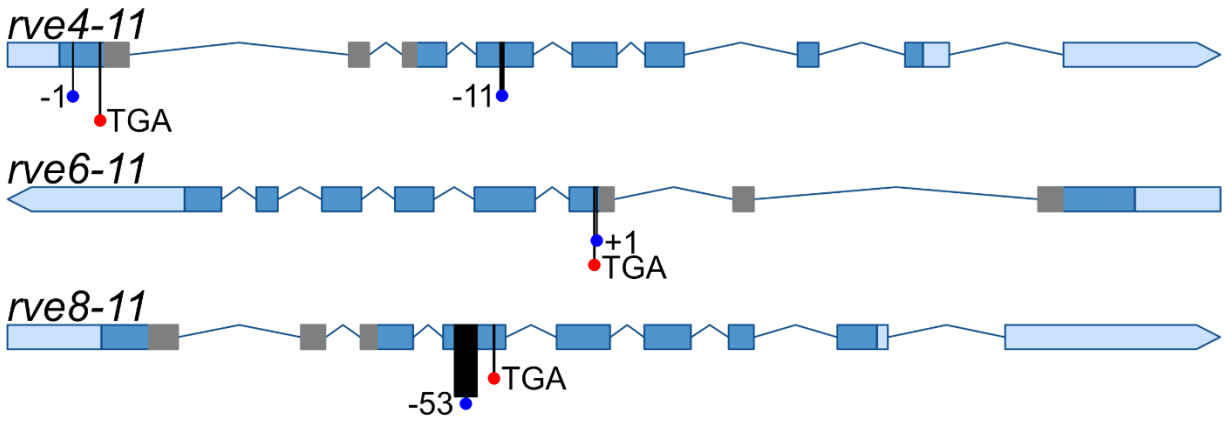

Figure S2.1: New *rve468* mutant alleles were generated using CRISPR-Cas9. Gene models of *rve4-11*, *rve6-11*, and *rve8-11* alleles. Positions of insertions or deletions are shown by blue circles and positions of resulting premature stop codons are shown by red circles. Light blue represents untranslated regions while dark blue represents coding regions. Gray shading represents the coding regions of the Myb-like DNA-binding domains.

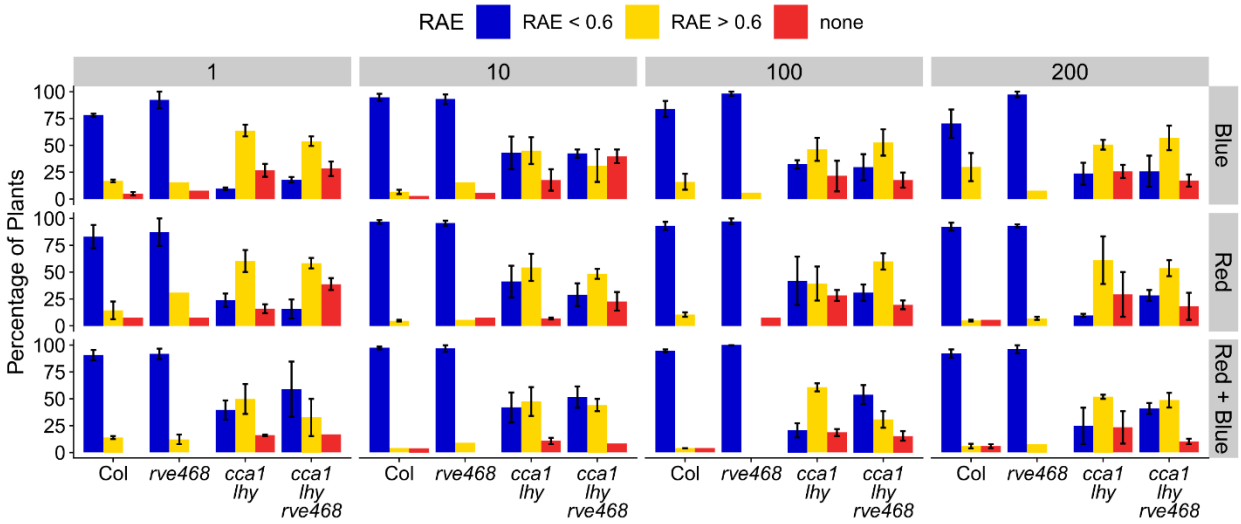

Figure S2.2: *cca1 lhy rve468* mutants have poor rhythms in all conditions tested. Rhythmicity as measured by relative amplitude error (RAE), where RAE < 0.6 is defined as rhythmic and RAE > 0.6 defined as arrhythmic. Seedlings with luciferase activity that could not be fit to any cosine curve did not return an RAE. Error bars indicate ± SEM. After entrainment, seedlings were transferred to constant monochromatic red, monochromatic blue, or red plus blue light of the specified intensities (from 1-200 µmol m^{-2} s^{-1}) at 22°C. Data from three trials, n = 10-36 per trial.

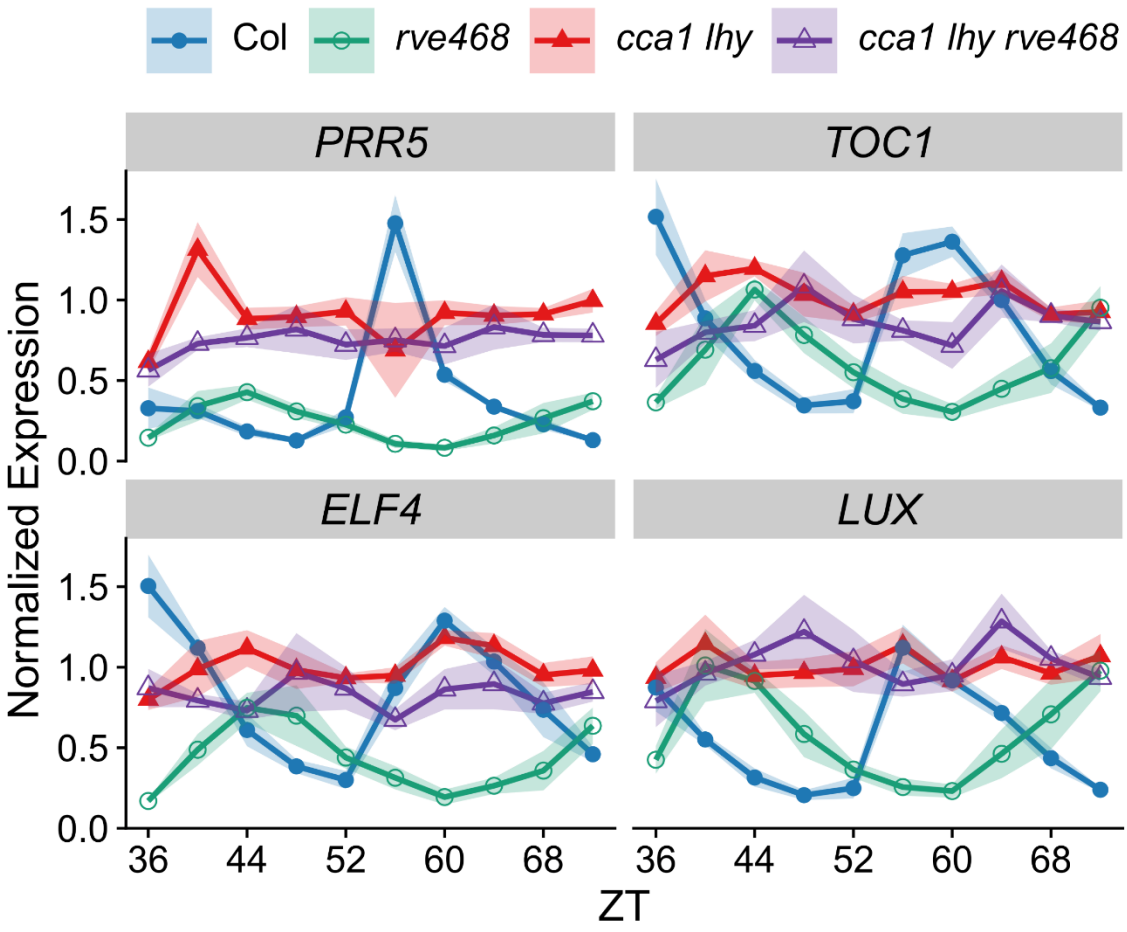

Figure 2.2: Rhythmicity of core clock gene expression is severely reduced in *cca1 lhy* and *cca1 lhy rve468* mutants. After entrainment, seedlings were transferred at ZT0 to constant 50-60 µmol m^{-2} s^{-1} white light at 22°C. Expression of the specified genes was determined by qRT-PCR and normalized to reference genes *PP2A* and *IPP2*. Ribbon indicates ± SEM for four biological replicates.

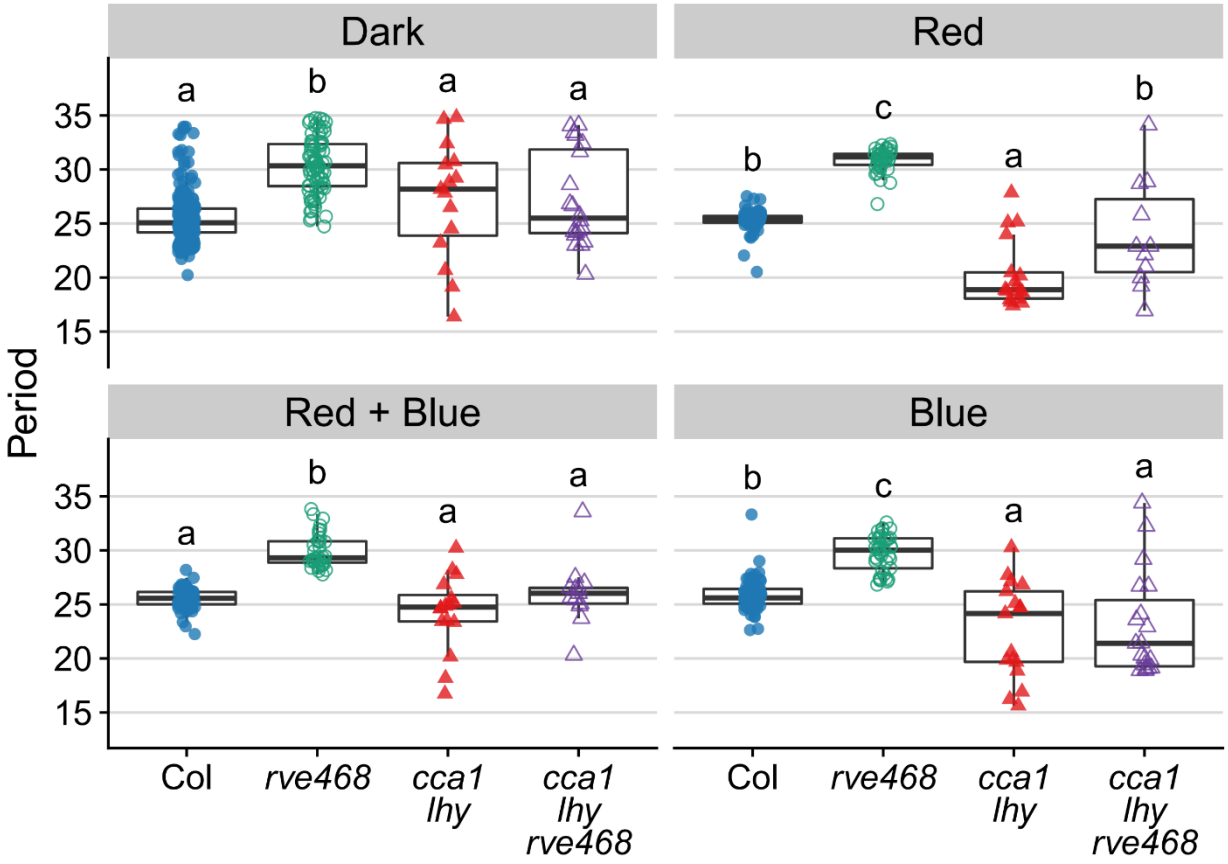

Figure S2.3: *CCA1* and *LHY* are epistatic to *RVE4*, *RVE6*, and *RVE8* for circadian period phenotypes.

Period estimates of rhythmic seedlings (RAE < 0.6) of the indicated genotypes. After entrainment at 22°C, seedlings were either transferred to constant darkness or constant 10 µmol m^{-2} s^{-1} light of the specified quality at 22°C. Data from these plants also shown in Fig. 1. Different letters denote significant differences between genotypes within each condition ($p < 0.01$), determined by one-way ANOVA followed by Tukey's post hoc test. The lines within the boxes are the medians, and the lower and upper hinges represent the first and third quartiles. Data from three trials, n = 11-106 per trial.

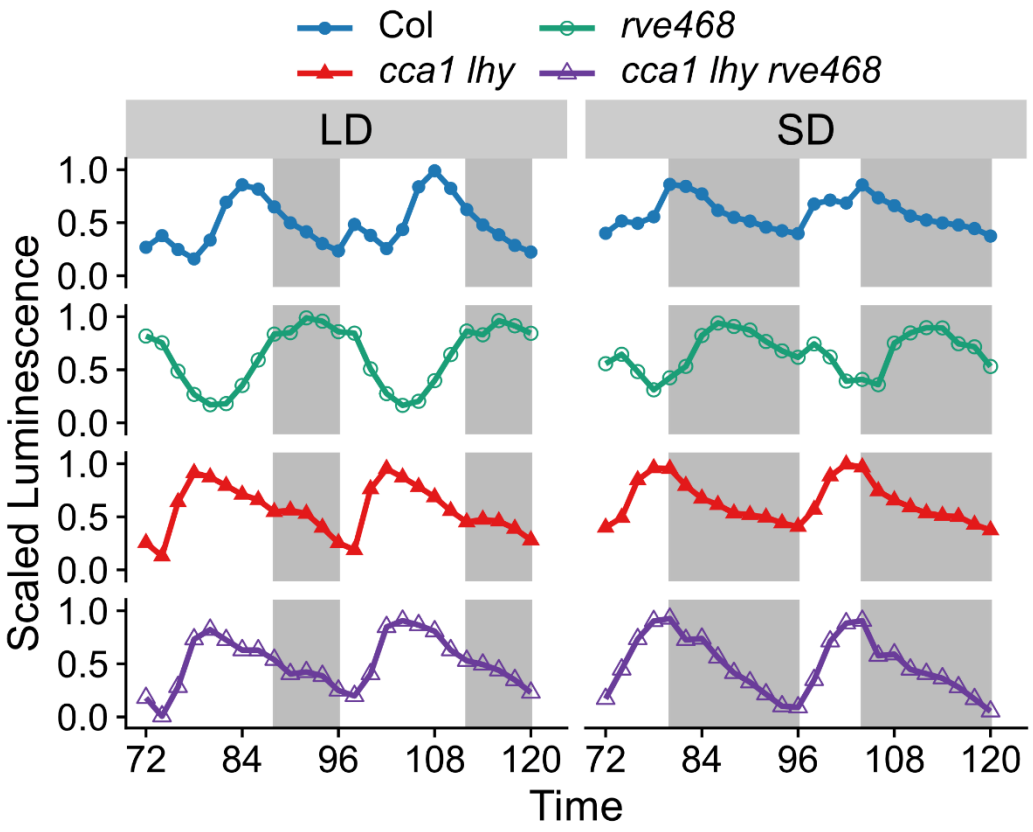

Figure 2.3: Diel waveforms of gene expression in *cca1 lhy* and *cca1 lhy rve468* mutants are similar to each other. Average traces of luminescence from *CCR2::LUC2* transgene in the indicated genotypes. Gray boxes show periods of darkness. Seedlings were entrained in 12:12 light-dark cycles, then transferred at time 0 to 12:12 light-dark cycles with 35 µmol m^{-2} s^{-1} red plus 35 µmol m^{-2} s^{-1} blue light at 22°C. At time 48, light-dark cycles were changed to either 16:8 (LD) or 8:16 (SD) under the same light intensities. n = 16-18, experiment was conducted twice with similar results. The full time course is presented in Fig. S2.4.

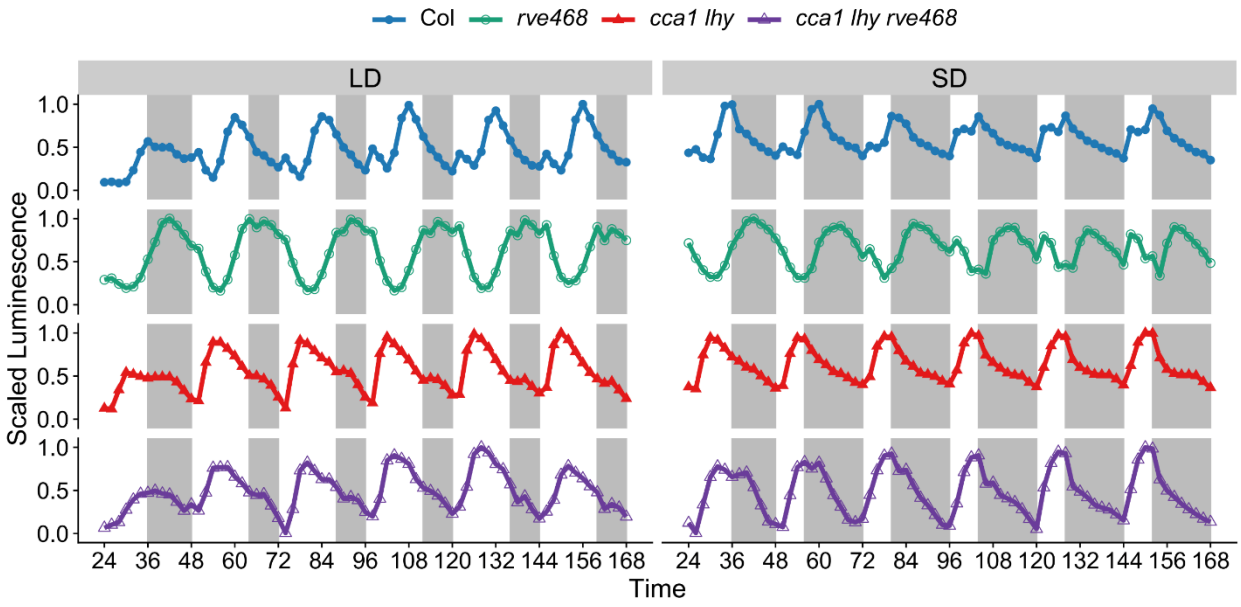

Figure S2.4: Diel waveforms of gene expression in *cca1 lhy* and *cca1 lhy rve468* mutants are similar to each other. Average traces of luminescence from *CCR2::LUC2* transgene in the indicated genotypes. Gray boxes show periods of darkness. Seedlings were entrained in 12:12 light-dark cycles, then transferred at time 0 to 12:12 light-dark cycles with 35 µmol m^{-2} s^{-1} red plus 35 µmol m^{-2} s^{-1} blue light at 22°C. At time 48, light-dark cycles were changed to either 16:8 (LD) or 8:16 (SD) under the same light intensities. n = 16-18, experiment was conducted twice with similar results. Data are the same as those presented in Fig. 2.3.

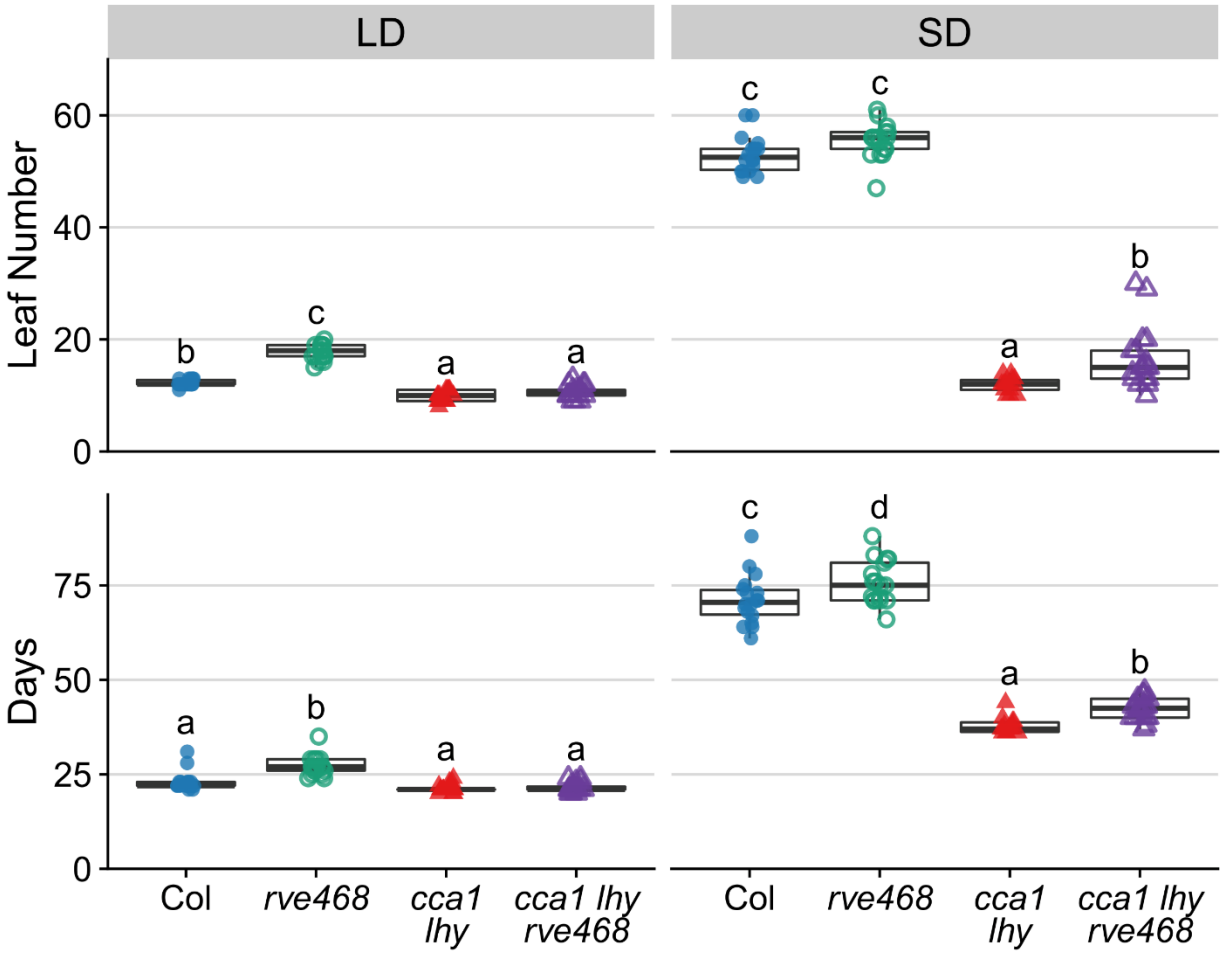

Figure 2.4: *CCA1* and *LHY* are epistatic to *RVE4*, *RVE6*, and *RVE8* for flowering time regulation.

Flowering time of the indicated genotypes was assessed by leaf number at bolting and days to bolting. Bolting was defined as the time when the inflorescence stem reached 1 cm. Plants were grown at 22°C under 150-200 µmol m^{-2} s^{-1} white light in the specified photoperiods (16:8 LD or 8:16 SD). Different letters denote significant differences between genotypes within each condition ($p < 0.01$), determined by one-way ANOVA followed by Tukey's post hoc test. The lines within the boxes are the medians, and the lower and upper hinges represent the first and third quartiles. n = 14-18, experiment was conducted twice with similar results.

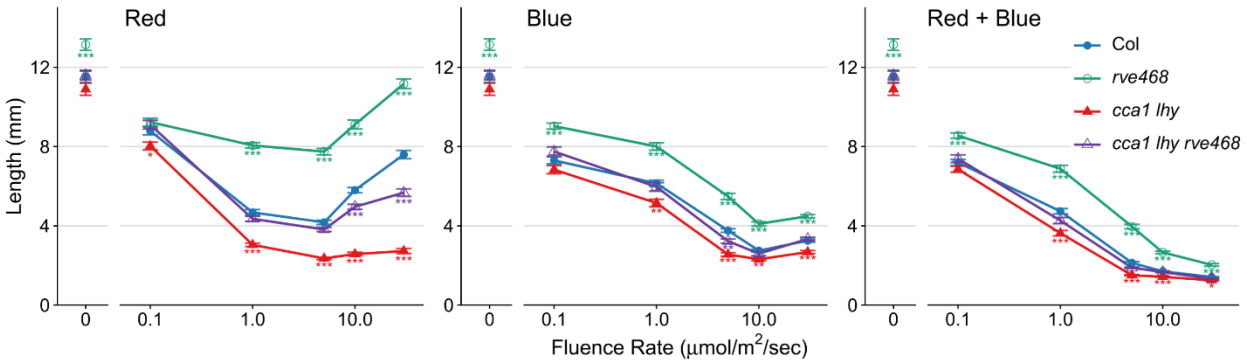

Figure 2.5: *CCA1*, *LHY*, *RVE4*, *RVE6*, and *RVE8* interact additively to regulate hypocotyl length.

Hypocotyl length of the indicated genotypes was determined in different light qualities and intensities. Seedlings were grown at 22°C under constant darkness or monochromatic red, monochromatic blue, or red plus blue light of the specified intensity (0.1-30 µmol m^{-2} s^{-1}). Points are the mean hypocotyl length, error bars indicate ± SEM. Significant differences between genotypes in each light quality and fluence rate determined by one-way ANOVA followed by Tukey's post hoc test (* $p < 0.05$, ** $p < 0.01$, *** $p < 0.001$). In constant light conditions, data from three trials (n = 15-22 per trial). In constant darkness, data from six trials (n = 7-21 per trial).

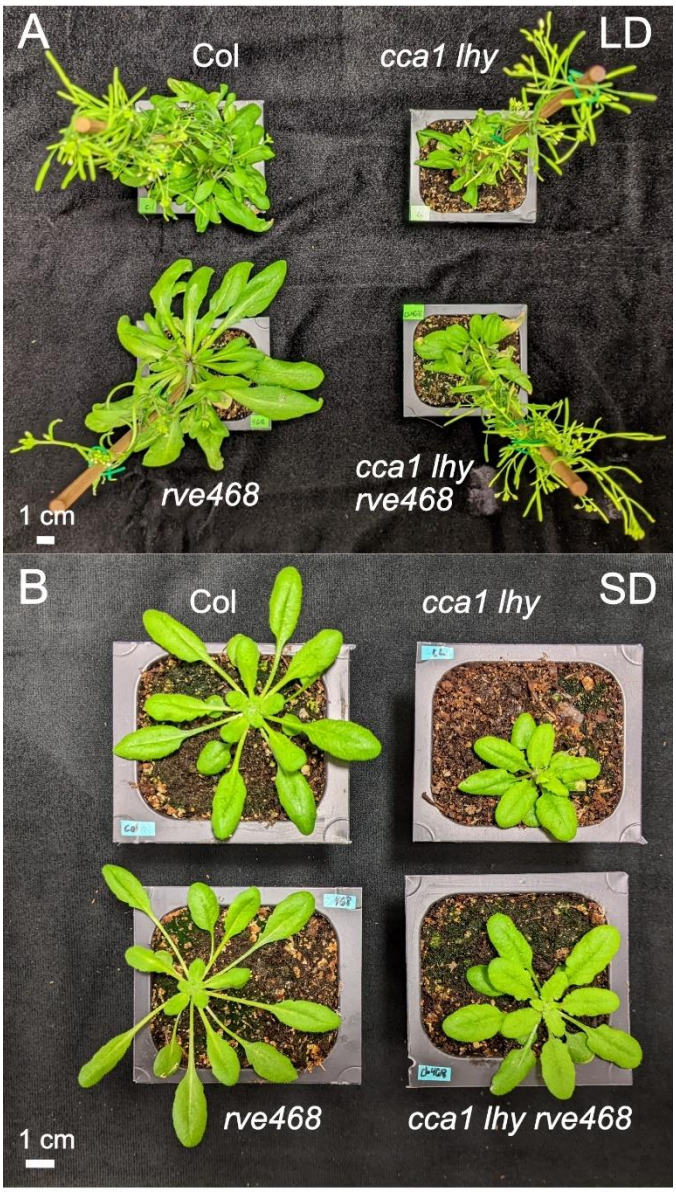
A
Col
cca1 lhy
LD
rve468
cca1 lhy
rve468
1 cm
B
Col
cca1 lhy
SD
rve468
cca1 lhy rve468
1 cm
C
LD
SD
Petiole Length (cm)
Blade Area (cm²)
Col
rve468
cca1 lhy
cca1 lhy rve468

Figure 2.6: *CCA1*, *LHY*, *RVE4*, *RVE6*, and *RVE8* interact additively to regulate leaf growth. (A) Representative images of plants grown for 35 days in 16:8 light-dark cycles (LD) at 22°C. (B) Representative images of plants grown for 35 days in 8:16 light-dark cycles (SD) at 22°C. (C) Petiole length and blade area of rosette leaf 5 of the indicated genotypes were assessed after 30 days of growth in the specified photoperiods. Different letters denote significant differences between genotypes within each condition ($p < 0.01$), determined by one-way ANOVA followed by Tukey's post hoc test. The lines within the boxes are the medians, and the lower and upper hinges represent the first and third quartiles. n = 17-18, experiment was conducted twice with similar results. Plants were grown at 22°C under 150-200 µmol m^{-2} s^{-1} white light (A-C).

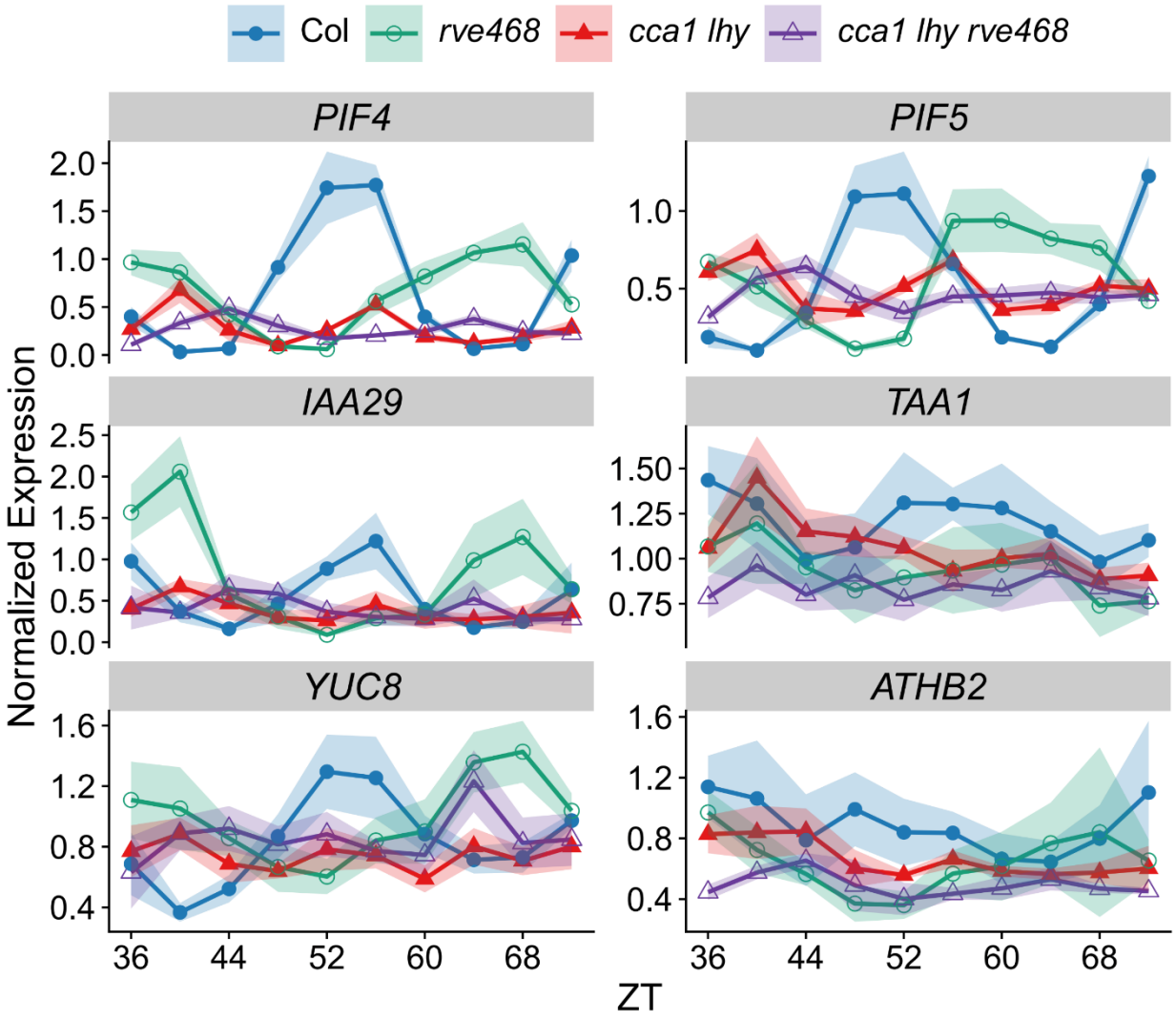

Figure 2.7: Expression of *PIF4*, *PIF5*, and PIF target genes is low and arrhythmic in *cca1 lhy* and *cca1 lhy rve468* mutants. After entrainment, seedlings were transferred at ZT0 to constant 50-60 µmol m^{-2} s^{-1} white light at 22°C. Expression of the specified genes was determined by qRT-PCR and normalized to reference genes *PP2A* and *IPP2*. Ribbon indicates ± SEM for four biological replicates.

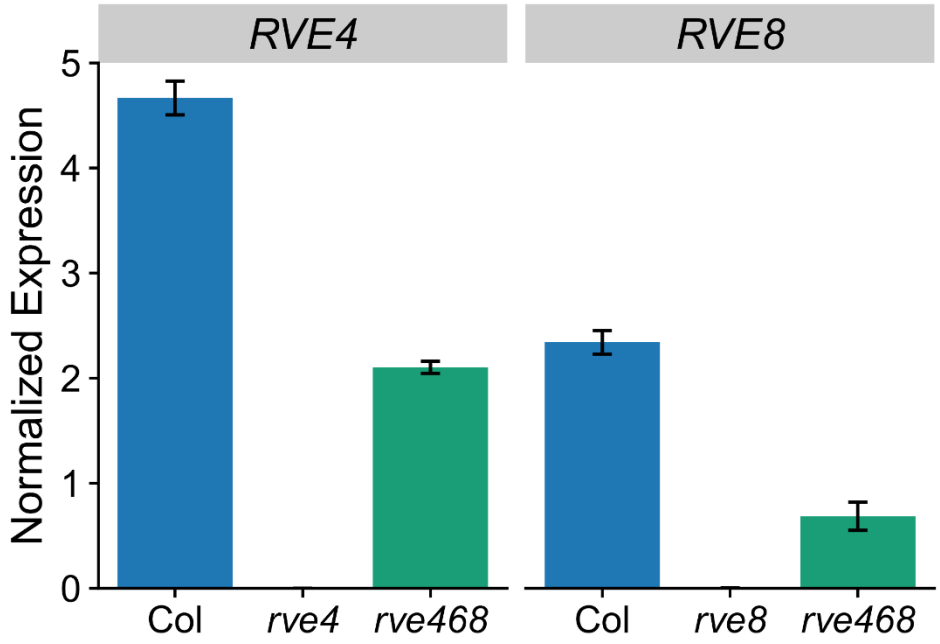

Figure S2.5: Expression levels of *RVE4* and *RVE8* are increased in *rve4-1 rve6-1 rve8-1* triple mutants compared to *rve4-1* and *rve8-1* single mutants. After entrainment, seedlings were released to 50-60 µmol m^{-2} s^{-1} constant white light at 22°C. Expression was determined by qRT-PCR and normalized to reference gene *PP2A*. Error bars indicate ± SEM for three biological replicates.

Chapter 3: Light quality-dependent roles of RVE proteins in the circadian system

Abstract

The closely related Myb-like activator proteins are known to have partially redundant functions within the plant circadian clock, but their specific roles are not well understood. To clarify the function of the *REVEILLE 4* (*RVE4*), *REVEILLE* (*RVE6*), and *REVEILLE* (*RVE8*) transcriptional activators, we characterized the growth and clock phenotypes of CRISPR-Cas9-generated single, double, and triple *rve* mutants. We found that these genes act synergistically to regulate flowering time, redundantly to regulate leaf growth, and antagonistically to regulate hypocotyl elongation. We previously found that increasing intensities of blue but not red light lengthen the period of triple *rve468* mutants, unlike the period-shortening effects of both light qualities in wild-type plants. We further investigated light quality-specific phenotypes of *rve* mutants and found that *rve468* mutants also lose the blue light-specific increase in expression of some clock genes observed in wild type. To investigate the basis of these blue-light specific clock phenotypes, we examined RVE protein abundances and degradation rates in blue and red light and found no significant differences between these conditions. We next examined genetic interactions between *RVE* genes and *ZEITLUPE* (*ZTL*) and *ELONGATED HYPOCOTYL5* (*HY5*), two factors with blue light-specific functions in the clock. We found that the *RVEs* interact additively with both *ZTL* and *HY5* to regulate circadian period, which suggests that neither of these factors are required for the blue light-specific differences that we observed. Overall, our results suggest that the *RVEs* have separable functions in plant growth and circadian regulation and that they are involved in blue light-specific circadian signaling via a novel mechanism.

Keywords: *Arabidopsis thaliana*; *RVE4*, *RVE6*, *RVE8*; blue light; flowering time; hypocotyl elongation

Introduction

The circadian clock provides a time-keeping mechanism to predict daily and seasonal changes. Circadian components also regulate physiological outputs, such as plant growth and photoperiodic

regulation of flowering[60,61,102], which is critical for increasing an organism's fitness by ensuring it is well-adapted to its environment[6,19,20]. These biological rhythms have a period of approximately twenty-four hours and persist in a constant environment with a similar free-running period[8].

While circadian rhythms continue in the absence of environmental signals, the circadian system is sensitive to a variety of environmental cues. Abrupt changes in light and temperature can re-set clock phase, and in addition, changes in light intensity and temperature can affect the free-running pace of the circadian oscillator[8]. In plants, as in most diurnal organisms, increased light intensity shortens circadian period, while in most nocturnal organisms increased light intensity causes period lengthening[103]. This general relationship is termed 'Aschoff's rule' and is speculated to underlie appropriate entrainment, which matches circadian phase with the environment[104,105].

In eukaryotes, the circadian system is made up of multiple interacting transcriptional feedback loops. Most plant circadian clock components are repressors of transcription[10]. However, several transcriptional activators have been identified. *REVEILLE 4* (*RVE4*), *REVEILLE 6* (*RVE6*), and *REVEILLE 8* (*RVE8*) are the primary known transcriptional activators within the plant circadian clock and act partially redundantly with each other. These *RVEs* are responsible for activating expression of afternoon and evening-phased genes, including *TIMING OF CAB EXPRESSION 1* (*TOC1*), the related *PSEUDO-RESPONSE REGULATORs* genes (*PRR5*, *PRR7*, and *PRR9*), and the evening complex genes *EARLY FLOWERING 3* (*ELF3*), *EARLY FLOWERING 4* (*ELF4*), and *LUX ARRHYTHMO* (*LUX*)[17,33,106]. Acting in opposition to the *RVEs* are the related Myb-like transcription factors *CIRCADIAN CLOCK ASSOCIATED 1* (*CCA1*) and *LATE ELONGATED HYPOCOTYL* (*LHY*), which repress these same targets[22,25,29–32]. Together, *CCA1*, *LHY*, *RVE4*, *RVE6*, and *RVE8* increase robustness of circadian rhythms and regulate clock pace[11].

Studies conducted over the past twenty years have led to considerable insight into how light signaling components interact with the circadian machinery. Phytochromes, which are red light photoreceptors, can affect circadian period and are known to physically interact with the ELF3

protein[104]. Multiple blue light photoreceptors influence the clock, including cryptochromes and the F-box protein ZEITLUPE (ZTL). CRYPTOCHROME2 (CRY2) physically interacts with PRR9 to repress its activity[107]. ZTL also inhibits the function of PRR proteins by promoting the degradation of TOC1 and PRR5 in a blue light-dependent manner[108,109]. In addition to the photoreceptors, downstream light signaling components connect light inputs to the circadian clock. For example, *ELONGATED HYPOCOTYL 5* (*HY5*) is a transcription factor that acts downstream of multiple types of photoreceptors and also affects circadian clock function[110,111]. Binding of HY5 to its targets, including clock gene promoters, is promoted by blue light[112]. This leads to an enhanced short-period phenotype of *hy5* mutants in blue light compared to red light[112].

The study of light responses in controlled environmental conditions has revealed both inhibitory and synergistic interactions between light signaling pathways[104,113,114]. Many circadian assays are performed in constant white or red plus blue light conditions, but separately examining the effects of monochromatic red and monochromatic blue light may uncover more detailed interactions between the clock and light input pathways. The *rve4-1 rve6-1 rve8-1* triple mutant was initially characterized as having a long period in constant red plus blue light conditions, a proxy for natural white light[17]. Subsequent experiments in monochromatic red and monochromatic blue light found that the period of *rve4-1 rve6-1 rve8-1* is consistently longer than wild type in both light qualities but the slope is opposite that of wild type specifically in blue light[18]. In red light, the period of *rve4-1 rve6-1 rve8-1* shortens as the fluence rate increases, as is also seen in wild type. However, while the period of wild-type plants also decreases under increasing intensities of blue light, the period of *rve4-1 rve6-1 rve8-1* mutants lengthens[18]. This change in responsiveness between monochromatic red and monochromatic blue light suggests that *RVE4*, *RVE6*, and *RVE8* may be involved in light quality-specific circadian regulation.

We wanted to further investigate the light quality-specific roles of *RVE4*, *RVE6*, and *RVE8* within the plant circadian system. However, we found that previously generated T-DNA alleles within the *rve4-*

1 rve6-1 rve8-1 triple mutant have regained significant *RVE* gene expression[11]. To circumvent this problem, we generated new *rve* alleles using CRISPR-Cas9. Here, we report the characterization of single, double, and triple mutants containing CRISPR-Cas9-generated alleles of *RVE4*, *RVE6*, and *RVE8*. We assessed the phenotypes of these new mutants in monochromatic red and monochromatic blue light and found blue light-specific phenotypes similar to those observed in the T-DNA *rve468* mutant. We then investigated whether RVE protein differences or interactions with light quality-specific factors could account for the observed light quality-specific differences in *rve468* mutants. We find that RVE protein abundance and degradation rate are not different between monochromatic red and monochromatic blue light. We also find that interactions between *RVE4*, *RVE6*, *RVE8* and *ZTL* or *HY5* are likely not responsible for the blue-specific phenotypes of *rve468* mutants. These data suggest that the RVEs interact with novel blue-specific signaling factors to influence circadian clock function in a light-quality specific manner.

Results

Synergistic, additive, and epistatic interactions between *rve* genes in control of plant growth.

We used CRISPR-Cas9 technology with multiple guide RNAs (Chapter 2) to generate a novel *rve4 rve6 rve8* triple mutant. A mutant with frameshift mutations predicted to cause premature stop codons in all three genes was selected and named *rve4-11 rve6-11 rve8-11* (Fig. 3.1A). The premature stop codon is upstream of the Myb-like DNA-binding domain in *RVE4*, downstream of the Myb-like DNA-binding domain but within the conserved proline-rich region in *RVE6*, and upstream of the conserved C-terminal domain in *RVE8* (Fig. 3.1A). We then isolated all possible single and double mutant combinations and assessed growth and circadian clock phenotypes in these lines and the original triple mutant. These mutants will hereafter be referred to as *rve4*, *rve6*, *rve8*, *rve46*, *rve48*, *rve68*, and *rve468* respectively. We first determined the free-running circadian period of seedlings by monitoring expression of a clock-regulated reporter gene, *CCR2::LUC2*, in each genotype. In constant red plus blue

light, the *rve8* single, all three double, and the triple mutants have a significantly longer period than Col-0 (Fig. 3.1B). We also examined the growth of these *rve* mutants in long and short photoperiods (Fig. 3.1C – D) and saw that *rve468* appears larger than Col-0 in long day conditions. These results are consistent with previous observations of *rve* triple mutants containing *rve4-1*, *rve6-1*, and *rve8-1* T-DNA alleles [17].

An important trait governed by the circadian clock is the photoperiodic control of the transition from vegetative to reproductive growth[60,61]. It has previously been shown that *rve4-1 rve6-1 rve8-1* triple mutant plants flower significantly later than Col-0 in long day (LD) photoperiods[18], so we hypothesized that other long-period *rve* mutants would also flower late. However, only *rve46*, *rve68*, and *rve468* flower significantly later than Col-0 in long days when measured by leaf number at flowering (Fig. S3.1A). The *rve4*, *rve6*, *rve8*, and *rve48* mutants do not flower later than Col-0 (Fig. 3.2A, Fig. S3.1A), even though *rve8* and *rve48* also have long circadian periods (Fig. 3.1B). In short day (SD) photoperiods, none of the *rve* mutants have a significantly different flowering time from Col-0 when measured by leaf number at flowering (Fig. 3.2A, Fig. S3.1A), but *rve468* flowers significantly later when measured by days to flowering (Fig. 3.2B). Overall, the delayed flowering time of *rve468* triple mutants compared to the single and double mutants in long days suggests that *RVE4, RVE6, and RVE8* act synergistically in regulation of flowering time.

We continued to examine the phenotypes of adult *rve* mutants in long and short photoperiods by measuring the petiole length and blade area of the fully-expanded fifth rosette leaf. In long and short days, the median petiole length of the *rve* single mutants is not significantly different from that of Col-0, but *rve68* and *rve468* have significantly longer petioles in short days (Fig. 3.2C, Fig. S3.1C). The median blade area of all *rve* mutants trends larger than Col-0 in long days, although this only reaches statistical significance for *rve468* (Fig. 3.2D, Fig. S3.1D). This is consistent with our previous findings that *rve468* T-DNA mutants have larger leaf blades than Col-0 when grown in long days[18]. Surprisingly, in short days

the median blade area of *rve* mutants trends smaller than Col-0, with *rve468* again being the only mutant with a significantly smaller blade area (Fig. 3.2D, Fig. S3.1D). Although there are not many significant differences in leaf growth between the *rve* mutants and Col-0, together these data suggest that these three RVE proteins act redundantly in control of leaf growth, dependent on day length.

We next investigated the roles for RVE proteins in photomorphogenesis. Seedlings were grown in constant darkness or in a range of fluence rates of constant monochromatic red, monochromatic blue, or red plus blue light and hypocotyl lengths were measured. In constant darkness, all *rve* mutants except *rve48* have significantly longer hypocotyls than Col-0 (Fig. 3.3, Fig. S3.2), suggesting a role in light-independent regulation of development. In all three light qualities tested, all *rve* single mutants have significantly longer hypocotyls than wild type at one or more light intensities (Fig. S3.2), with loss of *RVE6* giving the strongest phenotype. Intriguingly, hypocotyl elongation in *rve48* double mutants is not significantly different from wild type in the dark or at lower light intensities, despite the significantly long hypocotyls of *rve4* and *rve8* single mutants in these conditions (Fig. 3.3). These data suggest a light-independent, antagonistic relationship between RVE4 and RVE8 in the control of hypocotyl elongation.

The stronger hypocotyl phenotypes seen for *rve6* than for *rve4* and *rve8* suggest that *RVE6* is more important than these other Myb-like factors in the regulation of photomorphogenesis. Consistent with a major role for *RVE6*, while the *rve46* and *rve68* double mutants both have significantly elongated hypocotyls at most fluence rates in all three conditions, the *rve68* phenotypes are generally quite similar to the long hypocotyl phenotypes of the triple *rve468* mutant seedlings (Fig. S3.2). Together, these data suggest that all three *RVE* genes contribute to regulation of photomorphogenesis in response to both red and blue light, but that RVE6 plays a predominant role.

***rve468* mutants follow Aschoff's Rule in monochromatic red but not monochromatic blue light.**

We next examined the circadian phenotypes of the *rve* single, double, and triple mutants in a variety of light conditions (constant darkness, monochromatic red, monochromatic blue, and constant

red plus blue light) and across a range of light intensities (from 1-200 µmol m^{-2} s^{-1}). We previously found that the T-DNA alleles of *rve4* and *rve6* did not have period phenotypes[17]. While the new CRISPR allele of *rve4* does not have a period significantly different from wild type in the conditions tested, the new *rve6* allele has a significantly long-period phenotype in red light, and both *rve6* and *rve8* mutants trend long-period in red plus blue but not monochromatic blue light (Fig. 3.4). This suggests RVE6 and RVE8 play more important roles in clock function than RVE4. Indeed, while all three double mutant combinations have long-period phenotypes, the *rve68* mutant has a consistently longer period than the other two double mutants (Fig. S3.3). However, since free-running period is longest in the triple *rve468* mutant (Fig. S3.3), all three *RVE* genes contribute to period shortening in Arabidopsis.

We previously noted that increasing intensities of monochromatic red and monochromatic blue light have opposite effects on *rve4-1 rve6-1 rve8-1* period[18]. We therefore wanted to determine if other *rve* mutants have similar differences in circadian responsiveness to light. To investigate this, we assessed the slopes of free-running period relative to fluence rate in red, blue, and red plus blue light. In red light, the period of all single, double, and triple *rve* mutants decreases as light intensity increases (Fig. 3.4, Fig. S3.3), with slopes not significantly different from Col-0 (two-way ANOVA and Tukey's post hoc test, $p > 0.05$). Thus in red light these genotypes obey Aschoff's rule for diurnal organisms[103]. However, in blue light the period of *rve468* and *rve48* increases as light intensity increases (Fig. S3.3), with slopes that are not significantly different from each other (two-way ANOVA and Tukey's post hoc test, $p > 0.05$) but that are significantly different from wild type (two-way ANOVA and Tukey's post hoc test, $p < 0.05$). This pattern of period lengthening at higher light intensities is reminiscent of responses seen in many nocturnal organisms. This difference in response of circadian period to red and blue light in *rve468* and *rve48* mutants suggests that *RVE* regulation or function is altered between these two light qualities.

Blue light-mediated enhancement of expression of some clock genes is lost in *rve468* mutants.

Given the different effects of red and blue light on circadian period in *rve468* mutants, we hypothesized that expression of clock genes might be altered in *rve468* in a light quality-specific manner. To assess this, we grew Col-0 and *rve468* seedlings in monochromatic blue or monochromatic red light, collected samples over a 24-hour period, extracted RNA, and carried out quantitative reverse-transcriptase polymerase chain reaction (qRT-PCR) assays. In wild-type plants, the amplitude of the evening-phased clock gene *ELF4* is significantly higher in blue than in red light (Fig. 3.5, Fig. S3.5). A similar trend is seen for the other evening-phased genes *TOC1* and *PRR5*, although these values do not reach statistical significance (Fig. S3.5). In the case of *PRR5*, this may be because its expression pattern in blue light poorly matches a cosine curve, leading to an underestimate of its amplitude. A previous study found a significant increase in peak levels of *PRR5* expression in blue light compared to red[112], suggesting that its levels are indeed induced by blue light. However, we found that blue light did not cause a significant increase in peak levels of *CCA1*, *LUX*, and *BOA* when compared to red light. These data show that blue light enhances expression of a subset of evening-phased clock genes in wild type.

We next compared expression patterns of these genes in *rve468* mutants maintained in constant red or blue light. Unlike in wild type, blue light does not cause an increase in amplitude of *ELF4*, *TOC1*, or *PRR5* expression in *rve468* (Fig. 3.5, Fig. S3.5). We observed similar patterns when this experiment was conducted using the *rve4-1 rve6-1 rve8-1* T-DNA mutant (Fig. S3.4, Fig. S3.5). These data show that RVE function is required for the blue-light mediated enhancement of expression of a subset of clock genes, which may help explain the stronger period phenotype observed in *rve468* maintained in high-intensity blue compared to high-intensity red light (Fig. 3.4). Intriguingly, *ELF4*, *TOC1*, and *PRR5* are all direct targets of RVE8 transactivation activity[17].

Blue-specific *rve* mutant phenotypes are not due to differences in RVE protein abundance or degradation rate.

We hypothesized that the blue light-specific phenotypes observed in *rve* mutants might be due to higher *RVE* transcript levels in this condition. However, we did not observe any differences in *RVE4*, *RVE6*, or *RVE8* transcript abundance in plants maintained in constant red or blue light (Fig S6). We next assessed protein levels in the two conditions, making use of plants expressing epitope-tagged RVE4 or RVE8 under control of their native promoters. We focused on these two proteins because of the blue light-specific period responses in *rve48* and *rve468* mutants (Fig. S3.3). The *RVE8::RVE8-HA* transgene has previously been reported to rescue *rve8-1* phenotypes[106] and we similarly found that *RVE4::RVE4-FLAG* rescues RVE4 function in the *rve4-1* and *rve4-1 rve8-1* mutant backgrounds (Fig. S3.7). Seedlings were grown in various light conditions (monochromatic blue, monochromatic red, constant white light, 12:12 light-dark cycles, or constant darkness), samples were collected at four-hour intervals, and proteins were extracted and detected by western blotting. We found that the pattern of both RVE4-FLAG and RVE8-HA abundance is similar across light conditions (Fig. 3.6A), but that abundance of both proteins decreases rapidly in constant darkness (Fig. 3.6A, Fig. S3.8). However, RVE4-FLAG and RVE8-HA abundance is similar between monochromatic blue and monochromatic red light (Fig. 3.6A, Fig. S3.8), indicating that the stronger *rve* phenotypes in blue light compared to red are not due to a difference in RVE protein levels.

For many activators of transcription, activity is tightly coupled to proteasome-mediated degradation[115–118]. Since RVE8 is a transcriptional activator of genes such as *PRR5*, *ELF4*, and *TOC1*[17], which have enhanced peak levels in blue light compared to red (Fig. 3.5, Fig. S3.4), we speculated that higher RVE activity in blue light might be accompanied by a decrease in protein degradation in this condition. To test this, we exposed seedlings expressing RVE4-FLAG or RVE8-HA to various light conditions (monochromatic blue, monochromatic red light, or constant darkness), applied cycloheximide (CHX) during the day or subjective night to inhibit translation of new proteins, and assessed RVE protein abundance over time by western blotting. RVE4-FLAG is a relatively stable protein

during both the day (ZT5) and subjective night (ZT17), and its degradation rate is not significantly different in plants maintained in monochromatic blue or red light at either time (Fig. 3.6B, Bayesian non-linear regression, 0.05 confidence interval). Similarly, there is no significant difference in RVE8-HA protein degradation rate between monochromatic blue and monochromatic red light during the day or the subjective night (Fig. 3.6B, Bayesian non-linear regression, 0.05 confidence interval). These data suggest that the observed differences in *rve* circadian phenotypes in plants maintained in red and blue light (Fig. 3.4, Fig. 3.5) are not due to a difference in RVE4 or RVE8 protein degradation in these conditions.

Blue-specific *rve* mutant phenotypes do not require *ZTL* or *HY5*.

We next hypothesized that the *rve468* blue-light specific phenotypes might be caused by interactions between the *RVEs* and a blue light-specific factor. Two such factors known to influence the circadian system are the blue-light photoreceptor ZTL and the blue-light stabilized transcription factor HY5. We first tested for a genetic interaction between *RVE8* and *ZTL* by assessing free-running circadian period in *rve8-1 ztl* double mutants and *rve8-1* and *ztl* single mutants in a range of fluence rates of monochromatic blue light. Both *rve8-1* and *ztl* have long-period phenotypes, and the period of *rve8-1 ztl* is additively longer than the single mutants (Fig. S3.9A). We also examined the degradation of RVE8-HA protein in a *ztl* mutant background and found no significant difference in protein degradation rate between monochromatic blue and monochromatic red light during the subjective night (Fig. S3.9B, Bayesian non-linear regression, 0.05 confidence interval). Bayesian analysis reveals that during the day the RVE8-HA protein degradation rate is faster in *ztl* mutants in red light than in blue light and also faster in blue light in wild type than in *ztl* mutants, suggesting that ZTL may normally promote RVE8 degradation in blue light (Fig. S3.9B, Bayesian non-linear regression, 0.05 confidence interval). However, the additive effects of the *rve8* and *ztl* mutations on circadian period (Fig. S3.9A) suggest that these proteins affect the circadian system via different mechanisms. Overall, these data suggest that an

interaction between *RVE8* and *ZTL* is not responsible for the observed blue light-specific phenotypes of *rve* mutants.

We next tested for a genetic interaction between *RVE4*, *RVE6*, *RVE8*, and *HY5* by examining the circadian and growth phenotypes of *rve468 hy5* mutants compared to *rve468* and *hy5*. In constant monochromatic blue light of moderate intensity, *hy5* has a significantly shorter period and *rve468* has a significantly longer period than Col-0 (Fig. 3.7A), consistent with previous observations[18,112]. Interestingly, *rve468 hy5* has a significantly longer period than Col-0 but a significantly shorter period than *rve468* (Fig. 3.7A), which suggests that the *RVEs* and *HY5* interact additively to regulate circadian period in monochromatic blue light. We next assessed blue-light mediated inhibition of hypocotyl elongation in these mutants. We found that the *rve468 hy5* hypocotyls are significantly longer than *rve468* hypocotyls at all light intensities (Fig. 3.7B). Moreover, the *rve468 hy5* slope is significantly flatter than that of Col-0, *rve468*, and *hy5* (two-way ANOVA and Tukey's post hoc test, $p < 0.01$), indicating that these quadruple mutant seedlings have lower sensitivity to blue light than the other genotypes. Similar to our findings for *RVE8* and *ZTL*, the additive interaction between *RVE4*, *RVE6*, *RVE8*, and *HY5* in these assays suggests that an interaction between the *RVEs* and *HY5* is not responsible for the observed blue light-specific phenotypes of *rve* mutants.

Discussion

Here we present new mutant alleles of *RVE4*, *RVE6*, and *RVE8* in various combinations and show that they have similar clock and growth phenotypes to the previously studied T-DNA alleles[17,18]. However, we find that the *rve6* truncation mutant has a circadian clock phenotype not seen for the *rve6* T-DNA allele and that the new, likely null, *rve468* mutant characterized here has a stronger circadian phenotype than the *rve4-1 rve6-1 rve8-1* T-DNA line we originally characterized[17]. These results are likely because the original *rve6-1* allele reduced rather than abolished *RVE6* expression. We believe that the single, double, and triple mutant CRISPR-Cas9-generated alleles we have generated will be extremely

useful in future studies, especially given that after generations of propagation the original *rve4-1 rve6-1 rve8-1* mutants have also regained moderate expression of *RVE4* and *RVE8* (Chapter 2).

Severity of *rve* growth and clock phenotypes depends on light quality and intensity.

Our detailed characterization of *rve* single, double, and triple mutants has allowed us to assess their relative importance for regulation of plant growth and the circadian clock. When examining phenotypes in monochromatic red and monochromatic blue light, we found it surprising that the severity of growth and clock phenotypes does not always match based on the light conditions. For example, all *rve* single mutants have a long-hypocotyl phenotype in lower levels of monochromatic blue light, particularly at 0.1 µmol m^{-2} s^{-1} (Fig. S3.2), but none of these mutants have a period phenotype in any of the tested fluence rates of blue light (Fig. 3.4). Similarly, all *rve* single mutants have significantly long hypocotyls in constant darkness (Fig. S3.2), but only *rve6* has a significantly long period in constant darkness (Fig. 3.4). With the double mutants, *rve46* has significantly long hypocotyls in 0.1 and 1 µmol m^{-2} s^{-1} monochromatic blue light (Fig. S3.2), but no period phenotype in those same light conditions (Fig. S3.3). Conversely, *rve48* has no hypocotyl phenotype in almost all tested light qualities and fluence rates (Fig. 3.3) but has a significantly long period in both monochromatic red and monochromatic blue light of 10 µmol m^{-2} s^{-1} and above (Fig. S3.3). These phenotypic differences suggest that the RVE proteins have separate functions in regulation of growth and the clock.

We also noted differences in the effects of loss of the *RVE*s on the sensitivity of photomorphogenesis and the circadian system to light. As noted above, the circadian period of both *rve48* and *rve468* increases with higher fluence rates of monochromatic blue light while that of wild type decreases (Fig. 3.4, Fig. S3.3). However, all the tested *rve* mutants respond similarly to wild type in the inhibition of hypocotyl elongation in both red and blue light (Fig. 3.3, Fig. S3.2). These results suggest that in addition to playing separable roles in control of photomorphogenesis and circadian clock

function, *RVE4*, *RVE6*, and *RVE8* are also separately involved in different photoreceptor signaling pathways to the clock.

Possible mechanisms underlying light quality-dependent regulation of *RVE* function.

Our initial hypothesis that the enhanced circadian period phenotype of *rve48* and *rve468* mutants in response to blue light (Fig. S3.3) might be due to increased RVE4 or RVE8 protein abundance in this condition proved incorrect (Fig. 3.6, Fig. S3.8). However, there may be a light quality-specific difference in *RVE* transcript instead of RVE protein. While the overall abundance of *RVE4*, *RVE6*, and *RVE8* transcript in Col-0 is similar in monochromatic blue and monochromatic red light (Fig. S3.6), alternative splicing of these transcripts could differ between light qualities. Alternative splicing of *RVE8* has been observed to be regulated in response to white light[119], and increased abundance of a particular *RVE8* isoform has been associated with increased amplitude of *RVE8* target gene expression[120]. Perhaps alternative splicing to produce this isoform is increased in monochromatic blue light compared to monochromatic red light, leading to the observed *ELF4* amplitude difference between these two light qualities (Fig. 3.5).

Another possibility is that the localization of RVE proteins could differ in blue and in red light. The nuclear localization of both RVE4 and RVE8 has been shown to increase in seedlings moved from 22°C to 4°C and subsequently decrease when the seedlings were moved back to 22°C[12]. RVE proteins might be primarily localized in the nucleus when exposed to monochromatic blue light but primarily localized in the cytoplasm under monochromatic red light. Increased nuclear localization in blue light conditions would allow for increased activation of *RVE* targets, which could account for the enhanced expression of RVE8 target genes in blue compared to red light seen in wild type but not in *rve468* (Fig. 3.5).

Finally, another possibility is that RVE4 and RVE8 interact with a blue-light specific signaling component that helps control clock period. Our genetic analysis suggests that the RVEs are not

specifically working with ZTL or HY5 in control of clock pace in blue light (Fig. S3.9, Fig. 3.7). However, a recent report has revealed roles for the clock protein PRR9 and the blue light photoreceptor CRY2 in circadian clock sensitivity to blue light[107]. It is possible that the RVEs act with these or other, yet unidentified factors, in the transduction of blue light signals to the circadian system.

Materials and Methods

Plant Materials

All plants used are in the Columbia (Col-0) wild-type background. Col *CCR2::LUC2* and *rve4-11 rve6-11 rve8-11 CCR2::LUC2* were generated as previously described (Chapter 2). The *rve4-11 rve6-11 rve8-11 CCR2::LUC2* mutant was then backcrossed to Col *CCR2::LUC2* to generate *rve4-11 CCR2::LUC2*, *rve6-11 CCR2::LUC2*, *rve8-11 CCR2::LUC2*, *rve4-11 rve6-11 CCR2::LUC2*, *rve4-11 rve8-11 CCR2::LUC2*, and *rve6-11 rve8-11 CCR2::LUC2* mutants. *RVE4::RVE4-FLAG rve4-1 CCR2::LUC+* and *RVE4::RVE4-FLAG rve4-1 rve8-1 CCR2::LUC+* were generated by transforming *rve4-1 CCR2::LUC+* and *rve4-1 rve8-1 CCR2::LUC+* respectively with *RVE4::RVE4-FLAG* via floral dip[76]. *RVE8::RVE8-HA rve8-1* was previously described[106]. Col *CCR2::LUC2* was crossed to *hy5* (SALK_096651)[121] to generate *hy5 CCR2::LUC2*. *rve4-11 rve6-11 rve8-11 hy5 CCR2::LUC+* was crossed to *rve4-11 rve6-11 rve8-11 CCR2::LUC2* to generate *rve4-11 rve6-11 rve8-11 hy5 CCR2::LUC2*. For Fig. S3.4, Col *CCR2::LUC+* and *rve4-1 rve6-1 rve8-1 CCR2::LUC+* are as previously described[24,106]. For Fig. S3.9, Col *CCR2::LUC+*, *rve8-1 CCR2::LUC+*, and *ztl-103 CCR2::LUC+* are as previously described[58,106]. The *rve8-1 ztl-103 CCR2::LUC+* mutant was generated by crossing *rve8-1 CCR2::LUC+* to *ztl-103 CCR2::LUC+*. *RVE8::RVE8-HA rve8-1 ztl-103* was generated by crossing *RVE8::RVE8-HA rve8-1* to *ztl-103 CCR2::LUC+*.

Plasmids

RVE4::RVE4-FLAG was created by first amplifying the *RVE4* genomic region using primers 5'-CGGCAAGTATCTCCATTAGAT-3' and 5'-AGAGCTTAAGTGTTCATGACC-3'. The amplified region, including

approximately 2kb upstream of the transcriptional start site, was cloned into pCR8 (Invitrogen, Carlsbad, CA), which was then recombined with pEarleyGate302 by Gateway cloning[78].

Genotyping

CRISPR-Cas9 alleles were identified through PCR amplification followed by Sanger sequencing, as previously described (Chapter 2). Mutant lines without Cas9 were selected for use in experiments. Homozygous mutants of all alleles used in this research were identified through PCR amplification of genomic DNA. Primers used for genotyping are included in Appendix V.

Growth Conditions

Seeds were surface sterilized with chlorine gas and stratified in the dark for 2-4 days at 4°C. For luciferase imaging, qRT-PCR, and western blotting seeds were plated on 1X Murashige and Skoog, 0.7% agar, 3% sucrose. Seedlings were entrained in light-dark cycles (12h light, 12h dark) under 50-60 µmol m^{-2} s^{-1} white light at 22°C for 6 days. For hypocotyl length assays, seeds were plated on 0.5X Murashige and Skoog, 0.7% agar and exposed to a 4-hour pulse of 50-60 µmol m^{-2} s^{-1} white light at 22°C to induce germination. Seedlings were then grown in the specified light conditions using monochromatic red and/or blue LEDs (XtremeLUX, Santa Clara, CA) at 22°C for 6 days. For flowering time and rosette growth assays, seeds were sown directly on soil and grown in light-dark cycles of the specified photoperiod under 150-200 µmol m^{-2} s^{-1} white light at 22°C.

***CCR2::LUC2* and *CCR2::LUC+* luciferase imaging**

Seedlings were sprayed with 3 mM D-luciferin, moved to the specified light conditions using red and/or blue LEDs (XtremeLUX, Santa Clara, CA), and imaged for 5-6 days under a cooled CCD camera (DU434-BV, Andor Technology, or iKon M-934, Andor Technology, or ORCA II ER CCD, Hamamatsu Photonics). Neutral density filters (Rosco Laboratories or LEE Filters) were used to generate the specified light intensities of monochromatic red, monochromatic blue, or red plus blue light (Fig. 3.4, Fig. S3.3).

Quantification of bioluminescence was performed using MetaMorph software (Molecular Devices) and circadian rhythms were analyzed with Biological Rhythm Analysis Software System (BRASS)[53].

qRT-PCR analysis

After entrainment, seedlings were exposed to constant 60 µmol m^{-2} s^{-1} monochromatic blue or red light under LEDs (XtremeLUX, Santa Clara, CA) at 22°C. Seedlings were moved at dawn (ZT0) and collected every 3 hours from ZT21 to ZT48 (Fig. 3.5, Fig. S3.6) or every 3 hours from ZT24 to ZT48 (Fig. S3.4). Sample preparation and qRT-PCR were performed as previously described[11] using a BioRad CFX96 thermocycler (Bio-Rad Laboratories, Hercules, CA). Relative expression and SEM values were obtained from the BioRad CFX96 software package, amplitudes were calculated using BioDare2[122]. Primers used for qRT-PCR are included in Appendix V.

Hypocotyl length assays

After 6 days of growth, seedlings were transferred to transparent sheets and scanned at 600 dpi. Hypocotyls were individually measured using ImageJ[83].

Flowering time analysis

Date of flowering was recorded as the day the inflorescence stem reached 1 cm long. At that time, rosette leaves were counted to determine flowering time by leaf number. Cauline leaves were not included.

Rosette leaf measurements

After 30 days of growth, rosette leaf 5 was transferred to transparent sheets and scanned at 600 dpi. Blade area and petiole length were measured using LeafJ[84].

Protein abundance assays

After entrainment, seedlings were exposed to constant darkness, constant 60 µmol m^{-2} s^{-1} monochromatic blue or red light under LEDs (XtremeLUX, Santa Clara, CA), or 50-60 µmol m^{-2} s^{-1} white light at 22°C. Seedlings were moved at dawn (time 0) and collected every 4 hours from time 0 to time 48

(RVE4-FLAG) or every 3 hours from 3 hours before dawn to time 33 (RVE8-HA). Samples were prepared and quantified as previously described[11]. Total protein was analyzed by western blotting using mouse monoclonal anti-FLAG M2-HRP antibody (Sigma-Aldrich, St. Louis, MO) for RVE4-FLAG and rat monoclonal anti-HA-HRP antibody (Roche, Basel, Switzerland) for RVE8-HA. Prometheus ProSignal Dura (Genesee Scientific, Rochester, NY) was used to generate peroxidase activity and a Chemidoc analyzer (Bio-Rad Laboratories, Hercules, CA) was used for detection. Membranes were re-probed with mouse anti-actin antibody and anti-mouse-HRP antibody to normalize between samples. Protein abundance was quantified using Image Lab software (Bio-Rad Laboratories, Hercules, CA).

Protein degradation assays

After entrainment, seedlings were moved at dawn (ZT0) to constant darkness or constant 60 µmol m^{-2} s^{-1} monochromatic blue or red light under LEDs (XtremeLUX, Santa Clara, CA) at 22°C. During the day (ZT5 or ZT7) or subjective night (ZT17 or ZT19), seedlings were treated with cycloheximide by submerging them in liquid 1X Murashige and Skoog, 3% sucrose, 200 uM cycloheximide on a shaker and collected 0, 1, 2, or 4 hours later. Samples were prepared and quantified as previously described[11], western blotting and protein quantification were performed as described above.

Statistical Analysis and Data Visualization

All statistical analyses and data visualization were performed using R[85]. Figures were generated using the tidyverse[86], RColorBrewer[87], cowplot[88], gridExtra[89], glue[90], and ggtext[91] packages. Gene models were created using the genemodel package[92]. Linear mixed-effect models were used in one-way ANOVA and Tukey's post hoc tests. To compare flowering time and rosette growth differences between genotypes within each condition (LD or SD), used model "growth phenotype ~ genotype + (1|rep) + (1|flat)". To compare hypocotyl length differences between genotypes at each fluence rate, used model "length ~ genotype + (1|rep)". To compare period phenotype differences between genotypes at each fluence rate, used model "period ~ genotype + (1|rep)". Linear mixed-effect models were also used in two-way

ANOVA and Tukey's post hoc tests. To compare the effect of fluence rate on circadian period between genotypes, used model "period ~ genotype * fluence rate + (1|rep)". To compare the effect of fluence rate on hypocotyl length between genotypes, used model "length ~ genotype * fluence rate + (1|rep)". Modeling was done with the lme4[95] and lmerTest[96] packages, tests were performed using the lattice[97], broom[98], and emmeans[99] packages. Results were visualized with the multcomp[100] and multcompView[101] packages. Bayesian analysis for protein degradation was performed using the posterior[123] and brms[124] packages.

Accession Numbers

Accession numbers for *Arabidopsis thaliana* genes referenced here:

CCA1	AT4G16780
CRY2	AT1G04400
ELF3	AT2G25930
ELF4	AT2G40080
HY5	AT5G11260
LHY	AT1G01060
LUX	AT3G46640
PRR5	AT3G59060
PRR7	AT5G02810
PRR9	AT2G46790
RVE4	AT5G02840
RVE6	AT5G52660
RVE8	AT3G09600
TOC1	AT5G61380
ZTL	AT5G57360

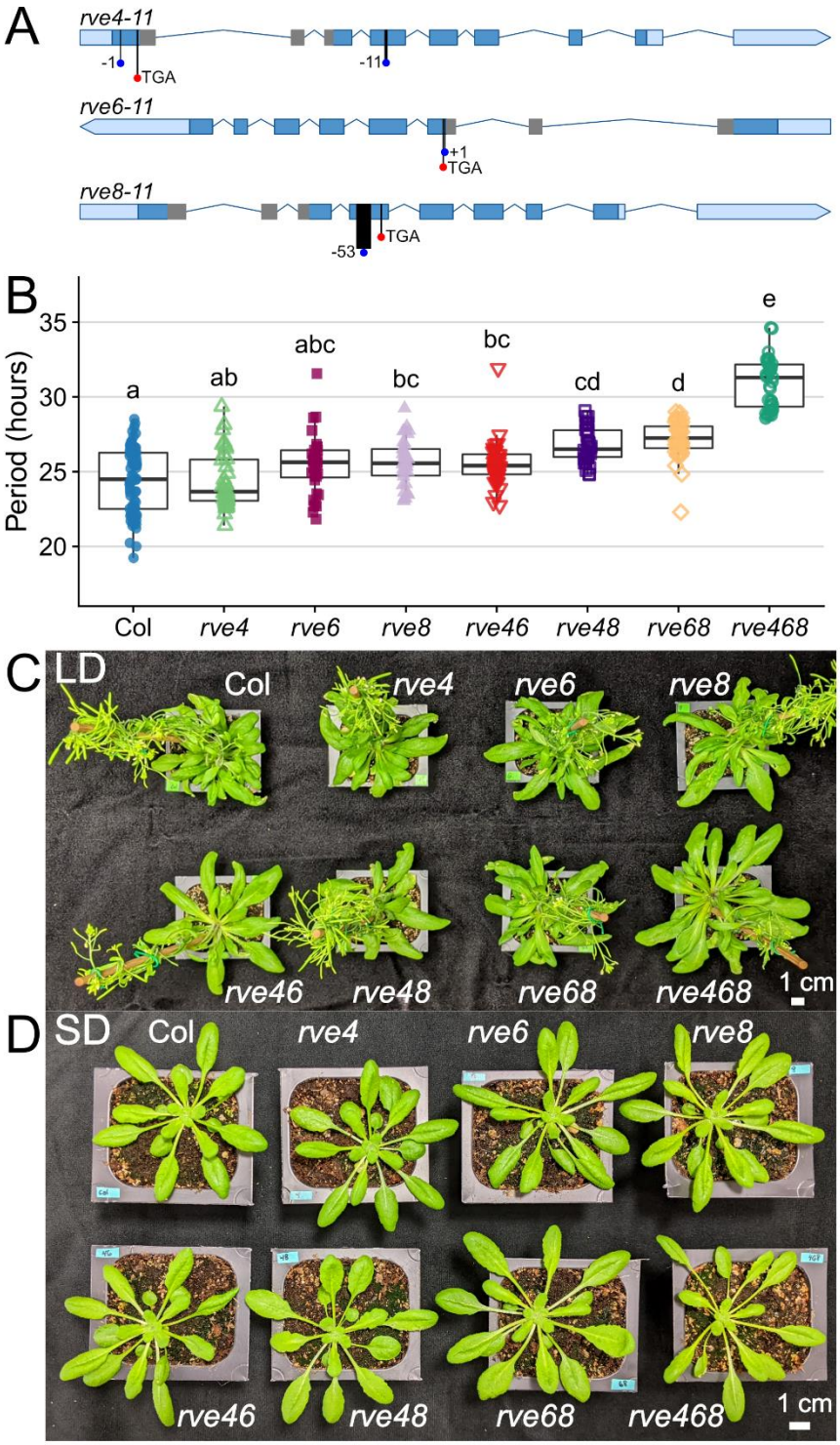

Figure 3.1: CRISPR-Cas9-generated *rve* mutants have phenotypes consistent with previously studied T-DNA *rve* mutants. (A) Gene models of *rve4-11*, *rve6-11*, and *rve8-11* alleles. Positions of insertions or deletions are shown by blue circles and positions of resulting premature stop codons are shown by red

circles. Light blue represents untranslated regions while dark blue represents coding regions. Gray shading represents the coding regions of the Myb-like DNA-binding domains. (B) Period estimates of rhythmic seedlings (RAE < 0.6) for the indicated genotypes were determined by monitoring *CCR2::LUC2* expression. After entrainment, seedlings were transferred to constant 50 µmol m^{-2} s^{-1} red plus 50 µmol m^{-2} s^{-1} blue light. Different letters denote significant differences between genotypes ($p < 0.05$), determined by one-way ANOVA followed by Tukey's post hoc test. The lines within the boxes are the medians, and the lower and upper hinges represent the first and third quartiles. Data from three trials (n = 10-25 per trial). (C – D) Representative images of plants grown for 35 days in (C) 16:8 light-dark cycles (LD) and (D) 8:16 light-dark cycles (SD).

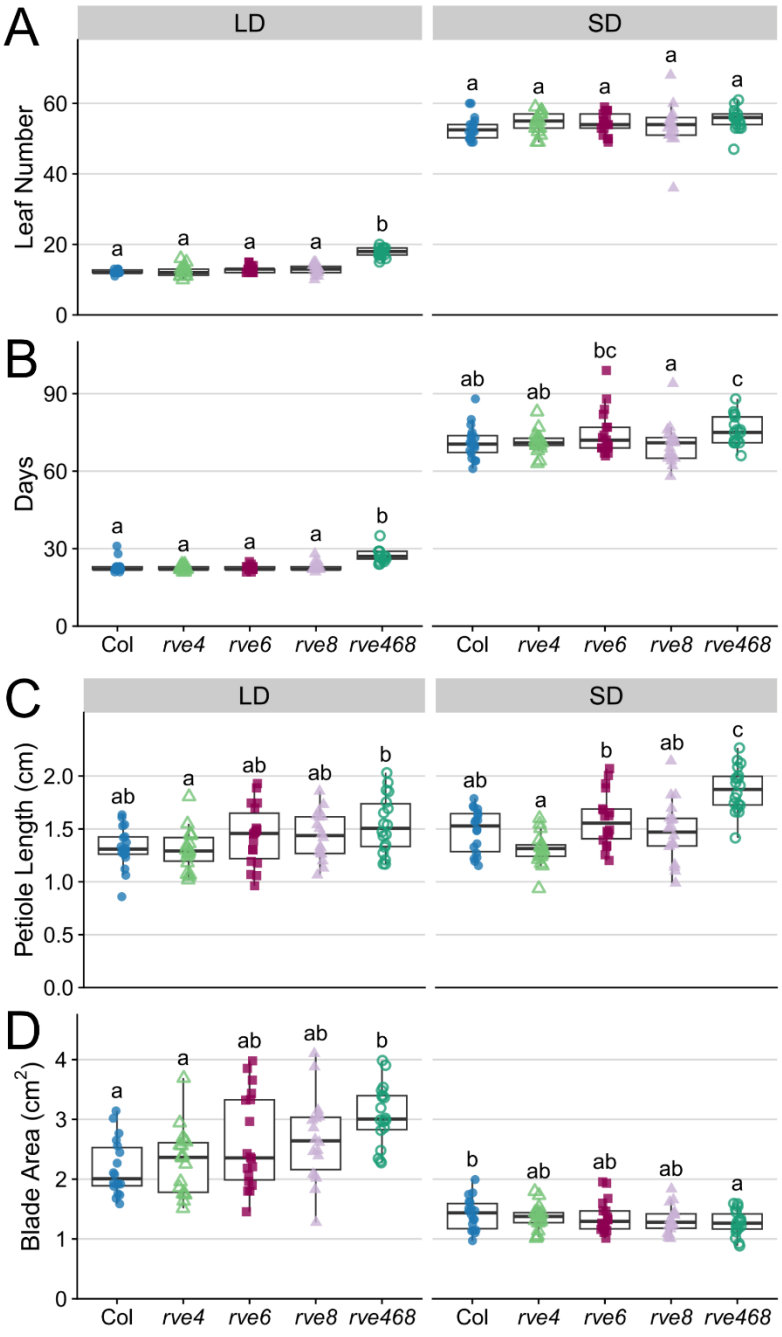

Figure 3.2: RVEs act redundantly to control flowering time and leaf growth. (A – B) Flowering times of the indicated genotypes were assessed by leaf number at bolting (A) and days to bolting (B). n = 17-18, experiment was conducted twice with similar results. (C – D) Petiole length (C) and blade area (D) of rosette leaf 5 of the indicated genotypes were assessed after 30 days of growth in the specified photoperiods. n = 18, experiment was conducted twice with similar results. (A – D) Plants were grown

under 150-200 µmol m^{-2} s^{-1} white light in the specified photoperiods (16:8 LD or 8:16 SD). Different letters denote significant differences between genotypes within each condition ($p < 0.05$), determined by one-way ANOVA followed by Tukey's post hoc test. The lines within the boxes are the medians, and the lower and upper hinges represent the first and third quartiles.

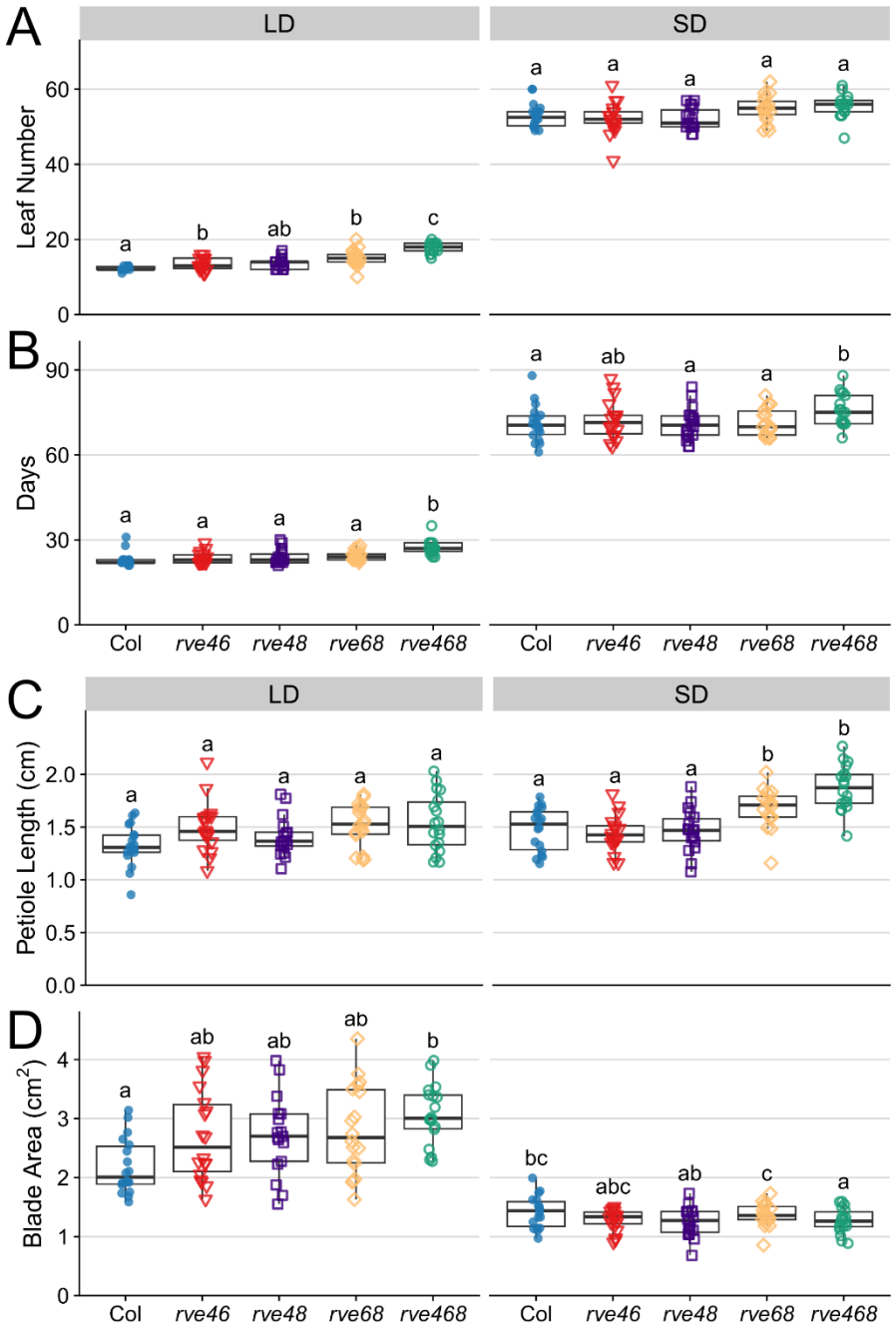

Figure S3.1: RVEs act redundantly to control flowering time and leaf growth. (A – B) Flowering time of the indicated genotypes was assessed by leaf number at bolting (A) and days to bolting (B). n = 17-18, experiment was conducted twice with similar results. (C – D) Petiole length (C) and blade area (D) of rosette leaf 5 of the indicated genotypes were assessed after 30 days of growth in the specified photoperiods. n = 17-18, experiment was conducted twice with similar results. (A – D) Plants were

grown under 150-200 µmol m^{-2} s^{-1} white light in the specified photoperiods (16:8 LD or 8:16 SD). Different letters denote significant differences between genotypes within each condition ($p < 0.05$), determined by one-way ANOVA followed by Tukey's post hoc test. The lines within the boxes are the medians, and the lower and upper hinges represent the first and third quartiles.

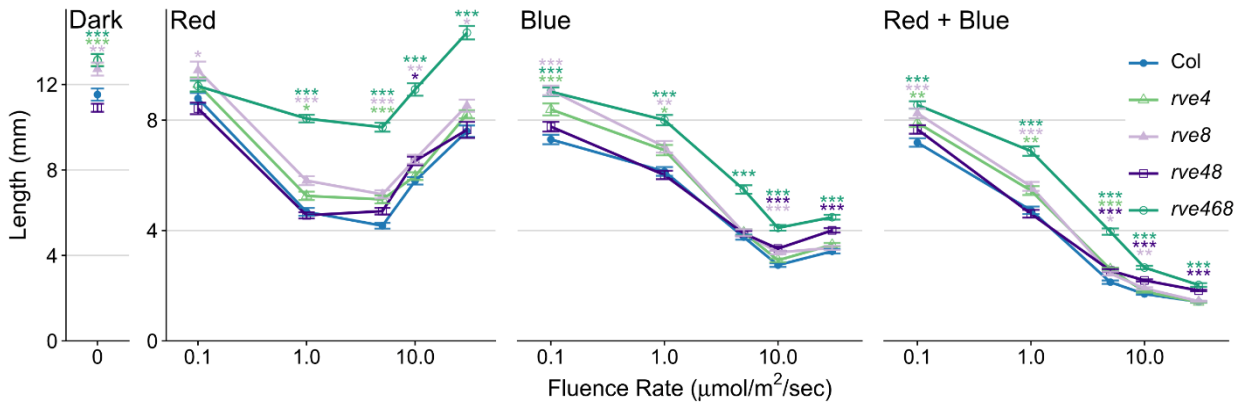

Figure 3.3: RVE4 and RVE8 have epistatic effects on hypocotyl elongation. Hypocotyl lengths of the indicated genotypes were determined in constant darkness or monochromatic red, monochromatic blue, or red plus blue light of the specified intensities (0.1-30 µmol m^{-2} s^{-1}). Points indicate mean hypocotyl lengths, error bars indicate ± SEM. Significant differences between genotypes determined by one-way ANOVA followed by Tukey's post hoc test (* $p < 0.05$, ** $p < 0.01$, *** $p < 0.001$). Data are from three (light conditions) or six (constant darkness) trials (n = 7-24 per trial).

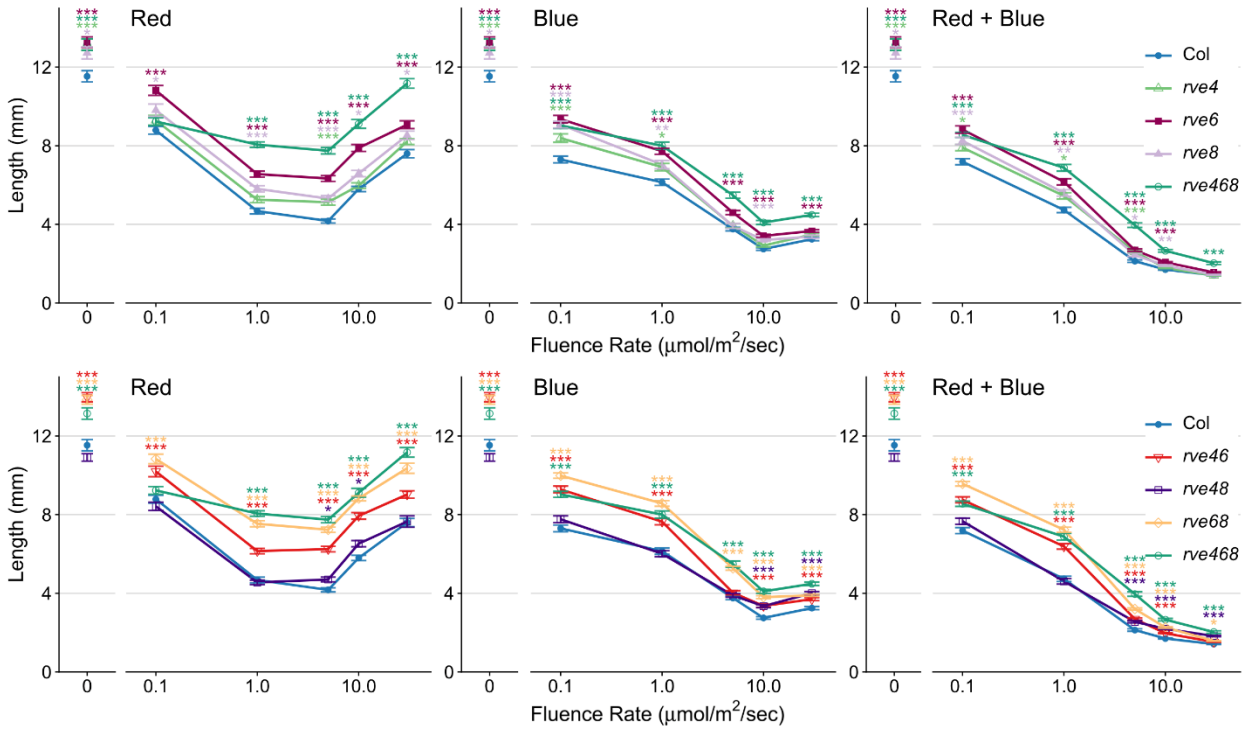

Figure S3.2: RVEs act redundantly and epistatically to control hypocotyl elongation. Hypocotyl lengths of the indicated genotypes were determined in the indicated light qualities and intensities. Seedlings were grown under constant darkness or monochromatic red, monochromatic blue, or red plus blue light of the specified intensities (0.1-30 µmol m^{-2} s^{-1}). Points indicate mean hypocotyl lengths, error bars indicate ± SEM. Significant differences between genotypes determined by one-way ANOVA followed by Tukey's post hoc test (* $p < 0.05$, ** $p < 0.01$, *** $p < 0.001$). Data are from three (light conditions) or six (constant darkness) trials (n = 7-24 per trial).

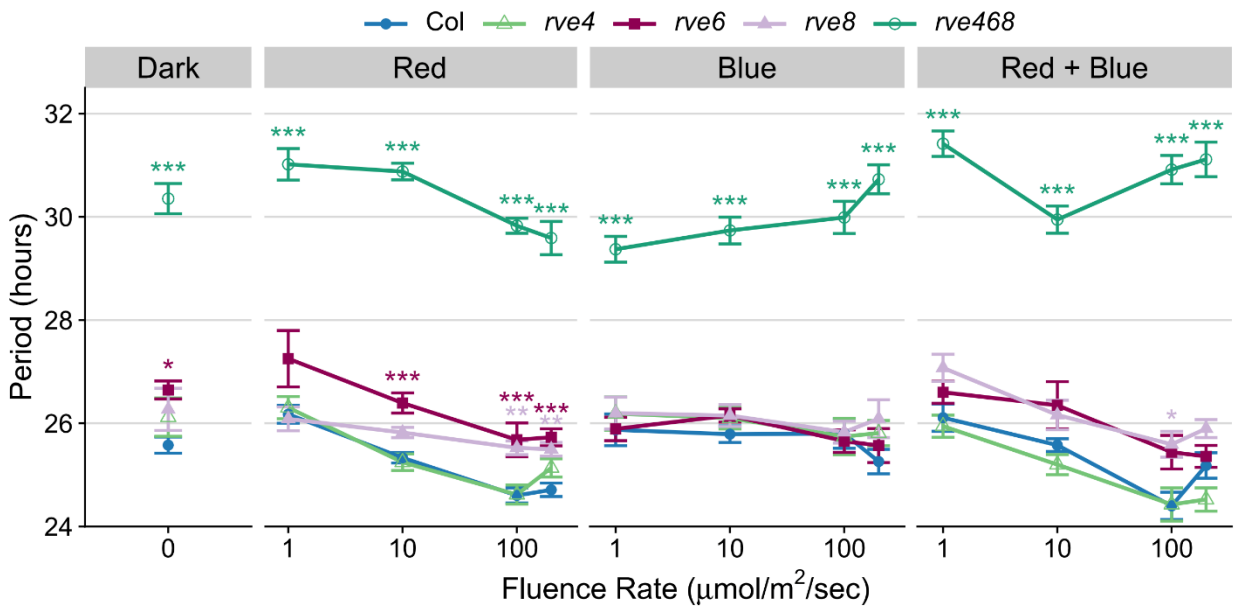

Figure 3.4: Increasing intensities of blue and red light have opposite effects on circadian period in *rve468* mutants. Period estimates of rhythmic seedlings (RAE < 0.6) for the indicated genotypes were determined in constant darkness or constant monochromatic red, monochromatic blue, or red plus blue light of the specified intensities (1-200 µmol m^{-2} s^{-1}) by monitoring *CCR2::LUC2* expression. Points indicate mean periods, error bars indicate ± SEM. Significant differences between genotypes determined by one-way ANOVA followed by Tukey's post hoc test (* $p < 0.05$, ** $p < 0.01$, *** $p < 0.001$). Data from three trials (n = 6-81 per trial).

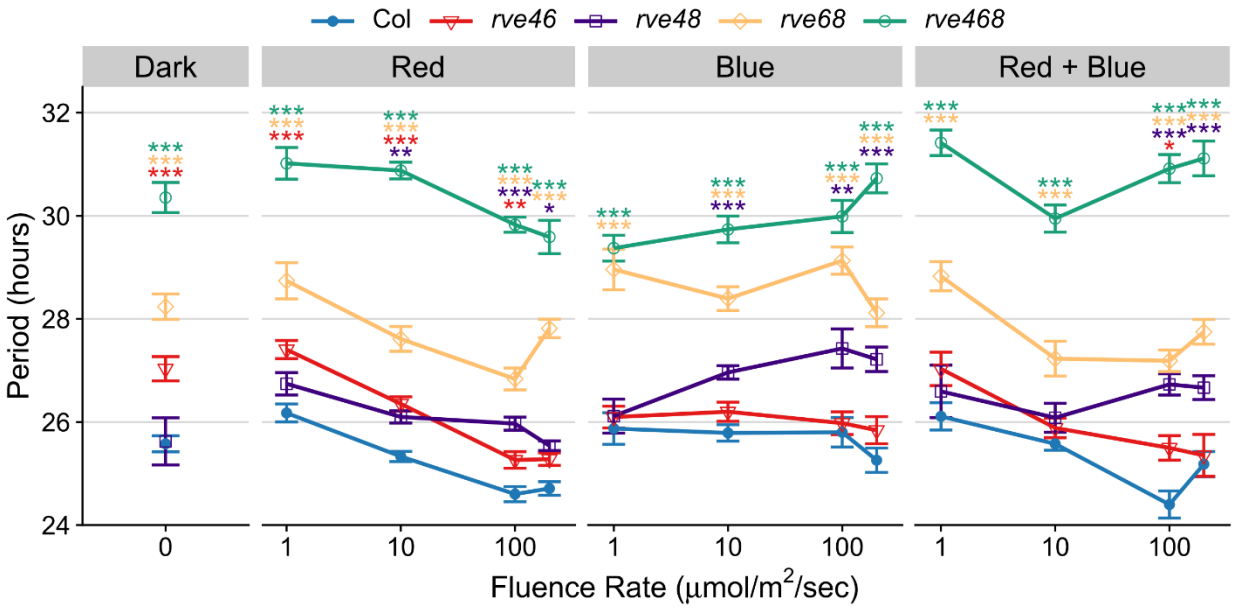

Figure S3.3: Increasing intensities of blue light lengthen but increasing intensities of red light shorten period in *rve468* and *rve48* mutants. Period estimates of rhythmic seedlings (RAE < 0.6) for the indicated genotypes were determined in constant darkness, constant monochromatic red, monochromatic blue, or red plus blue light of the specified intensities (1-200 µmol m^{-2} s^{-1}) by monitoring *CCR2::LUC2* expression. Points indicate mean period, error bars indicate ± SEM. Significant differences between genotypes determined by one-way ANOVA followed by Tukey's post hoc test (* $p < 0.05$, ** $p < 0.01$, *** $p < 0.001$). Data from three trials (n = 4-81 per trial).

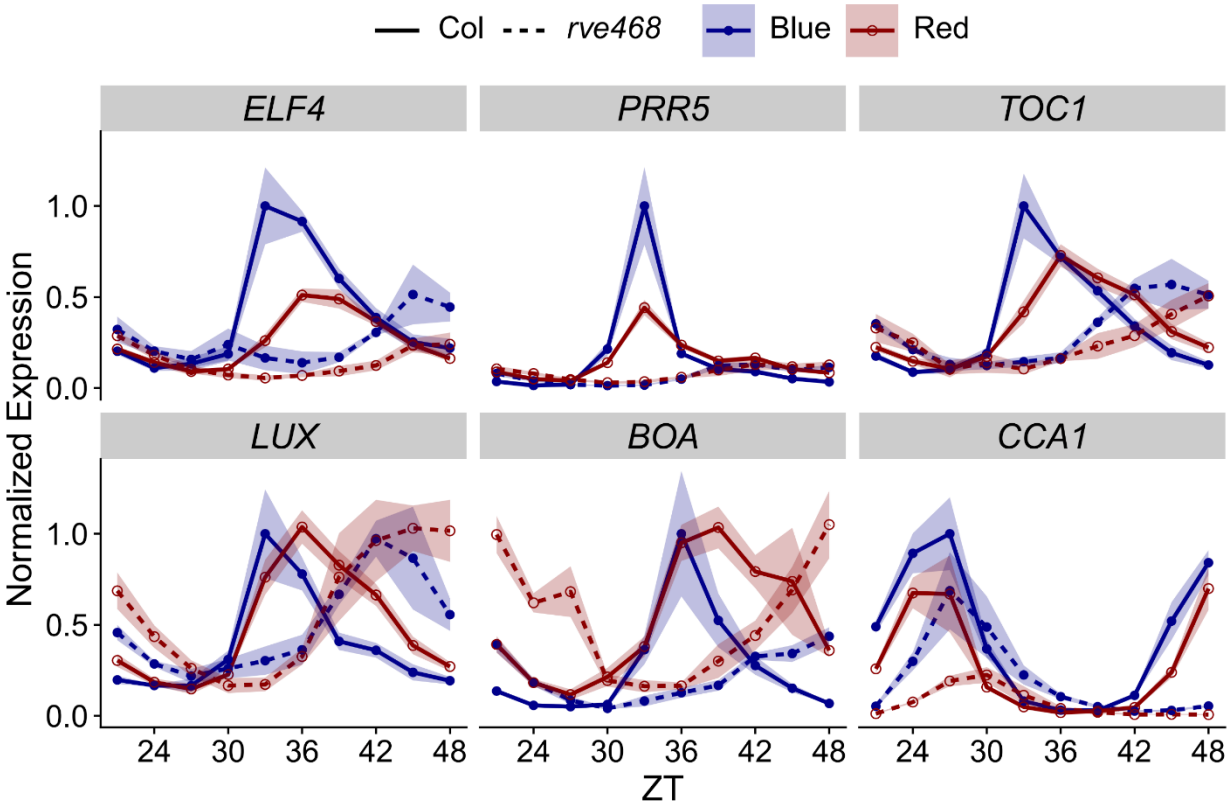

Figure 3.5: Blue-mediated enhancement of clock gene expression is reduced in *rve468* mutants. After entrainment, Col-0 and *rve4-11 rve6-11 rve8-11* seedlings were transferred at ZT0 to constant 60 µmol m^{-2} s^{-1} monochromatic blue or monochromatic red light. Expression of the specified genes was determined by qRT-PCR and normalized to reference genes *PP2A* and *IPP2*. Ribbon indicates ± SEM for three biological replicates.

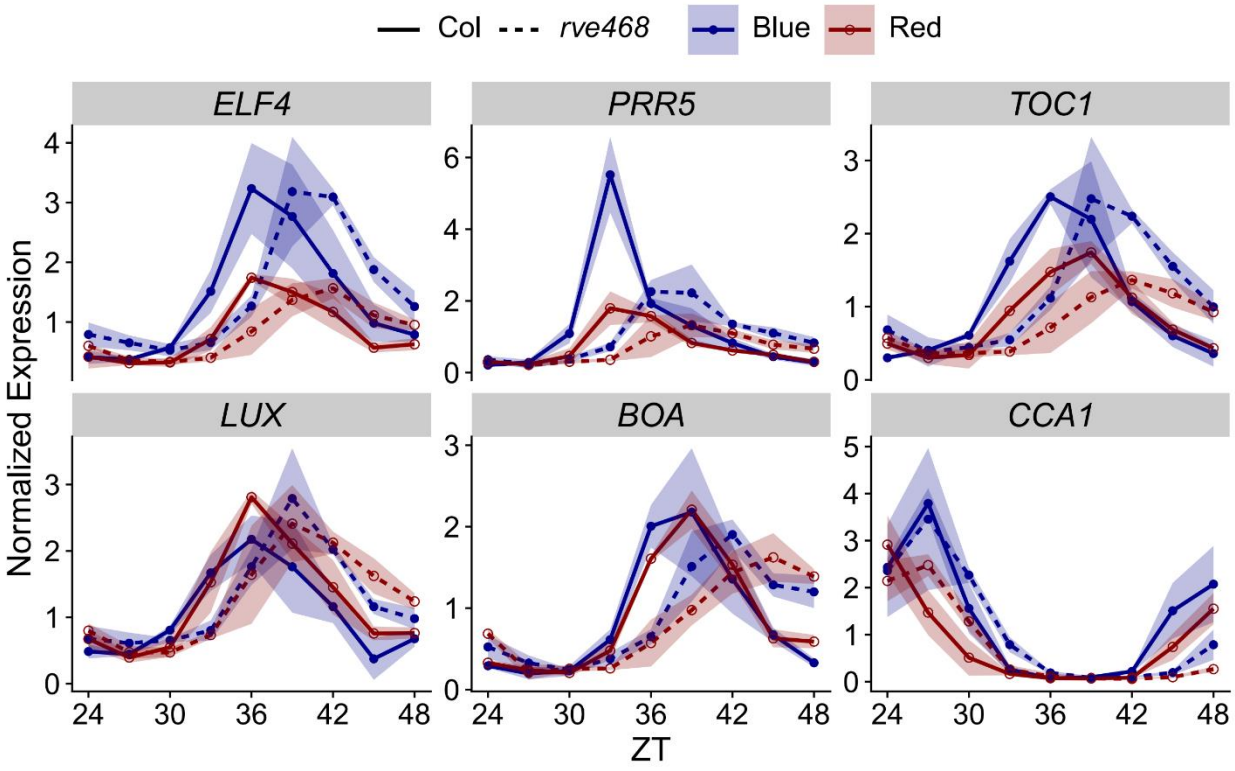

Figure S3.4: Amplitude of *PRR5* expression is reduced in T-DNA *rve468* mutants in monochromatic blue light. After entrainment, Col-0 and *rve4-1 rve6-1 rve8-1* seedlings were transferred at ZT0 to constant 60 µmol m^{-2} s^{-1} monochromatic blue or 60 µmol m^{-2} s^{-1} monochromatic red light. Expression of the specified genes was determined by qRT-PCR and normalized to reference gene *PP2A*. Ribbon indicates ± SEM for two biological replicates.

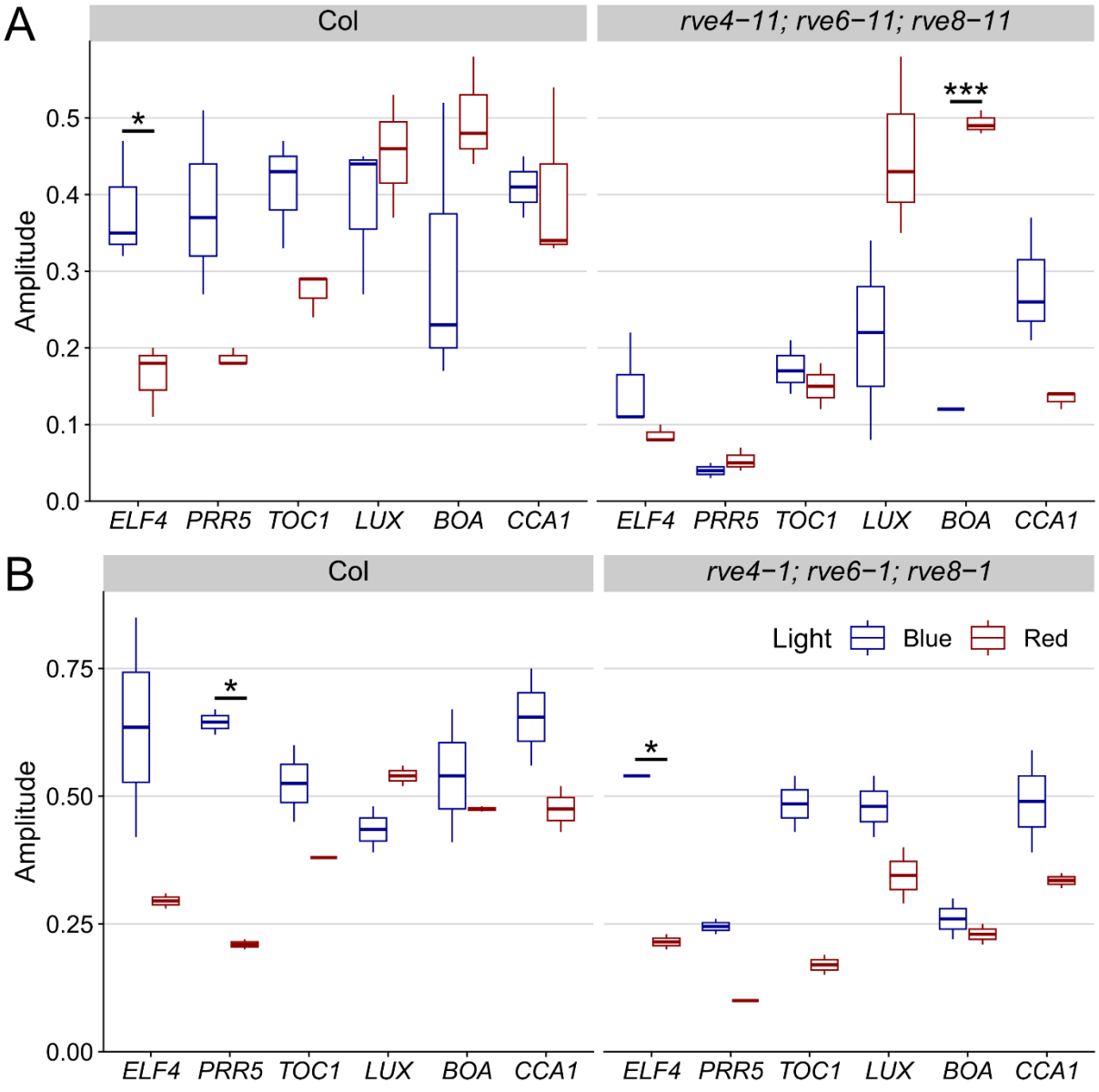

Figure S3.5: Amplitude of RVE target expression is reduced in *rve468* mutants in monochromatic blue light. (A – B) After entrainment, Col-0 and (A) *rve4-11 rve6-11 rve8-11* or (B) *rve4-1 rve6-1 rve8-1* seedlings were transferred at ZT0 to constant 60 µmol m^{-2} s^{-1} monochromatic blue or 60 µmol m^{-2} s^{-1} monochromatic red light. Expression of the specified genes was determined by qRT-PCR and normalized to reference genes (A) *PP2A* and *IPP2* or (B) *PP2A*. Amplitude was calculated by MFourFit using the first peak. Significant differences between light qualities determined by Student's t-test (* $p < 0.05$, ** $p <$

0.01, *** $p < 0.001$). The lines within the boxes are the medians, and the lower and upper hinges represent the first and third quartiles. Data from (A) three or (B) two biological replicates.

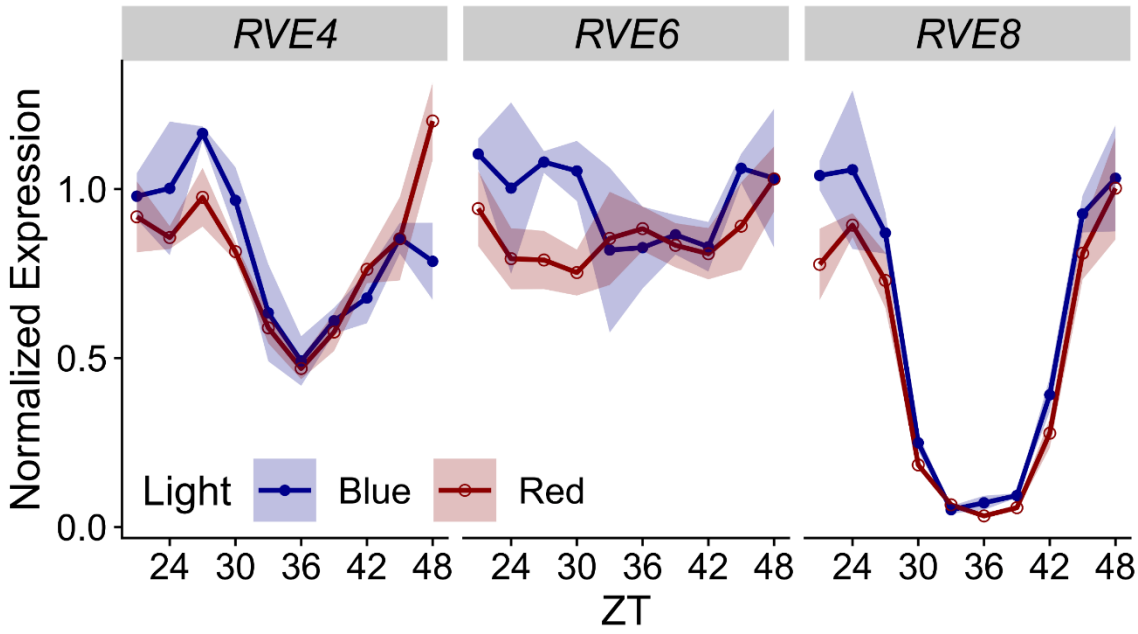

Figure S3.6: *RVE4*, *RVE6*, and *RVE8* expression levels are similar in monochromatic red and monochromatic blue light. After entrainment, Col-0 seedlings were transferred at ZT0 to constant 60 µmol m^{-2} s^{-1} monochromatic blue or 60 µmol m^{-2} s^{-1} monochromatic red light. Expression of the specified genes was determined by qRT-PCR and normalized to reference genes *PP2A* and *IPP2*. Ribbon indicates ± SEM for three biological replicates.

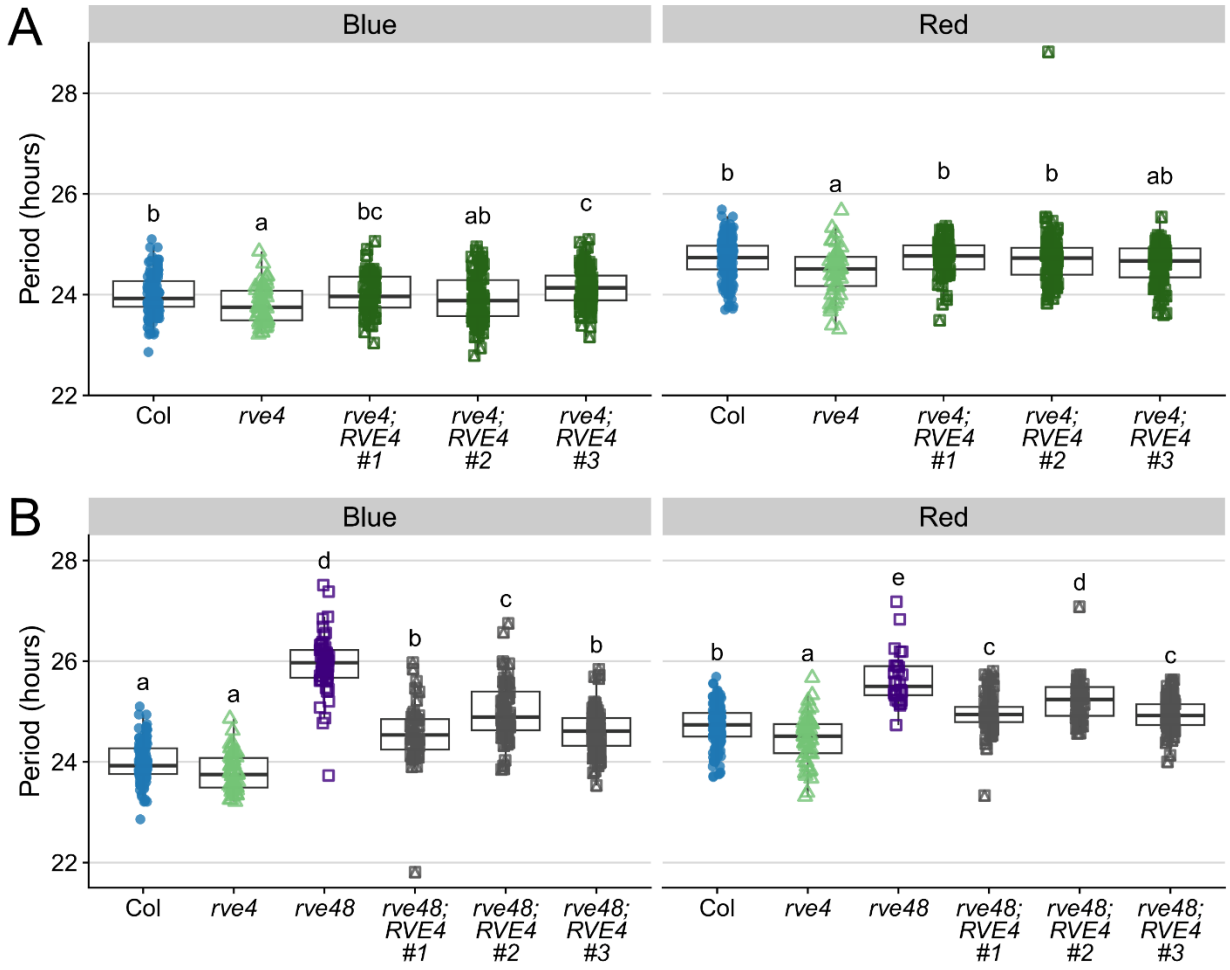

Figure S3.7: The *RVE4::RVE4-FLAG* transgene restores RVE4 activity. (A - B) Period estimates of rhythmic seedlings (RAE < 0.6) for the indicated genotypes were determined by monitoring *CCR2::LUC+* expression. Three independent lines of *RVE4::RVE4-FLAG* in the (A) *rve4-1* mutant background or (B) *rve4-1 rve8-1* mutant background were assessed for complementation. After entrainment, seedlings were transferred to constant 30 µmol m^{-2} s^{-1} monochromatic red or 30 µmol m^{-2} s^{-1} monochromatic blue light. Different letters denote significant differences between genotypes within each light quality ($p < 0.05$), determined by one-way ANOVA followed by Tukey's post hoc test. The lines within the boxes are the medians, and the lower and upper hinges represent the first and third quartiles. Data from two trials (n = 14-94 per trial).

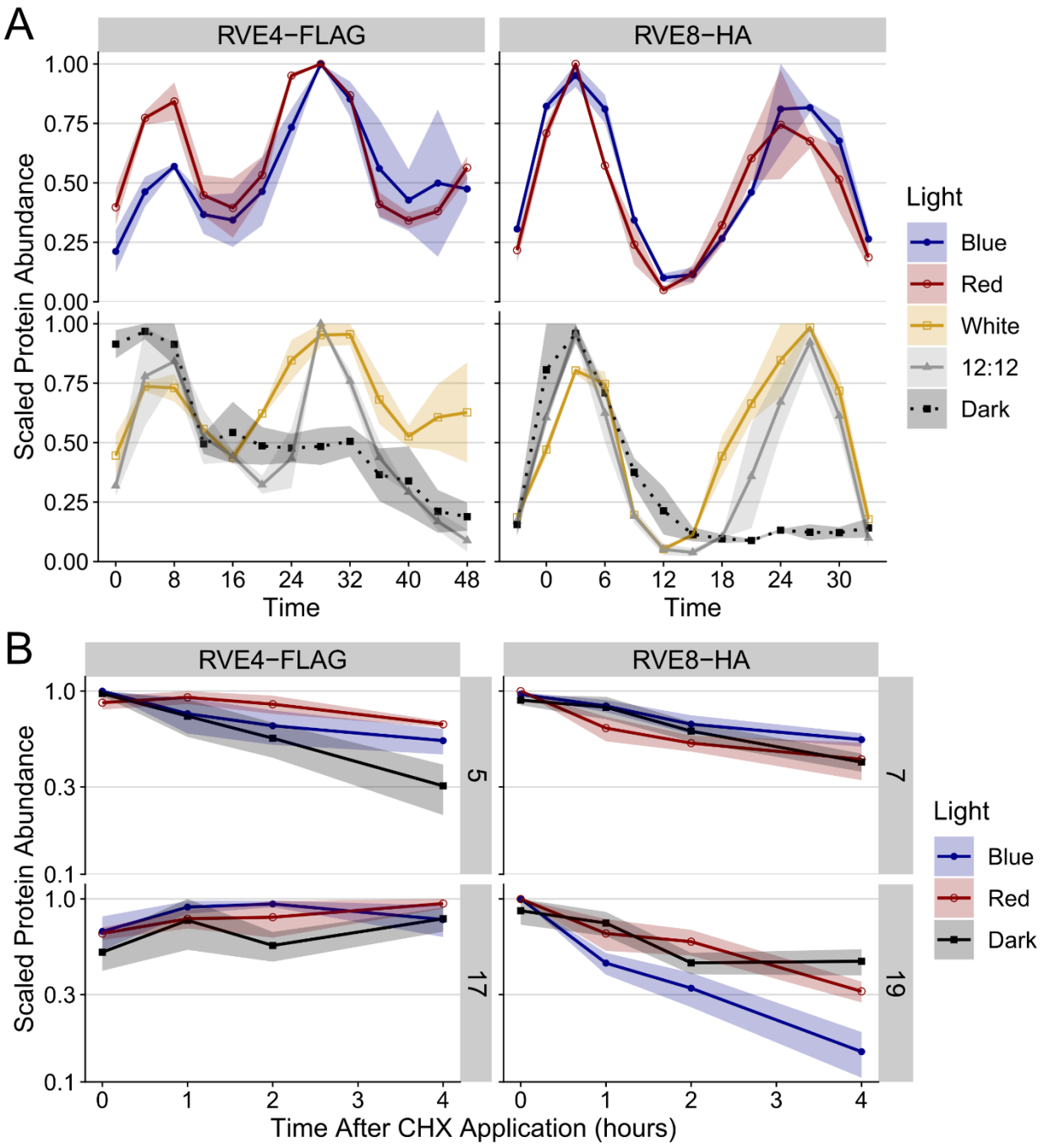

Figure 3.6: RVE4-FLAG and RVE8-HA protein abundance and degradation rates are similar in monochromatic red and monochromatic blue light. (A) After entrainment, seedlings were kept in 12:12 light-dark cycles under 50-60 µmol m^{-2} s^{-1} white light or transferred at time 0 to constant darkness, constant 50-60 µmol m^{-2} s^{-1} white, 60 µmol m^{-2} s^{-1} monochromatic blue, or 60 µmol m^{-2} s^{-1} monochromatic red light. Abundance of the specified proteins was determined by western blot and

normalized to abundance of actin. Ribbon indicates ± SEM for two biological replicates. (B) After entrainment, seedlings were transferred at ZT0 to constant darkness, 60 µmol m^{-2} s^{-1} monochromatic blue, or 60 µmol m^{-2} s^{-1} monochromatic red light. Seedlings were treated with cycloheximide (CHX) during the day (at ZT5 or ZT7) or during the subjective night (at ZT17 or ZT19). Abundance of the specified proteins was determined by western blot and normalized to abundance of actin. For RVE4-FLAG, ribbon indicates ± SEM for three biological replicates. For RVE8-HA, ribbon indicates ± SEM for seven biological replicates in blue, four biological replicates in red, and five biological replicates in dark.

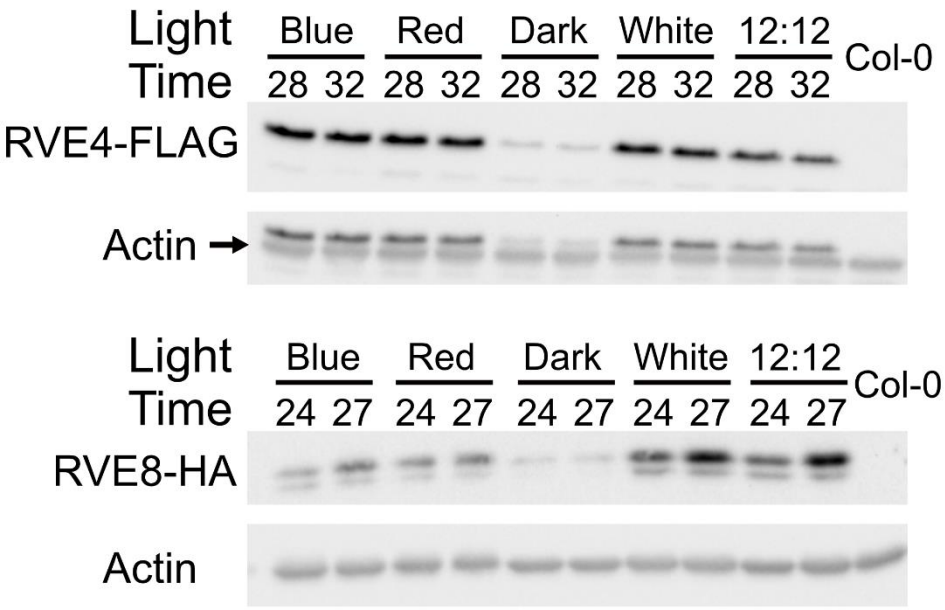

Figure S3.8: RVE4-FLAG and RVE8-HA have similar abundance in monochromatic red and monochromatic blue light. After entrainment, seedlings were kept in 12:12 light-dark cycles under 50-60 µmol m^{-2} s^{-1} white light or transferred at time 0 to constant darkness, constant 50-60 µmol m^{-2} s^{-1} white, 60 µmol m^{-2} s^{-1} monochromatic blue, or 60 µmol m^{-2} s^{-1} monochromatic red light. The specified proteins were visualized by western blotting.

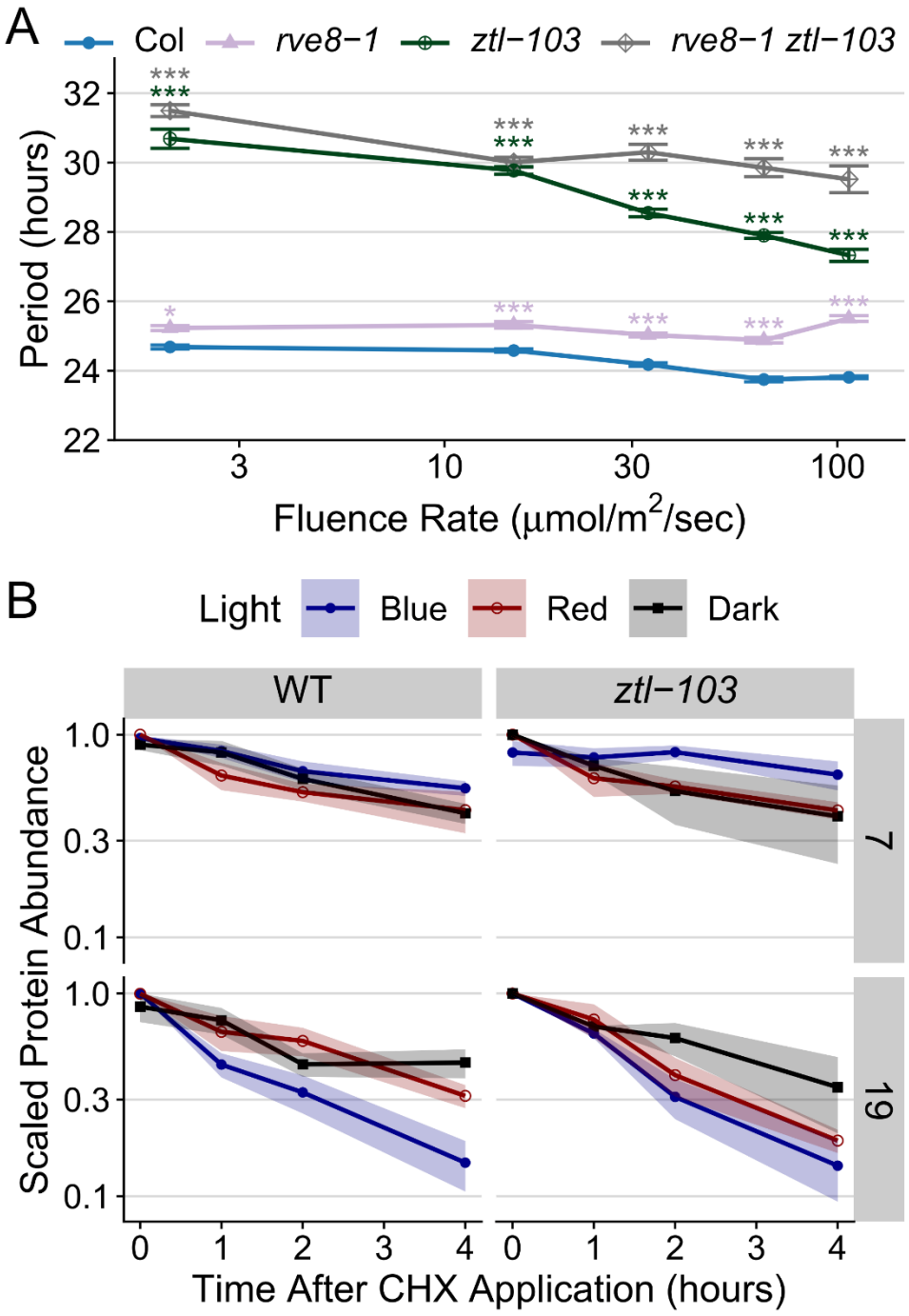

Figure S3.9: *RVE8* and *ZTL* interact additively to regulate circadian function. (A) Period estimates of rhythmic seedlings (RAE < 0.6) for the indicated genotypes were determined in different light intensities by monitoring *CCR2::LUC+* expression. After entrainment, seedlings were transferred to constant monochromatic blue light of the specified intensities (2-107 µmol m^{-2} s^{-1}). Points indicate mean period,

error bars indicate ± SEM. Significant differences between genotypes determined by one-way ANOVA followed by Tukey's post hoc test (* $p < 0.05$, ** $p < 0.01$, *** $p < 0.001$). Data from three trials (n = 9-41 per trial). (B) After entrainment, seedlings were transferred at ZT0 to constant darkness, 60 µmol m^{-2} s^{-1} monochromatic blue, or 60 µmol m^{-2} s^{-1} monochromatic red light. Seedlings were treated with cycloheximide (CHX) at ZT7 or ZT19. Abundance of RVE8-HA protein in the specified backgrounds was determined by western blot and normalized to abundance of actin. Wild-type data are the same as those presented in Fig. 6, ribbon indicates ± SEM for seven biological replicates in blue, four biological replicates in red, and five biological replicates in dark. For *ztl* background, ribbon indicates ± SEM for five biological replicates in blue and two biological replicates in red and dark.

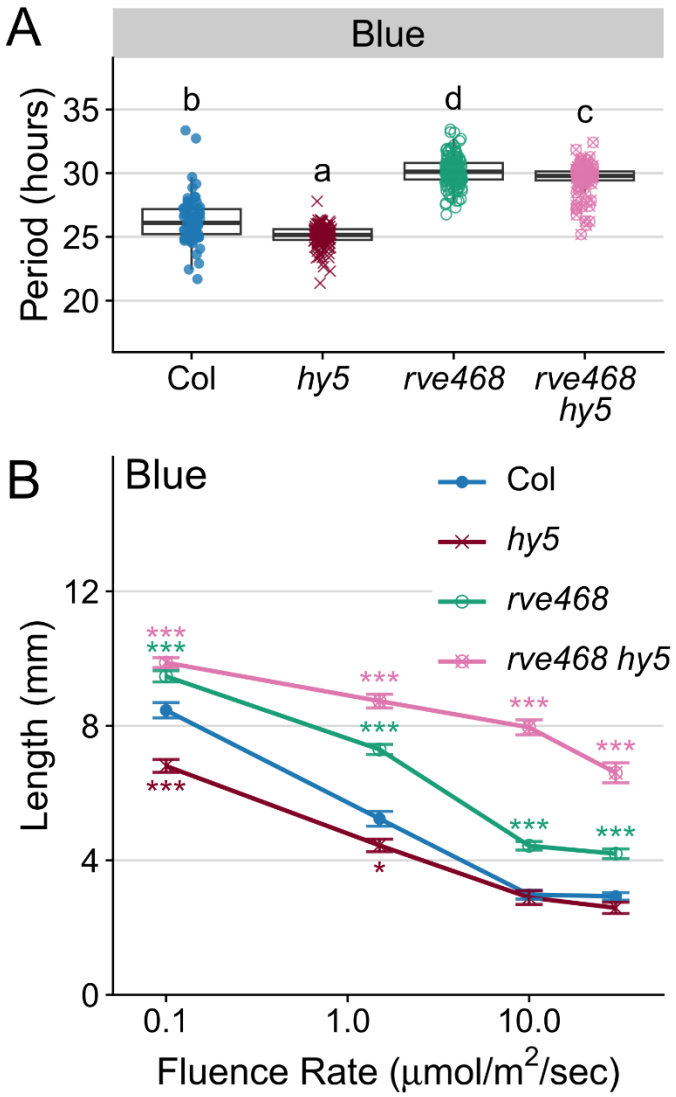

Figure 3.7: *RVE4*, *RVE6*, *RVE8*, and *HY5* interact additively to control clock function but epistatically to control hypocotyl elongation. (A) Period estimates of rhythmic seedlings (RAE < 0.6) for the indicated genotypes were determined by monitoring *CCR2::LUC2* expression. After entrainment, seedlings were transferred to constant 15 µmol m^{-2} s^{-1} monochromatic blue light. Different letters denote significant differences between genotypes ($p < 0.01$), determined by one-way ANOVA followed by Tukey's post hoc test. The lines within the boxes are the medians, and the lower and upper hinges represent the first and third quartiles. Data from two trials (n = 42-77 per trial). (B) Hypocotyl lengths of the indicated genotypes were determined in constant monochromatic blue light of the specified intensities (0.1-30

μmol m^{-2} s^{-1}). Points indicate mean hypocotyl length, error bars indicate ± SEM. Significant differences between genotypes determined by one-way ANOVA followed by Tukey's post hoc test (* $p < 0.05$, ** $p < 0.01$, *** $p < 0.001$). Data from two trials (n = 16-24 per trial).

Conclusions and Future Directions

I generated a null *cca1 lhy rve468* quintuple mutant and investigated its circadian and growth phenotypes. I hypothesized that *CCA1*, *LHY*, *RVE4*, *RVE6*, and *RVE8* would interact additively to regulate both circadian and growth phenotypes. I found that both *cca1 lhy rve468* and *cca1 lhy* have poor circadian rhythmicity in a range of light qualities and fluence rates and flower early in long and short day photoperiods. Together, my data suggest that *CCA1*, *LHY*, and the *RVEs* interact epistatically to regulate circadian phenotypes. However, *cca1 lhy rve468* mutant hypocotyl elongation and rosette leaf growth phenotypes are intermediate between those of *cca1 lhy* and *rve468* mutants and similar to wild-type plants, which suggests that *CCA1*, *LHY*, and the *RVEs* interact additively to regulate growth phenotypes. Overall, this study shows that a functional circadian oscillator is not required for near-normal phenotypes of clock-regulated outputs.

I additionally generated a new null *rve468* triple mutant and isolated all single and double mutants for characterization. My data suggest that the *RVEs* act synergistically in the regulation of flowering time, redundantly in the regulation of leaf growth, and antagonistically in the regulation of hypocotyl elongation. I also examined circadian phenotypes of these *rve* mutants in monochromatic red and monochromatic blue light and found that the mutants' period shortens in increasing fluence rates of red light, like wild type. However, the period of *rve468* and *rve48* mutants lengthens in increasing fluence rates of blue light, opposite from the wild-type response. Additionally, blue light-enhanced expression of several clock genes is reduced in *rve468* triple mutants. I hypothesized that these blue light-specific *rve* phenotypes are caused by light quality-specific differences in RVE protein abundance or degradation, but I found that both RVE protein abundance and degradation are similar between blue and red light. Furthermore, *ZTL* and *HY5*, which both have blue light-specific circadian functions, interact additively with the *RVEs* to regulate circadian phenotypes. Overall, this study shows that the *RVEs*

function separately within the circadian system and regulation of growth and that a novel mechanism controls *RVE* involvement in blue light-specific circadian function.

Do *RVE3* and *RVE5* have similar roles regulating the clock and growth as *RVE4*, *RVE6*, and *RVE8*?

Together, *RVE4*, *RVE6*, and *RVE8* were initially identified as transcriptional activators within the *Arabidopsis thaliana* circadian clock[24]. However, *REVEILLE 3* (*RVE3*) and *REVEILLE 5* (*RVE5*) are also Myb-like transcription factors that are closely related to these other *RVEs*, as well as *CCA1* and *LHY*. The period of a *rve34568* quintuple T-DNA mutant is longer than that of the *rve468* T-DNA triple mutant[55], suggesting that *RVE3* and *RVE5* also act with *RVE4*, *RVE6*, and *RVE8* to regulate the clock. Therefore, a *cca1 lhy rve34568* mutant would likely have more complete disruption of the clock feedback loops than the *cca1 lhy rve468* mutant studied here. Examining the phenotypes of a *cca1 lhy rve34568* septuple null mutant would enhance our understanding of the roles of these Myb-like transcription factors within the circadian oscillator as well as regulation of growth. I hypothesize that the *cca1 lhy rve34568* mutant will have poor circadian rhythms like *cca1 lhy rve468* and *cca1 lhy*, but growth phenotypes similar to *cca1 lhy rve468* and wild-type plants. This would suggest that *RVE3* and *RVE5* interact epistatically to *CCA1* and *LHY* to regulate circadian phenotypes and additively to regulate growth phenotypes, like *RVE4*, *RVE6*, and *RVE8*.

Is RVE protein preferentially localized in the nucleus in blue light but not red light?

While the overall abundance of RVE protein is not altered between monochromatic red and monochromatic blue light, the localization of these proteins may be light quality-dependent. Both RVE4 and RVE8 move into the nucleus in low-temperature conditions[12], and perhaps the RVEs also move preferentially into the nucleus under blue light. This would increase activation of RVE targets in blue light compared to red light and may account for the observed blue light-specific phenotypes of *rve* mutants. When assessing RVE protein abundance, we extracted protein from whole cells and did not

separately examine the nuclear and cytoplasmic fractions. Therefore, visualizing RVE localization *in vivo* and examining RVE association with target promoters in monochromatic blue and monochromatic red light may be informative for further investigation of light quality-dependent *RVE* regulation.

Acknowledgements

I would first like to thank Dr. Stacey Harmer for all her advice and support throughout my time in graduate school. She was always available to flesh out ideas and to problem solve when something unexpected happened, and her mentorship has been invaluable for helping me grow as a scientist.

Thank you to my thesis committee, Dr. Joanna Chiu and Dr. Siobhan Brady, for their helpful feedback on experimental analysis and the writing of my thesis.

A big thank you to everyone who contributed to this project. To Dr. Julin Maloof for the Bayesian analysis of protein degradation rate. To Dr. Yuyan An for verifying the *RVE4::RVE4-FLAG* plant lines, examining RVE4-FLAG protein degradation, and assessing *rve8 ztl* circadian phenotypes. To all the undergraduate students I've worked with, but especially Hongtao Qian for diligently measuring thousands of hypocotyls.

Thank you to the past and present members of the Harmer and Maloof labs for their suggestions and friendship. Thank you to Dr. Akiva Shalit-Kaneh and Dr. Roderick Kumimoto for teaching me how to work with plants and for passing on protocols. I am extra grateful to Veronica Thompson-Lim for being the best caffeine buddy and sounding board.

Finally, thank you to my family for their love and support over the years. An extra thank you to my husband, Clay Hughes, for his patience and help throughout this process, particularly during my last year while I was pregnant and after the birth of our twins.

References

1. Jabbur ML, Johnson CH. Spectres of Clock Evolution: Past, Present, and Yet to Come. *Front Physiol*. 2022;12. https://www.frontiersin.org/articles/10.3389/fphys.2021.815847

2. McClung CR. The Plant Circadian Oscillator. *Biology (Basel)*. 2019;8(1). doi:10.3390/biology8010014

3. Takahashi JS. Transcriptional architecture of the mammalian circadian clock. *Nat Rev Genet*. 2017;18(3):164-179. doi:10.1038/nrg.2016.150

4. Young MW, Kay SA. Time zones: a comparative genetics of circadian clocks. *Nat Rev Genet*. 2001;2(9):702-715. doi:10.1038/35088576

5. Rosbash M. The Implications of Multiple Circadian Clock Origins. *PLoS Biol*. 2009;7(3):e1000062-. https://doi.org/10.1371/journal.pbio.1000062

6. Dodd AN, Salathia N, Hall A, et al. Plant Circadian Clocks Increase Photosynthesis, Growth, Survival, and Competitive Advantage. *Science (1979)*. 2005;309(5734):630-633. doi:10.1126/science.1115581

7. McClung CR. Circadian Clock Components Offer Targets for Crop Domestication and Improvement. *Genes (Basel)*. 2021;12(3). doi:10.3390/genes12030374

8. Creux N, Harmer S. Circadian Rhythms in Plants. *Cold Spring Harb Perspect Biol*. 2019;11(9). doi:10.1101/cshperspect.a034611

9. Sanchez SE, Rugnone ML, Kay SA. Light Perception: A Matter of Time. *Mol Plant*. 2020;13(3):363-385. doi:10.1016/j.molp.2020.02.006

10. Hsu PY, Harmer SL. Wheels within wheels: the plant circadian system. *Trends Plant Sci*. 2014;19(4):240-249. doi:https://doi.org/10.1016/j.tplants.2013.11.007

11. Shalit-Kaneh A, Kumimoto RW, Filkov V, Harmer SL. Multiple feedback loops of the Arabidopsis circadian clock provide rhythmic robustness across environmental conditions. *Proceedings of the National Academy of Sciences*. 2018;115(27):7147-7152. doi:10.1073/pnas.1805524115

12. Kidokoro S, Hayashi K, Haraguchi H, et al. Posttranslational regulation of multiple clock-related transcription factors triggers cold-inducible gene expression in Arabidopsis. *Proceedings of the National Academy of Sciences*. 2021;118(10):e2021048118. doi:10.1073/pnas.2021048118

13. Pérez-García P, Ma Y, Yanovsky MJ, Mas P. Time-dependent sequestration of RVE8 by LNK proteins shapes the diurnal oscillation of anthocyanin biosynthesis. *Proceedings of the National Academy of Sciences*. 2015;112(16):5249-5253. doi:10.1073/pnas.1420792112

14. Chalker-Scott L. Environmental Significance of Anthocyanins in Plant Stress Responses. *Photochem Photobiol*. 1999;70(1):1-9. doi:https://doi.org/10.1111/j.1751-1097.1999.tb01944.x

15. Li B, Gao Z, Liu X, Sun D, Tang W. Transcriptional Profiling Reveals a Time-of-Day-Specific Role of REVEILLE 4/8 in Regulating the First Wave of Heat Shock–Induced Gene Expression in Arabidopsis. *Plant Cell*. 2019;31(10):2353-2369. doi:10.1105/tpc.19.00519

16. Scandola S, Mehta D, Li Q, Rodriguez Gallo MC, Castillo B, Uhrig RG. Multi-omic analysis shows REVEILLE clock genes are involved in carbohydrate metabolism and proteasome function. *Plant Physiol*. 2022;190(2):1005-1023. doi:10.1093/plphys/kiac269

17. Hsu PY, Devisetty UK, Harmer SL. Accurate timekeeping is controlled by a cycling activator in Arabidopsis. Chory J, ed. *Elife*. 2013;2:e00473. doi:10.7554/eLife.00473

18. Gray JA, Shalit-Kaneh A, Chu DN, Hsu PY, Harmer SL. The REVEILLE Clock Genes Inhibit Growth of Juvenile and Adult Plants by Control of Cell Size. *Plant Physiol*. 2017;173(4):2308-2322. doi:10.1104/pp.17.00109

19. Spoelstra K, Wikelski M, Daan S, Loudon ASI, Hau M. Natural selection against a circadian clock gene mutation in mice. *Proceedings of the National Academy of Sciences*. 2016;113(3):686-691. doi:10.1073/pnas.1516442113

20. Ouyang Y, Andersson CR, Kondo T, Golden SS, Johnson CH. Resonating circadian clocks enhance fitness in cyanobacteria. *Proceedings of the National Academy of Sciences*. 1998;95(15):8660-8664. doi:10.1073/pnas.95.15.8660

21. Harmer SL, Kay SA. Positive and Negative Factors Confer Phase-Specific Circadian Regulation of Transcription in Arabidopsis. *Plant Cell*. 2005;17(7):1926-1940. doi:10.1105/tpc.105.033035

22. Alabadí D, Oyama T, Yanovsky MJ, Harmon FG, Más P, Kay SA. Reciprocal Regulation Between TOC1 and LHY/CCA1 Within the Arabidopsis Circadian Clock. *Science (1979)*. 2001;293(5531):880-883. doi:10.1126/science.1061320

23. Rawat R, Takahashi N, Hsu PY, et al. REVEILLE8 and PSEUDO-REPONSE REGULATOR5 Form a Negative Feedback Loop within the Arabidopsis Circadian Clock. *PLoS Genet*. 2011;7(3):e1001350-. https://doi.org/10.1371/journal.pgen.1001350

24. Hsu PY, Devisetty UK, Harmer SL. Accurate timekeeping is controlled by a cycling activator in Arabidopsis. Chory J, ed. *Elife*. 2013;2:e00473. doi:10.7554/eLife.00473

25. Kamioka M, Takao S, Suzuki T, et al. Direct Repression of Evening Genes by CIRCADIAN CLOCK-ASSOCIATED1 in the Arabidopsis Circadian Clock. *Plant Cell*. 2016;28(3):696-711. doi:10.1105/tpc.15.00737

26. Nakamichi N, Kiba T, Henriques R, Mizuno T, Chua NH, Sakakibara H. PSEUDO-RESPONSE REGULATORS 9, 7, and 5 Are Transcriptional Repressors in the Arabidopsis Circadian Clock . *Plant Cell*. 2010;22(3):594-605. doi:10.1105/tpc.109.072892

27. Huang W, Pérez-García P, Pokhilko A, et al. Mapping the Core of the Arabidopsis Circadian Clock Defines the Network Structure of the Oscillator. *Science (1979)*. 2012;336(6077):75-79. doi:10.1126/science.1219075

28. Gendron JM, Pruneda-Paz JL, Doherty CJ, Gross AM, Kang SE, Kay SA. Arabidopsis circadian clock protein, TOC1, is a DNA-binding transcription factor. *Proceedings of the National Academy of Sciences*. 2012;109(8):3167-3172. doi:10.1073/pnas.1200355109

29. Adams S, Grundy J, Veflingstad SR, et al. Circadian control of abscisic acid biosynthesis and signalling pathways revealed by genome-wide analysis of LHY binding targets. *New Phytologist*. 2018;220(3):893-907. doi:https://doi.org/10.1111/nph.15415

30. Nagel DH, Doherty CJ, Pruneda-Paz JL, Schmitz RJ, Ecker JR, Kay SA. Genome-wide identification of CCA1 targets uncovers an expanded clock network in Arabidopsis. *Proceedings of the National Academy of Sciences*. 2015;112(34):E4802-E4810. doi:10.1073/pnas.1513609112

31. Hazen SP, Schultz TF, Pruneda-Paz JL, Borevitz JO, Ecker JR, Kay SA. LUX ARRHYTHMO encodes a Myb domain protein essential for circadian rhythms. *Proceedings of the National Academy of Sciences*. 2005;102(29):10387-10392. doi:10.1073/pnas.0503029102

32. Li G, Siddiqui H, Teng Y, et al. Coordinated transcriptional regulation underlying the circadian clock in Arabidopsis. *Nat Cell Biol*. 2011;13(5):616-622. doi:10.1038/ncb2219

33. Farinas B, Mas P. Functional implication of the MYB transcription factor RVE8/LCL5 in the circadian control of histone acetylation. *The Plant Journal*. 2011;66(2):318-329. doi:https://doi.org/10.1111/j.1365-313X.2011.04484.x

34. Davis W, Endo M, Locke JCW. Spatially specific mechanisms and functions of the plant circadian clock. *Plant Physiol*. 2022;190(2):938-951. doi:10.1093/plphys/kiac236

35. Niwa Y, Ito S, Nakamichi N, et al. Genetic Linkages of the Circadian Clock-Associated Genes, TOC1, CCA1 and LHY, in the Photoperiodic Control of Flowering Time in Arabidopsis thaliana. *Plant Cell Physiol*. 2007;48(7):925-937. doi:10.1093/pcp/pcm067

36. Nakamichi N, Kiba T, Kamioka M, et al. Transcriptional repressor PRR5 directly regulates clock-output pathways. *Proceedings of the National Academy of Sciences*. 2012;109(42):17123-17128. doi:10.1073/pnas.1205156109

37. Fornara F, Panigrahi KCS, Gissot L, et al. Arabidopsis DOF Transcription Factors Act Redundantly to Reduce CONSTANS Expression and Are Essential for a Photoperiodic Flowering Response. *Dev Cell*. 2009;17(1):75-86. doi:https://doi.org/10.1016/j.devcel.2009.06.015

38. Kardailsky I, Shukla VK, Ahn JH, et al. Activation Tagging of the Floral Inducer FT. *Science (1979)*. 1999;286(5446):1962-1965. doi:10.1126/science.286.5446.1962

39. Kobayashi Y, Kaya H, Goto K, Iwabuchi M, Araki T. A Pair of Related Genes with Antagonistic Roles in Mediating Flowering Signals. *Science (1979)*. 1999;286(5446):1960-1962. doi:10.1126/science.286.5446.1960

40. Nusinow DA, Helfer A, Hamilton EE, et al. The ELF4–ELF3–LUX complex links the circadian clock to diurnal control of hypocotyl growth. *Nature*. 2011;475(7356):398-402. doi:10.1038/nature10182

41. Zhang Y, Pfeiffer A, Tepperman JM, et al. Central clock components modulate plant shade avoidance by directly repressing transcriptional activation activity of PIF proteins. *Proceedings of the National Academy of Sciences*. 2020;117(6):3261-3269. doi:10.1073/pnas.1918317117

42. Martín G, Rovira A, Veciana N, et al. Circadian Waves of Transcriptional Repression Shape PIF-Regulated Photoperiod-Responsive Growth in Arabidopsis. *Current Biology*. 2018;28(2):311-318.e5. doi:https://doi.org/10.1016/j.cub.2017.12.021

43. Soy J, Leivar P, González-Schain N, et al. Molecular convergence of clock and photosensory pathways through PIF3–TOC1 interaction and co-occupancy of target promoters. *Proceedings of the National Academy of Sciences*. 2016;113(17):4870-4875. doi:10.1073/pnas.1603745113

44. Nozue K, Harmer SL, Maloof JN. Genomic Analysis of Circadian Clock-, Light-, and Growth-Correlated Genes Reveals PHYTOCHROME-INTERACTING FACTOR5 as a Modulator of Auxin Signaling in Arabidopsis . *Plant Physiol*. 2011;156(1):357-372. doi:10.1104/pp.111.172684

45. Franklin KA, Lee SH, Patel D, et al. PHYTOCHROME-INTERACTING FACTOR 4 (PIF4) regulates auxin biosynthesis at high temperature. *Proceedings of the National Academy of Sciences*. 2011;108(50):20231-20235. doi:10.1073/pnas.1110682108

46. Kunihiro A, Yamashino T, Nakamichi N, Niwa Y, Nakanishi H, Mizuno T. PHYTOCHROME-INTERACTING FACTOR 4 and 5 (PIF4 and PIF5) Activate the Homeobox ATHB2 and Auxin-Inducible IAA29 Genes in the Coincidence Mechanism Underlying Photoperiodic Control of Plant Growth of Arabidopsis thaliana. *Plant Cell Physiol*. 2011;52(8):1315-1329. doi:10.1093/pcp/pcr076

47. Sun J, Qi L, Li Y, Chu J, Li C. PIF4–Mediated Activation of YUCCA8 Expression Integrates Temperature into the Auxin Pathway in Regulating Arabidopsis Hypocotyl Growth. *PLoS Genet*. 2012;8(3):e1002594-. https://doi.org/10.1371/journal.pgen.1002594

48. Koini MA, Alvey L, Allen T, et al. High Temperature-Mediated Adaptations in Plant Architecture Require the bHLH Transcription Factor PIF4. *Current Biology*. 2009;19(5):408-413. doi:10.1016/j.cub.2009.01.046

49. Hornitschek P, Kohnen M V, Lorrain S, et al. Phytochrome interacting factors 4 and 5 control seedling growth in changing light conditions by directly controlling auxin signaling. *The Plant Journal*. 2012;71(5):699-711. doi:https://doi.org/10.1111/j.1365-313X.2012.05033.x

50. Alabadí D, Yanovsky MJ, Más P, Harmer SL, Kay SA. Critical Role for CCA1 and LHY in Maintaining Circadian Rhythmicity in Arabidopsis. *Current Biology*. 2002;12(9):757-761. doi:https://doi.org/10.1016/S0960-9822(02)00815-1

51. Más P, Alabadí D, Yanovsky MJ, Oyama T, Kay SA. Dual Role of TOC1 in the Control of Circadian and Photomorphogenic Responses in Arabidopsis[W]. *Plant Cell*. 2003;15(1):223-236. doi:10.1105/tpc.006734

52. Mizoguchi T, Wheatley K, Hanzawa Y, et al. LHY and CCA1 Are Partially Redundant Genes Required to Maintain Circadian Rhythms in Arabidopsis. *Dev Cell*. 2002;2(5):629-641. doi:https://doi.org/10.1016/S1534-5807(02)00170-3

53. Locke JCW, Southern MM, Kozma-Bognár L, et al. Extension of a genetic network model by iterative experimentation and mathematical analysis. *Mol Syst Biol*. 2005;1(1):2005.0013. doi:https://doi.org/10.1038/msb4100018

54. Hall A, Bastow RM, Davis SJ, et al. The TIME FOR COFFEE Gene Maintains the Amplitude and Timing of Arabidopsis Circadian Clocks[W]. *Plant Cell*. 2003;15(11):2719-2729. doi:10.1105/tpc.013730

55. Gray JA, Shalit-Kaneh A, Chu DN, Hsu PY, Harmer SL. The REVEILLE Clock Genes Inhibit Growth of Juvenile and Adult Plants by Control of Cell Size. *Plant Physiol*. 2017;173(4):2308-2322. doi:10.1104/pp.17.00109

56. Wang ZY, Tobin EM. Constitutive Expression of the CIRCADIAN CLOCK ASSOCIATED 1 (CCA1) Gene Disrupts Circadian Rhythms and Suppresses Its Own Expression. *Cell*. 1998;93(7):1207-1217. doi:https://doi.org/10.1016/S0092-8674(00)81464-6

57. Green RM, Tobin EM. Loss of the circadian clock-associated protein 1 in Arabidopsis results in altered clock-regulated gene expression. *Proceedings of the National Academy of Sciences*. 1999;96(7):4176-4179. doi:10.1073/pnas.96.7.4176

58. Martin-Tryon EL, Kreps JA, Harmer SL. GIGANTEA Acts in Blue Light Signaling and Has Biochemically Separable Roles in Circadian Clock and Flowering Time Regulation. *Plant Physiol*. 2007;143(1):473-486. doi:10.1104/pp.106.088757

59. Michael TP, Salomé PA, Yu HJ, et al. Enhanced Fitness Conferred by Naturally Occurring Variation in the Circadian Clock. *Science (1979)*. 2003;302(5647):1049-1053. doi:10.1126/science.1082971

60. Maeda AE, Nakamichi N. Plant clock modifications for adapting flowering time to local environments. *Plant Physiol*. 2022;190(2):952-967. doi:10.1093/plphys/kiac107

61. Song YH, Shim JS, Kinmonth-Schultz HA, Imaizumi T. Photoperiodic Flowering: Time Measurement Mechanisms in Leaves. *Annu Rev Plant Biol*. 2015;66(1):441-464. doi:10.1146/annurev-arplant-043014-115555

62. Dowson-Day MJ, Millar AJ. Circadian dysfunction causes aberrant hypocotyl elongation patterns in Arabidopsis. *The Plant Journal*. 1999;17(1):63-71. doi:https://doi.org/10.1046/j.1365-313X.1999.00353.x

63. Tao Y, Ferrer JL, Ljung K, et al. Rapid Synthesis of Auxin via a New Tryptophan-Dependent Pathway Is Required for Shade Avoidance in Plants. *Cell*. 2008;133(1):164-176. doi:10.1016/j.cell.2008.01.049

64. Steindler C, Matteucci A, Sessa G, et al. Shade avoidance responses are mediated by the ATHB-2 HD-zip protein, a negative regulator of gene expression. *Development*. 1999;126(19):4235-4245. doi:10.1242/dev.126.19.4235

65. Yakir E, Hilman D, Kron I, Hassidim M, Melamed-Book N, Green RM. Posttranslational Regulation of CIRCADIAN CLOCK ASSOCIATED1 in the Circadian Oscillator of Arabidopsis . *Plant Physiol*. 2009;150(2):844-857. doi:10.1104/pp.109.137414

66. Zhang C, Xie Q, Anderson RG, et al. Crosstalk between the Circadian Clock and Innate Immunity in Arabidopsis. *PLoS Pathog*. 2013;9(6):e1003370-. https://doi.org/10.1371/journal.ppat.1003370

67. Marshall CM, Tartaglio V, Duarte M, Harmon FG. The Arabidopsis sickle Mutant Exhibits Altered Circadian Clock Responses to Cool Temperatures and Temperature-Dependent Alternative Splicing. *Plant Cell*. 2016;28(10):2560-2575. doi:10.1105/tpc.16.00223

68. Yuan L, Yu Y, Liu M, et al. BBX19 fine-tunes the circadian rhythm by interacting with PSEUDO-RESPONSE REGULATOR proteins to facilitate their repressive effect on morning-phased clock genes. *Plant Cell*. 2021;33(8):2602-2617. doi:10.1093/plcell/koab133

69. Lu SX, Knowles SM, Andronis C, Ong MS, Tobin EM. CIRCADIAN CLOCK ASSOCIATED1 and LATE ELONGATED HYPOCOTYL Function Synergistically in the Circadian Clock of Arabidopsis . *Plant Physiol*. 2009;150(2):834-843. doi:10.1104/pp.108.133272

70. Xue W, Ruprecht C, Street N, et al. Paramutation-Like Interaction of T-DNA Loci in Arabidopsis. *PLoS One*. 2012;7(12):e51651-. https://doi.org/10.1371/journal.pone.0051651

71. Sandhu KS, Koirala PS, Neff MM. The ben1-1 Brassinosteroid-Catabolism Mutation Is Unstable Due to Epigenetic Modifications of the Intronic T-DNA Insertion. *G3 Genes|Genomes|Genetics*. 2013;3(9):1587-1595. doi:10.1534/g3.113.006353

72. Gao Y, Zhao Y. Epigenetic Suppression of T-DNA Insertion Mutants in Arabidopsis. *Mol Plant*. 2013;6(2):539-545. doi:https://doi.org/10.1093/mp/sss093

73. Osabe K, Harukawa Y, Miura S, Saze H. Epigenetic Regulation of Intronic Transgenes in Arabidopsis. *Sci Rep*. 2017;7(1):45166. doi:10.1038/srep45166

74. Helfer A, Nusinow DA, Chow BY, Gehrke AR, Bulyk ML, Kay SA. LUX ARRHYTHMO Encodes a Nighttime Repressor of Circadian Gene Expression in the Arabidopsis Core Clock. *Current Biology*. 2011;21(2):126-133. doi:https://doi.org/10.1016/j.cub.2010.12.021

75. Dixon LE, Knox K, Kozma-Bognar L, Southern MM, Pokhilko A, Millar AJ. Temporal Repression of Core Circadian Genes Is Mediated through EARLY FLOWERING 3 in Arabidopsis. *Current Biology*. 2011;21(2):120-125. doi:https://doi.org/10.1016/j.cub.2010.12.013

76. Clough SJ, Bent AF. Floral dip: a simplified method for Agrobacterium -mediated transformation of Arabidopsis thaliana. *The Plant Journal*. 1998;16(6):735-743. doi:https://doi.org/10.1046/j.1365-313x.1998.00343.x

77. Strayer C, Oyama T, Schultz TF, et al. Cloning of the Arabidopsis Clock Gene TOC1, an Autoregulatory Response Regulator Homolog. *Science (1979)*. 2000;289(5480):768-771. doi:10.1126/science.289.5480.768

78. Hartley JL, Temple GF, Brasch MA. DNA Cloning Using In Vitro Site-Specific Recombination. *Genome Res*. 2000;10(11):1788-1795. doi:10.1101/gr.143000

79. Concordet JP, Haeussler M. CRISPOR: intuitive guide selection for CRISPR/Cas9 genome editing experiments and screens. *Nucleic Acids Res*. 2018;46(W1):W242-W245. doi:10.1093/nar/gky354

80. Haeussler M, Schönig K, Eckert H, et al. Evaluation of off-target and on-target scoring algorithms and integration into the guide RNA selection tool CRISPOR. *Genome Biol*. 2016;17(1):148. doi:10.1186/s13059-016-1012-2

81. Xie K, Minkenberg B, Yang Y. Boosting CRISPR/Cas9 multiplex editing capability with the endogenous tRNA-processing system. *Proceedings of the National Academy of Sciences*. 2015;112(11):3570-3575. doi:10.1073/pnas.1420294112

82. Fauser F, Schiml S, Puchta H. Both CRISPR/Cas-based nucleases and nickases can be used efficiently for genome engineering in Arabidopsis thaliana. *The Plant Journal*. 2014;79(2):348-359. doi:https://doi.org/10.1111/tpj.12554

83. Schneider CA, Rasband WS, Eliceiri KW. NIH Image to ImageJ: 25 years of image analysis. *Nat Methods*. 2012;9(7):671-675. doi:10.1038/nmeth.2089

84. Maloof JN, Nozue K, Mumbach MR, Palmer CM. LeafJ: An ImageJ Plugin for Semi-automated Leaf Shape Measurement. *JoVE*. 2013;(71):e50028. doi:doi:10.3791/50028

85. R Core Team. R: A Language and Environment for Statistical Computing. Published online 2021. https://www.R-project.org/

86. Wickham H, Averick M, Bryan J, et al. Welcome to the tidyverse. *J Open Source Softw*. 2019;4(43):1686. doi:10.21105/joss.01686

87. Neuwirth E. RColorBrewer: ColorBrewer Palettes. Published online 2014. https://CRAN.R-project.org/package=RColorBrewer

88. Wilke CO. cowplot: Streamlined Plot Theme and Plot Annotations for ggplot2. Published online 2020. https://wilkelab.org/cowplot/

89. Auguie B. gridExtra: Miscellaneous Functions for "Grid" Graphics. Published online 2017. https://CRAN.R-project.org/package=gridExtra

90. Hester J, Bryan J. glue: Interpreted String Literals. Published online 2022. https://CRAN.R-project.org/package=glue

91. Wilke CO. ggtext: Improved Text Rendering Support for ggplot2. Published online 2020. https://wilkelab.org/ggtext/

92. Monroe JG. genemodel: Gene Model Plotting in R. Published online 2017. https://github.com/greymonroe/genemodel

93. Kassambara A. rstatix: Pipe-Friendly Framework for Basic Statistical Tests. Published online 2021. https://rpkgs.datanovia.com/rstatix/

94. Parsons R, Parsons R, Garner N, Oster H, Rawashdeh O. CircaCompare: a method to estimate and statistically support differences in mesor, amplitude and phase, between circadian rhythms. *Bioinformatics*. 2020;36(4):1208-1212. doi:10.1093/bioinformatics/btz730

95. Bates D, Mächler M, Bolker B, Walker S. Fitting Linear Mixed-Effects Models Using lme4. *J Stat Softw*. 2015;67(1):1-48. doi:10.18637/jss.v067.i01

96. Kuznetsova A, Brockhoff PB, Christensen RHB. lmerTest Package: Tests in Linear Mixed Effects Models. *J Stat Softw*. 2017;82(13):1-26. doi:10.18637/jss.v082.i13

97. Sarkar D. *Lattice: Multivariate Data Visualization with R*. Springer; 2008. http://lmdvr.r-forge.r-project.org

98. Robinson D, Hayes A, Couch S. broom: Convert Statistical Objects into Tidy Tibbles. Published online 2021. https://CRAN.R-project.org/package=broom

99. Lenth R V. emmeans: Estimated Marginal Means, aka Least-Squares Means. Published online 2022. https://github.com/rvlenth/emmeans

100. Hothorn T, Bretz F, Westfall P. Simultaneous Inference in General Parametric Models. *Biometrical Journal*. 2008;50(3):346-363.

101. Graves S, Piepho HP, with help from Sundar Dorai-Raj LS. multcompView: Visualizations of Paired Comparisons. Published online 2019. https://CRAN.R-project.org/package=multcompView

102. Seluzicki A, Burko Y, Chory J. Dancing in the dark: darkness as a signal in plants. *Plant Cell Environ*. 2017;40(11):2487-2501. doi:https://doi.org/10.1111/pce.12900

103. Aschoff J. Circadian Rhythms: Influences of Internal and External Factors on the Period Measured in Constant Conditions1. *Z Tierpsychol*. 1979;49(3):225-249. doi:https://doi.org/10.1111/j.1439-0310.1979.tb00290.x

104. Oakenfull RJ, Davis SJ. Shining a light on the Arabidopsis circadian clock. *Plant Cell Environ*. 2017;40(11):2571-2585. doi:https://doi.org/10.1111/pce.13033

105. Sanchez SE, Rugnone ML, Kay SA. Light Perception: A Matter of Time. *Mol Plant*. 2020;13(3):363-385. doi:https://doi.org/10.1016/j.molp.2020.02.006

106. Rawat R, Takahashi N, Hsu PY, et al. REVEILLE8 and PSEUDO-REPONSE REGULATOR5 Form a Negative Feedback Loop within the Arabidopsis Circadian Clock. *PLoS Genet*. 2011;7(3):e1001350-. https://doi.org/10.1371/journal.pgen.1001350

107. He Y, Yu Y, Wang X, Qin Y, Su C, Wang L. Aschoff's rule on circadian rhythms orchestrated by blue light sensor CRY2 and clock component PRR9. *Nat Commun*. 2022;13(1):5869. doi:10.1038/s41467-022-33568-3

108. Fujiwara S, Wang L, Han L, et al. Post-translational Regulation of the Arabidopsis Circadian Clock through Selective Proteolysis and Phosphorylation of Pseudo-response Regulator Proteins*. *Journal of Biological Chemistry*. 2008;283(34):23073-23083. doi:https://doi.org/10.1074/jbc.M803471200

109. Más P, Kim WY, Somers DE, Kay SA. Targeted degradation of TOC1 by ZTL modulates circadian function in Arabidopsis thaliana. *Nature*. 2003;426(6966):567-570. doi:10.1038/nature02163

110. Xiao Y, Chu L, Zhang Y, Bian Y, Xiao J, Xu D. HY5: A Pivotal Regulator of Light-Dependent Development in Higher Plants. *Front Plant Sci*. 2022;12. https://www.frontiersin.org/articles/10.3389/fpls.2021.800989

111. Gangappa SN, Botto JF. The Multifaceted Roles of HY5 in Plant Growth and Development. *Mol Plant*. 2016;9(10):1353-1365. doi:https://doi.org/10.1016/j.molp.2016.07.002

112. Hajdu A, Dobos O, Domijan M, et al. ELONGATED HYPOCOTYL 5 mediates blue light signalling to the Arabidopsis circadian clock. *The Plant Journal*. 2018;96(6):1242-1254. doi:https://doi.org/10.1111/tpj.14106

113. Más P, Devlin PF, Panda S, Kay SA. Functional interaction of phytochrome B and cryptochrome 2. *Nature*. 2000;408(6809):207-211. doi:10.1038/35041583

114. Guo H, Yang H, Mockler TC, Lin C. Regulation of Flowering Time by Arabidopsis Photoreceptors. *Science (1979)*. 1998;279(5355):1360-1363. doi:10.1126/science.279.5355.1360

115. Lipford JR, Deshaies RJ. Diverse roles for ubiquitin-dependent proteolysis in transcriptional activation. *Nat Cell Biol*. 2003;5(10):845-850. doi:10.1038/ncb1003-845

116. Muratani M, Tansey WP. How the ubiquitin–proteasome system controls transcription. *Nat Rev Mol Cell Biol*. 2003;4(3):192-201. doi:10.1038/nrm1049

117. Geng F, Tansey WP. Similar temporal and spatial recruitment of native 19S and 20S proteasome subunits to transcriptionally active chromatin. *Proceedings of the National Academy of Sciences*. 2012;109(16):6060-6065. doi:10.1073/pnas.1200854109

118. Zhai Q, Yan L, Tan D, et al. Phosphorylation-Coupled Proteolysis of the Transcription Factor MYC2 Is Important for Jasmonate-Signaled Plant Immunity. *PLoS Genet*. 2013;9(4):e1003422-. https://doi.org/10.1371/journal.pgen.1003422

119. Mancini E, Sanchez SE, Romanowski A, et al. Acute Effects of Light on Alternative Splicing in Light-Grown Plants. *Photochem Photobiol*. 2016;92(1):126-133. doi:https://doi.org/10.1111/php.12550

120. Yan T, Heng Y, Wang W, Li J, Deng XW. SWELLMAP 2, a phyB-Interacting Splicing Factor, Negatively Regulates Seedling Photomorphogenesis in Arabidopsis. *Front Plant Sci*. 2022;13. doi:10.3389/fpls.2022.836519

121. Chen H, Zhang J, Neff MM, et al. Integration of light and abscisic acid signaling during seed germination and early seedling development. *Proceedings of the National Academy of Sciences*. 2008;105(11):4495-4500. doi:10.1073/pnas.0710778105

122. Zielinski T, Moore AM, Troup E, Halliday KJ, Millar AJ. Strengths and Limitations of Period Estimation Methods for Circadian Data. *PLoS One*. 2014;9(5):e96462-. https://doi.org/10.1371/journal.pone.0096462

123. Bürkner PC, Gabry J, Kay M, Vehtari A. posterior: Tools for Working with Posterior Distributions. Published online 2022. https://mc-stan.org/posterior/

124. Bürkner PC. brms: An R Package for Bayesian Multilevel Models Using Stan. *J Stat Softw*. 2017;80(1):1-28. doi:10.18637/jss.v080.i01

125. Czechowski T, Stitt M, Altmann T, Udvardi MK, Scheible WR. Genome-Wide Identification and Testing of Superior Reference Genes for Transcript Normalization in Arabidopsis. *Plant Physiol*. 2005;139(1):5-17. doi:10.1104/pp.105.063743

126. Mockler TC, Yu X, Shalitin D, et al. Regulation of flowering time in Arabidopsis by K homology domain proteins. *Proceedings of the National Academy of Sciences*. 2004;101(34):12759-12764. doi:10.1073/pnas.0404552101

127. Martin-Tryon EL, Harmer SL. XAP5 CIRCADIAN TIMEKEEPER Coordinates Light Signals for Proper Timing of Photomorphogenesis and the Circadian Clock in Arabidopsis . *Plant Cell*. 2008;20(5):1244-1259. doi:10.1105/tpc.107.056655

Appendix I: Generation of a *cca1 lhy rve34568* septuple mutant

In chapter 2 I examined the interactions between *CIRCADIAN CLOCK ASSOCIATED 1* (*CCA1*), *LATE ELONGATED HYPOCOTYL* (*LHY*), *REVEILLE 4* (*RVE4*), *REVEILLE 6* (*RVE6*), and *REVEILLE 8* (*RVE8*) by studying the circadian and growth phenotypes of a likely null *cca1 lhy rve468* quintuple mutant. However, these Myb-like transcription factors are also closely related to *REVEILLE 3* (*RVE3*) and *REVEILLE 5* (*RVE5*), which act with *RVE4*, *RVE6*, and *RVE8* to regulate circadian phenotypes[55]. I therefore wanted to generate a *cca1 lhy rve34568* septuple mutant to further understand how these Myb-like transcription factors regulate the clock and growth.

To begin generating the septuple mutant, I started with the *cca1 lhy rve468 CCR2::LUC2* mutant described in chapter 2. I designed CRISPR-Cas9 guides targeting *RVE3* and *RVE5* using the CRISPOR algorithm[79,80] and created a 6X-*RVE*_pMR333 plasmid containing the guides and Cas9. Guide sequences are listed in Appendix III. The *6X-RVE*_pMR333 plasmid was created through Gateway cloning[78] between 6X-*RVE*_pEn-Chimera and pMR333 (generously donated by Dr. Mily Ron). I then transformed *cca1 lhy rve468 CCR2::LUC2* with 6X-*RVE*_pMR333 via floral dip[76]. T1 seeds were collected from twelve transformed pots (D5 – D16, Appendix VI). Transgenic plants were selected on media containing 30 mg/L Basta, then transferred to soil and allowed to self-pollinate. T2 seeds were collected from three T1 families (D1 – D4, Appendix VI) and are ready for screening.

In the future, T2 plants should be sequenced around the six guide locations to identify new *rve3* and *rve5* mutant alleles. Plants with mutations of interest should also be checked for the presence of Cas9. Ideally a T2 plant would be identified that lacks Cas9 and has mutations in both *RVE3* and *RVE5*, which could then be propagated to create the *cca1 lhy rve34568 CCR2::LUC2* mutant of interest.

Appendix II: Mutant allele sequences

***rve4-11* genomic sequence**

ATGACCTCAACCAATCCGGTGGTCGCCGAAGTAATACGGCGGAAACTTCTACAGATGCTACAGAGACGACGAT
TGCAACGACGGAAGCTGGTGAAGCACCGGAGAAGAAGGTGAGGAAAGCTTACACAATCACCAAGTCTAGAGA
GAGTTGGACTGAAGGAGAACACGACAAGTTTCTGGAAGCTCTTCAATTGTAATTTTACCGCGCTCTTTTTTTCTT
CCACCAGCTATTTGATTGACTGATTCTTTGTGTTTCGAGCTCTAATTTATAGCTGAATTTTGCGTAATTTCGCGTA
ATTTCTACTTAATTTGCTTAATCAGATCGAAGTTTGGTTATGTGGTAGATCATCTGGAGTTTTGCGTATGCAATT
GGATTTTGCAGAAGCAACAATGTCTTCTTTGATTTGTTAGGTTGGATTGTATATTCGATAGATCAGAATTTATAT
TAATCGCTGATGAATGTTTCTTCTCATAAAACCGAAGTATGGTTTAAGCTTATCTTAGGTTGCCAAAATGATTGA
GTAGAGGACTTGGCATCTGGTTTCTGCATAAATAGTGGTATTTTGCAGAAGTCGTATCTTTCTTTATTAAAAATG
TTTAACATGAGAACTGAAAAAACTTACTACAAGTCAGCTTTTAGAGCTATGCATGAAACCAATTTCCAACTACAG
TCCTAAACTACAATTCAGATTTTGGTAATGGTTCGTTACTTCCACATATTACATTGCTCTTTTGTGTGTGTGAAAG
GCTTCTCTCTCTTTTAGAAAAAAGAATCTTACTTTGTCCTGACAATTTTCTCGTGTCCTTAGGTTTGATCGTGACT
GGAAAAAGATAGAAGATTTTGTTGGTTCAAAGACAGTTATTCAGGTTTGAGATCAGCTTCTTTGGATTTTTGGTT
TAATATACAACCTTGGCACATTTCCCCACTCAATCATCCTGTGCCTGTTTGATTTACTGCAGATCAGGAGCCATGC
CCAAAAATACTTTCTAAAGGTCCAAAAAAATGGGACTTTAGCACATGTTCCACCCCCTAGGCCTAAGCGCAAAG
CTGCTCATCCATATCCTCAAAAGGCATCGAAAAATGGTTAGTTCTATTGTAATAGATATTACTTTGGGTTGACAG
ATGGAGTAACATGTAATCAATCTGATTTCAACTCAAATCTGCAGCTCAAATGTCGCTTCACGTTTCCATGTCCTTT
CCTACTCAAATAAATAACCTGCCTGGATATACTCGATACATCTGCATTGTTAAACATTGCTGTAAGTGGGGTTAT
TCCACCAGAAGATGAACTTGATACTCTTTGTGGAGCAGAAGGCATGCGTTCTCATCTGTACTCAGTTTTTATATT
TTGCTTTGGTAGTCTAGTCACTCTATCTTCTGAAGTTTTCATATGCTAAATGCGGCTTACATATCATTGTTTCAGTT
GATGTTGGATCAAATGACATGATAAGTGAAACTAGTCCTTCAGCATCTGGTATCGGAAGCTCAAGCAGAACACT
ATCAGATTCTAAGGGTTTGAGACTGGCGAAACAAGCTCCCTCAATGCATGGTAATTATCTGAACAATTGAGGGA
CTATTTCTTAGTTTTCATTTTGTGGTGGACGCTGTTGTAATGGTTGCTTTGCAGGTCTTCCTGATTTTGCTGAGGT
TTATAACTTCATTGGGAGTGTGTTCGATCCTGACAGCAAAGGCCGCATGAAAAAGCTCAAGGAAATGGATCCTA
TAAATTTCGAAACTGTGAGTTGGAGCTTTACTTGCCTTTAGATTAACTGATATGTGTGTTGCAGCATATCAATCA
TTTAGTCTTCTTCTTTGAGTTCCCGAATAAATTCAGCTGTGTGAGAAGATAAATATAAAGATCAGTACTTGCAAT
ATATAGATTCACGAGTTGGAAACACCAAAAAGCCAAAGTACCATGATTCTATGGAGATGTTGGTCAAATAATGG
GATTGTTACAACCATGAGTCAGTTTTAGGTGTCATGGTACCTATTTGTAGCTGTCAGTGATTGTTCTTTTTCCTAG
TATCCGTCACTAATCACAGTTTTTCTTGCAGGTTTTGCTGTTGATGAGAAACCTCACAGTGAACTTGTCAAACCCT
GACTTTGAACCTACTGTAAGTTATAATTTTATCATTACTTCTGTGCTCGTTGAGTATGTGAGGCACATTTGTCTTT
TCGTGATAAGAATGAGTGAGAAAAAGTCTCTAACAGCTAACAAACCTACTTACTATCTGCCTTGAAGTTTAACTA
TAGAAATTAAGACTAGTTCGCCTTTAGTGTGTTATGTTTTTAACCGTTCCAATGATTAAATGAGGATTGTTGTGC
TCTATGAGATATAATCTAACCATAATTTAGTCTGAATATGTTGATGCTGCAGAGGAAGGTCATGAACACTTAAG
CTCTTAG

***rve6-11* genomic sequence**

ATGGTCTCTAGAAATTCTGACGGATATTTCTTGGATCCGACCGGTATGACTGTTCCTGGTCTCGGACCTTCCTTT
ACAGCCGCCGTTTCTTCTTCTTCTTCACCAACGACTTCTTCTACGGCCGTGGCTGTGGCGGATGTGACGGCGATG
GTTTCTTCTTCGGAGGAGGATTTGAGTAAGAAGATTAGGAAGCCTTATACTATTACTAAGTCTAGAGAGAGCTG
GACGGAGCCTGAGCATGATAAATTCCTTGAAGCTCTTCAATTGTGAGTTTTGTTCATTTTGTGCTTTACCATTTCT
CGTTAATGGCTATTTGGAGATTTGATTTGGGAAGAATTAGCATCAATTTTGGTTGATTAGGGTTTGTGGTGGAC
TTTATAGAATCATGTGAATATGCGTGGAGTTTCGATTAGGATAATGTGCAACTTTATGTTTCAGTAGGTTTCTGA
ATTGTACTGTGTTGAACCAGTGGAATTAGATTGGATTTGGGACATAGAATTGGAATCGAGAGTTGGATTTAGG

CAGATGGATTTGGCTATGTATGCACATTTTGTTGAATTAGGCGTCTGATAAGAATTGAGAAGATCAGGATGTCG
AAAAATGAGTATAGACTGTATTGAATTTGTGTAGTAGCTATTGAAATTGGATGAGCTAAATGTTCTTCTAAGAC
CTGTATGATCATTGATAGTGAAGAACGAAACAGGCAAGAAATTGAGCTGAGATTATGAGGAAATAGCGACGCA
AACTATATGTATCTTAGTAAAAAGAGGATTTAGTGAAAACTATTAGAGCTGCGTTTTTTTTTTTTTTGGTTACAAT
AGTGTCTATAAACACTGGTAAGTGAGTAATTGTAGTACTAAGGTTGGTATGTAGTGGGAAAGTCCTTGGGGTA
GGTTCTAGGGGAGGCGATGATGATTGTACTGTTCATTGCTTATTCTTCTGTGTATTGTGATGCGTACAATCTTAG
GCAAGGATTAGACACATGCTATATCCAGGTTGTTTGGTGGTGGATCTGATATCTCTTATGTTTGTGTTTTGATTA
TTTTAGGTTTGATAGAGACTGGAAGAAGATTGAAGCTTTTATTGGTTCAAAGACAGTGATTCAGGTACAGTAAA
AAGTAGATATATCTTCTGAGTTACTCTGTTTTTCGCCTACTCTAGTTGTTTGATTCTGTCATCTTTCTCTTGGGCCC
TCAGTGTTACTTTGGATTGAGGTTGTTTTCTCTCATTTGATATCTCCACAAAGTGTTCTGTTAAAACATCTTTATTG
TCTGTAACTGTTTTGAACTACTACTACTAGGAGAAAGAATGTCACATGCGTTTGTCGCTTATCACCACTTAATGA
AGTGTTATATGTAGTTATTTTTGCATTAGACAAGTGAGCTCGTTGAGCTCTTTTATGGCTTCTTATACGGACTCCT
TTAATACTGCAGATACGAAGTCATGCTCAGAAGTATTTTCTTAAGGTACAAAAGAGTGGTGACCGGTGAACATC
TCCCTCCTCCTCGACCTAAAAGGAAAGCCGCTCATCCATATCCTCAGAAGGCTCACAAGAATGGTACGTTATAG
CTACTGCTTTAAAAACTTTGAAGTTGTATTGTTGTTTGCTTACTGAAAACTATATTGATGCACTGTTTATGGCAAT
GTGCAGTGCAACTGCAAGTACCAGGGTCATTCAAGTCAACATCTGAACCAAATGACCCAAGTTTTATGTTTAGG
CCTGAGTCTTCTTCAATGCTGATGACTTCGCCAACCACTGCTGCTGCGGCTCCATGGACAAATAATGCGCAAACA
ATTAGCTTCACTCCCCTCCCAAAAGGTTCTATTCTCATTTACAAGCATTATGCAATTACTGTTACTCTCTTAATATA
ATCTCTGTTTCAAATTTTACTAAATGAAGCATATTGTTGTTCCACGTTGATGGAAACAGCAGGAGCAGGAGCTA
ATAACAATTGTTCTAGTAGTTCTGAAAATACTCCAAGACCACGATCCAACAGGGACGCAAGAGACCATGGAAAT
GTTGGCCATTCATTAAGAGGTAAGCATCGTTACATCGTCTCCTGTTAATCTTTTTGTTTGTACCATATTTACCATTT
CTTACTAGACAGTTCCGCCTTTTTTTTTTTCAGTTTTACCGGACTTTGCCCAAGTATACGGCTTCATTGGAAGTGT
GTTTGACCCATATGCAAGTAATCATCTACAAAAGCTGAAGAAGATGGACCCCATAGATGTTGAAACAGTACGTT
TCTTGTCTTTTCAGTTTTCACTTTTACATCAATCTTAATTGAAACCACGTCGGTCCAATGGAACAAATGGTTAAAC
TAATCATTTTTTTCCTTTGTTTGCCCCCACCAAACAGGTGTTACTATTGATGAGAAATCTATCCATCAACTTGTCTA
GTCCTGACTTTGAGGATCATGTAAGTATTTTACTCCACAAACTACTAGTCAATTTTAACTCGAAACCCTATACCAG
AACTAACCTCAAGACTCTTATTGATTTCAAAAACAATAGAGACGGCTTCTTTCGTCTTATGATATCGGATCTGAG
ACAGCAACTGATCATGGTGGAGTGAATAAAACCTTAAACAAAGACCCACCTGAAATCTCTACTTAATGTTTAAT
AGAAGAGGAGAACTGTGAAAAGTGTCTCAGGTGAGCCAGCCAACAACCAGATGGCTACAAAATACAGAGATT
CTGTTGTGGTTTTTTGTTTGTACATAGGAAGAAGATGAAGCTGATGTTACTCGGTTTAGTTGTTGTTACTGTTAT
AAATAGTCTGTTGGGTTAAGGATGGTATATGTACAGTGTATTATCATAAGTTAGATCTCAAGTTTAAACATATGT
ATCAGTCTCTTTGATGGGAGACCAAAATCTCTTAATAGAGTTGTCTTTGCTTTCGTTTTCATTCGTTTATAGAGGA
AGAAATAAGGTGACTGTGACCATTTGTATAACAATATGGATAAACTATTTTTAGTGGCATACTCTCGACTATAAG
AAAAGATGCATCCAAGGAATATCAAATCTTCTTGATCAAAA

***rve8-11* genomic sequence**

ATGAGCTCGTCGCCGTCAAGAAATCCAACGAACGCCGAAGCACCTCCGCCACCACCAACATCGACGGATGCTGT
GGCAGAGGGTTCGTCTAAGAAAGTGAGGAAACCATATACCATCACCAAGTCAAGAGAGAGCTGGACAGAGGA
AGAGCACGATAAGTTTCTTGAAGCACTTCAACTGTAATAATTTATCTCTGTTTCTCTGTTTTTAGAGACTTCAAAT
TTCTTAGTTTGCTGCTGATTTCTGAGTTTAGTTAGTTATAGACTGAACAAACAGAGGAAAGTTTATGTTACTTAG
CTTAGGTCTAGTAGTAACTTAGCTATAAAAAATCTGCTTAGCTAAAAAGATCTGCTTCTTGGAGCACTTCAACTG
TAATAAATTTATAGTTGTGTTGACTTTTTGAAAGTGTTATTGATGTAACTAGGACCTGATTCTGCTGATACTACTA
CTCCTCTATGTTCCTTAGGTTTGATCGTGACTGGAAGAAGATTGAAGATTTTGTTGGTTCAAAGACTGTGATTCA
GGTTTTAAAATAGCTTACTCTGCATTTTTGGTCGCAGTTACTTTGTGGCAATGTTTTCAACTTATTTGACTTTGTA
CTGCAGATAAGGAGTCATGCTCAAAAATACTTTCTCAAGGTTCAGAAAAACGGGACATTAGCTCATGTGCCACC

TCCTCGACCTAAGCGCAAAGCAGCTCATCCGTATCCTCAAAAGGCATCAAAGAACGGTTCGAATATTTTATAATA
CTTCTTAGTTTGGTTATAGAGTTGAGTTTTTAACTCACATTTTCTTGCAGCTCAAATGCCACTTCAAGTTTCCACG
TGCCTCAATGCTGCTAAACAGAGTTATTTCACCACAACATGAACTTGCTACTCTTCGTGGAGCAGAAGGCATGC
ACATTTGTCTATCCTTTTTGTTTTCTTCATTTTATTGGTAGTTGTAGTAAGAATAGGTTCCATCAAAGGACGTTTC
ATGTGCTTATTATGGCATATAACGCCACTGATTCAGCTGATATTGGATCAAAGGGCTTATTAAATGTTAGTAGCC
CTTCTACATCTGGCATGGGAAGCTCAAGCCGAACAGTATCAGGTTCTGAGATTGTAAGAAAGGCTAAACAGCCT
CCAGTGCTTCACGGTAACCATCTGTGAACAATTCCATGTTTTTTCACTAACTTTTATGCATGATGGAGACTGTACT
GATACTATCTTTGTAGGTGTTCCTGATTTTGCTGAAGTTTATAATTTCATTGGGAGTGTCTTTGATCCTGAAACGA
GAGGCCATGTGGAAAAGCTCAAGGAAATGGATCCTATAAATTTCGAAACTGTGAGTCAAGAGTTTACAAGCTT
TCAGATTAATTGGTGTTCAAGCTCTTAGCATTTCTTCACTAATCACATAGTATGGTGTTTACAGGTTCTGTTATTG
ATGAGAAACCTCACAGTTAACTTATCAAACCCTGATTTAGAATCCACTGTAAGTGTTAAATTTGCGATAAAAGAT
TTGTGATGACCAACTTTCTCAGAGTCTGAAACTATTTCACTCTCAACCAATGAGTTGGAGGCACTTCTTTTATGAT
CTTTGGTTCCTTACATTGAAATGAGTTTTTTTGCGCTTGCGTGATCAAATTTAATCTAACCTCAGCTAGTCGGATT
GTAATGATGCTGCAGAGGAAAGTCCTCTTATCATATGACAACGTGACGACCGAGCTCCCAAGCGTTGTTTCCCT
TGTCAAGAACTCAACAAGCGACAAATCAGCATAACAAAAATATGAGCCATCAGCTAGCAAGTAAGTGTTTTTCC
CTCTTTTTCCTCTGACCTTTTAAATTCAGTACAAGAAAACATTTCACTACTATTAGAAGTCACATGAGTTCATGGT
TAGATATAAGTCTAGTGACAGTTCTCTAACTCTAAGGTTTGCAATAAGAGTTCTATAGTTAGTCACAGTCTGGGA
TACAAGATATATACACTACGGTATTTTGAGTATTAGCACCAGTTCAGGCTTCTTGCAAACTTTGTAAAGTCTTGC
ATAAGAGTTATATGGTTCTCACCGTATTGGCAGGTTTACTCATTGGTTTCCCATGTTTAATAAACTTTGGTGTTAT
ACGTCACTGGAATCACAATCGTGTCACTGCATCATCATGTGGGAATTGTGTAAAAGGTCTTTGTTGTTTTGAGG
AGAAACATAAGCCAAGTTTTGAAGCTATAGGGGGCTTCCGCAGATTTTGACCAGGACTAGTTGGGTGAATGGT
AGGTATAATATATGTAAGGGGTTTTTCTACTAGTTGCAAGACAGCCTCATTCTCATCCACCCGTTACTCTTGTACT
AAAATCTCGTCATAACTTTTTGTTCAGTTGTTGTGTATTTGTGTAAAAGATAAGTCCTAGGACTGAGTGTAATGG
TTCAAGATCAGTGTTAAGTAAATGACGGCAACTCTATTGTTTTAAAGTTGACAGCTTTCTTTATATATTATGGGG
TTTGATTCAGAATTTTGTTTTTAATAAGGAAA

***rve4-12* genomic sequence**

ATGACCTCAACCAATCCGGTGGTCGCCGAAGTAATACGGCGGAAACTTCTACAGATGCTACAGAGACGACGAT
TGCAACGACGGAAGCTGGTGAAGCACCGGAGAAGAAGGTGAGGAAAGCTTACACAATCACCAAGTCTAGAGA
GAGTTGGACTGAAGGAGAACACGACAAGTTTCTGGAAGCTCTTCAATTGTAATTTTACCGCGCTCTTTTTTTCTT
CCACCAGCTATTTGATTGACTGATTCTTTGTGTTTCGAGCTCTAATTTATAGCTGAATTTTGCGTAATTTCGCGTA
ATTTCTACTTAATTTGCTTAATCAGATCGAAGTTTGGTTATGTGGTAGATCATCTGGAGTTTTGCGTATGCAATT
GGATTTTGCAGAAGCAACAATGTCTTCTTTGATTTGTTAGGTTGGATTGTATATTCGATAGATCAGAATTTATAT
TAATCGCTGATGAATGTTTCTTCTCATAAAACCGAAGTATGGTTTAAGCTTATCTTAGGTTGCCAAAATGATTGA
GTAGAGGACTTGGCATCTGGTTTCTGCATAAATAGTGGTATTTTGCAGAAGTCGTATCTTTCTTTATTAAAAATG
TTTAACATGAGAACTGAAAAAACTTACTACAAGTCAGCTTTTAGAGCTATGCATGAAACCAATTTCCAACTACAG
TCCTAAACTACAATTCAGATTTTGGTAATGGTTCGTTACTTCCACATATTACATTGCTCTTTTGTGTGTGTGAAAG
GCTTCTCTCTCTTTTAGAAAAAAGAATCTTACTTTGTCCTGACAATTTTCTCGTGTCCTTAGGTTTGATCGTGACT
GGAAAAAGATAGAAGATTTTGTTGGTTCAAAGACAGTTATTCAGGTTTGAGATCAGCTTCTTTGGATTTTTGGTT
TAATATACAACCTTGGCACATTTCCCCACTCAATCATCCTGTGCCTGTTTGATTTACTGCAGATCAGGAGCCATGC
CCAAAAATACTTTCTAAAGGTCCAAAAAAATGGGACTTTAGCACATGTTCCACCCCCTAGGCCTAAGCGCAAAG
CTGCTCATCCATATCCTCAAAAGGCATCGAAAAATGGTTAGTTCTATTGTAATAGATATTACTTTGGGTTGACAG
ATGGAGTAACATGTAATCAATCTGATTTCAACTCAAATCTGCAGCTCAAATGTCGCTTCACGTTTCCATGTCCTTT
CCTACTCAAATAAATAACCTGCCTGGATATACTCCATGGGATGATGATACATCTGCATTGTTAAACATTGCTGTA
AGTGGGGTTATTCCACCAGAAGATGAACTTGATACTCTTTGTGGAGCAGAAGGCATGCGTTCTCATCTGTACTC

AGTTTTTATATTTTGCTTTGGTAGTCTAGTCACTCTATCTTCTGAAGTTTTCATATGCTAAATGCGGCTTACATATC
ATTGTTTCAGTTGATGTTGGATCAAATGACATGATAAGTGAAACTAGTCCTTCAGCATCTGGTATCGGAAGCTC
AAGCAGAACACTATCAGATTCTAAGGGTTTGAGACTGGCGAAACAAGCTCCCTCAATGCATGGTAATTATCTGA
ACAATTGAGGGACTATTTCTTAGTTTTCATTTTGTGGTGGACGCTGTTGTAATGGTTGCTTTGCAGGTCTTCCTG
ATTTTGCTGAGGTTTATAACTTCATTGGGAGTGTGTTCGATCCTGACAGCAAAGGCCGCATGAAAAAGCTCAAG
GAAATGGATCCTATAAATTTCGAAACTGTGAGTTGGAGCTTTACTTGCCTTTAGATTAACTGATATGTGTGTTGC
AGCATATCAATCATTTAGTCTTCTTCTTTGAGTTCCCGAATAAATTCAGCTGTGTGAGAAGATAAATATAAAGAT
CAGTACTTGCAATATATAGATTCACGAGTTGGAAACACCAAAAAGCCAAAGTACCATGATTCTATGGAGATGTT
GGTCAAATAATGGGATTGTTACAACCATGAGTCAGTTTTAGGTGTCATGGTACCTATTTGTAGCTGTCAGTGATT
GTTCTTTTTCCTAGTATCCGTCACTAATCACAGTTTTTCTTGCAGGTTTTGCTGTTGATGAGAAACCTCACAGTGA
ACTTGTCAAACCCTGACTTTGAACCTACTGTAAGTTATAATTTTATCATTACTTCTGTGCTCGTTGAGTATGTGAG
GCACATTTGTCTTTTCGTGATAAGAATGAGTGAGAAAAAGTCTCTAACAGCTAACAAACCTACTTACTATCTGCC
TTGAAGTTTAACTATAGAAATTAAGACTAGTTCGCCTTTAGTGTGTTATGTTTTTAACCGTTCCAATGATTAAATG
AGGATTGTTGTGCTCTATGAGATATAATCTAACCATAATTTAGTCTGAATATGTTGATGCTGCAGAGGAAGGTC
ATGAACACTTAAGCTCTTAG

***rve6-12* genomic sequence**

ATGGTCTCTAGAAATTCTGACGGATATTTCTTGGATCCGACCGGTATGACTGTTCCTGGTCTCGGACCTTCCTTT
ACAGCCGCCGTTTCTTCTTCTTCTTCACCAACGACTTCTTCTACGGCCGTGGCTGTGGCGGATGTGACGGCGATG
GTTTCTTCTTCGGAGGAGGATTTGAGTAAGAAGATTAGGAAGCCTTATACTATTACTAAGTCTAGAGAGAGCTG
GACGGAGCCTGAGCATGATAAATTCCTTGAAGCTCTTCAATTGTGAGTTTTGTTCATTTTGTGCTTTACCATTTCT
CGTTAATGGCTATTTGGAGATTTGATTTGGGAAGAATTAGCATCAATTTTGGTTGATTAGGGTTTGTGGTGGAC
TTTATAGAATCATGTGAATATGCGTGGAGTTTCGATTAGGATAATGTGCAACTTTATGTTTCAGTAGGTTTCTGA
ATTGTACTGTGTTGAACCAGTGGAATTAGATTGGATTTGGGACATAGAATTGGAATCGAGAGTTGGATTTAGG
CAGATGGATTTGGCTATGTATGCACATTTTGTTGAATTAGGCGTCTGATAAGAATTGAGAAGATCAGGATGTCG
AAAAATGAGTATAGACTGTATTGAATTTGTGTAGTAGCTATTGAAATTGGATGAGCTAAATGTTCTTCTAAGAC
CTGTATGATCATTGATAGTGAAGAACGAAACAGGCAAGAAATTGAGCTGAGATTATGAGGAAATAGCGACGCA
AACTATATGTATCTTAGTAAAAAGAGGATTTAGTGAAAACTATTAGAGCTGCGTTTTTTTTTTTTTTGGTTACAAT
AGTGTCTATAAACACTGGTAAGTGAGTAATTGTAGTACTAAGGTTGGTATGTAGTGGGAAAGTCCTTGGGGTA
GGTTCTAGGGGAGGCGATGATGATTGTACTGTTCATTGCTTATTCTTCTGTGTATTGTGATGCGTACAATCTTAG
GCAAGGATTAGACACATGCTATATCCAGGTTGTTTGGTGGTGGATCTGATATCTCTTATGTTTGTGTTTTGATTA
TTTTAGGTTTGATAGAGACTGGAAGAAGATTGAAGCTTTTATTGGTTCAAAGACAGTGATTCAGGTACAGTAAA
AAGTAGATATATCTTCTGAGTTACTCTGTTTTTCGCCTACTCTAGTTGTTTGATTCTGTCATCTTTCTCTTGGGCCC
TCAGTGTTACTTTGGATTGAGGTTGTTTTCTCTCATTTGATATCTCCACAAAGTGTTCTGTTAAAACATCTTTATTG
TCTGTAACTGTTTTGAACTACTACTACTAGGAGAAAGAATGTCACATGCGTTTGTCGCTTATCACCACTTAATGA
AGTGTTATATGTAGTTATTTTTGCATTAGACAAGTGAGCTCGTTGAGCTCTTTTATGGCTTCTTATACGGACTCCT
TTAATACTGCAGATACGAAGTCATGCTCAGAAGTATTTTCTTAAGGTACAAAAGAGTGGTGAACACTGCTTAAG
ACCGGTGAACATCTCCCTCCTCCTCGACCTAAAAGGAAAGCCGCTCATCCATATCCTCAGAAGGCTCACAAGAA
TGGTACGTTATAGCTACTGCTTTAAAAACTTTGAAGTTGTATTGTTGTTTGCTTACTGAAAACTATATTGATGCAC
TGTTTATGGCAATGTGCAGTGCAACTGCAAGTACCAGGGTCATTCAAGTCAACATCTGAACCAAATGACCCAAG
TTTTATGTTTAGGCCTGAGTCTTCTTCAATGCTGATGACTTCGCCAACCACTGCTGCTGCGGCTCCATGGACAAA
TAATGCGCAAACAATTAGCTTCACTCCCCTCCCAAAAGGTTCTATTCTCATTTACAAGCATTATGCAATTACTGTT
ACTCTCTTAATATAATCTCTGTTTCAAATTTTACTAAATGAAGCATATTGTTGTTCCACGTTGATGGAAACAGCAG
GAGCAGGAGCTAATAACAATTGTTCTAGTAGTTCTGAAAATACTCCAAGACCACGATCCAACAGGGACGCAAG
AGACCATGGAAATGTTGGCCATTCATTAAGAGGTAAGCATCGTTACATCGTCTCCTGTTAATCTTTTTGTTTGTA

CCATATTTACCATTTCTTACTAGACAGTTCCGCCTTTTTTTTTTTCAGTTTTACCGGACTTTGCCCAAGTATACGGC
TTCATTGGAAGTGTGTTTGACCCATATGCAAGTAATCATCTACAAAAGCTGAAGAAGATGGACCCCATAGATGT
TGAAACAGTACGTTTCTTGTCTTTTCAGTTTTCACTTTTACATCAATCTTAATTGAAACCACGTCGGTCCAATGGA
ACAAATGGTTAAACTAATCATTTTTTTCCTTTGTTTGCCCCCACCAAACAGGTGTTACTATTGATGAGAAATCTAT
CCATCAACTTGTCTAGTCCTGACTTTGAGGATCATGTAAGTATTTTACTCCACAAACTACTAGTCAATTTTAACTC
GAAACCCTATACCAGAACTAACCTCAAGACTCTTATTGATTTCAAAAACAATAGAGACGGCTTCTTTCGTCTTAT
GATATCGGATCTGAGACAGCAACTGATCATGGTGGAGTGAATAAAACCTTAAACAAAGACCCACCTGAAATCTC
TACTTAATGTTTAATAGAAGAGGAGAACTGTGAAAAGTGTCTCAGGTGAGCCAGCCAACAACCAGATGGCTAC
AAAATACAGAGATTCTGTTGTGGTTTTTTGTTTGTACATAGGAAGAAGATGAAGCTGATGTTACTCGGTTTAGTT
GTTGTTACTGTTATAAATAGTCTGTTGGGTTAAGGATGGTATATGTACAGTGTATTATCATAAGTTAGATCTCAA
GTTTAAACATATGTATCAGTCTCTTTGATGGGAGACCAAAATCTCTTAATAGAGTTGTCTTTGCTTTCGTTTTCAT
TCGTTTATAGAGGAAGAAATAAGGTGACTGTGACCATTTGTATAACAATATGGATAAACTATTTTTAGTGGCAT
ACTCTCGACTATAAGAAAAGATGCATCCAAGGAATATCAAATCTTCTTGATCAAAA

***rve8-12* genomic sequence**

ATGAGCTCGTCGCCGTCAAGAAATCCAACGAACGCCGAAGCACCTCCGCCACCACCAACATCGACGGATGCTGT
GGCAGAGGGTTCGTCTAAGAAAGTGAGGAAACCATATACCATCACCAAGTCAAGAGAGAGCTGGACAGAGGA
AGAGCACGATAAGTTTCTTGAAGCACTTCAACTGTAATAATTTATCTCTGTTTCTCTGTTTTTAGAGACTTCAAAT
TTCTTAGTTTGCTGCTGATTTCTGAGTTTAGTTAGTTATAGACTGAACAAACAGAGGAAAGTTTATGTTACTTAG
CTTAGGTCTAGTAGTAACTTAGCTATAAAAAATCTGCTTAGCTAAAAAGATCTGCTTCTTGGAGCACTTCAACTG
TAATAAATTTATAGTTGTGTTGACTTTTTGAAAGTGTTATTGATGTAACTAGGACCTGATTCTGCTGATACTACTA
CTCCTCTATGTTCCTTAGGTTTGATCGTGACTGGAAGAAGATTGAAGATTTTGTTGGTTCAAAGACTGTGATTCA
GGTTTTAAAATAGCTTACTCTGCATTTTTGGTCGCAGTTACTTTGTGGCAATGTTTTCAACTTATTTGACTTTGTA
CTGCAGATAAGGAGTCATGCTCAAAAATACTTTCTCAAGGTTCAGAAAAACGGGACATTAGCTCATGTGCCACC
TCCTCGACCTAAGCGCAAAGCAGCTCATCCGTATCCTCAAAAGGCATCAAAGAACGGTTCGAATATTTTATAATA
CTTCTTAGTTTGGTTATAGAGTTGAGTTTTTAACTCACATTTTCTTGCAGCTCAAATGCCACTTCAAGTTTCCACG
TTCTTTTACTACTACGCGAAATGGCGACATGCCGGGATATGCTTCATGGGATGATGCCTCAATGCTGCTAAACA
GAGTTATTTCACCACAACATGAACTTGCTACTCTTCGTGGAGCAGAAGGCATGCACATTTGTCTATCCTTTTTGTT
TTCTTCATTTTATTGGTAGTTGTAGTAAGAATAGGTTCCATCAAAGGACGTTTCATGTGCTTATTATGGCATATA
ACGCCACTGATTCAGCTGATATTGGATCAAAGGGCTTATTAAATGTTAGTAGCCCTTCTACATCTGGCATGGGA
AGCTCAAGCCGAACAGTATCAGGTTCTGAGATTGTAAGAAAGGCTAAACAGCCTCCAGTGCTTCACGGTAACC
ATCTGTGAACAATTCCATGTTTTTTCACTAACTTTTATGCATGATGGAGACTGTACTGATACTATCTTTGTAGGTG
TTCCTGATTTTGCTGAAGTTTATAATTTCATTGGGAGTGTCTTTGATCCTGAAACGAGAGGCCATGTGGAAAAGC
TCAAGGAAATGGATCCTATAAATTTCGAAACTGTGAGTCAAGAGTTTACAAGCTTTCAGATTAATTGGTGTTCA
AGCTCTTAGCATTTCTTCACTAATCACATAGTATGGTGTTTACAGGTTCTGTTATTGATGAGAAACCTCACAGTTA
ACTTATCAAACCCTGATTTAGAATCCACTGTAAGTGTTAAATTTGCGATAAAAGATTTGTGATGACCAACTTTCT
CAGAGTCTGAAACTATTTCACTCTCAACCAATGAGTTGGAGGCACTTCTTTTATGATCTTTGGTTCCTTACATTGA
AATGAGTTTTTTTGCGCTTGCGTGATCAAATTTAATCTAACCTCAGCTAGTCGGATTGTAATGATGCTGCAGAGG
AAAGTCCTCTTATCATATGACAACGTGACGACCGAGCTCCCAAGCGTTGTTTCCCTTGTCAAGAACTCAACAAGC
GACAAATCAGCATAACAAAAATATGAGCCATCAGCTAGCAAGTAAGTGTTTTTCCCTCTTTTTCCTCTGACCTTTT
AAATTCAGTACAAGAAAACATTTCACTACTATTAGAAGTCACATGAGTTCATGGTTAGATATAAGTCTAGTGACA
GTTCTCTAACTCTAAGGTTTGCAATAAGAGTTCTATAGTTAGTCACAGTCTGGGATACAAGATATATACACTACG
GTATTTTGAGTATTAGCACCAGTTCAGGCTTCTTGCAAACTTTGTAAAGTCTTGCATAAGAGTTATATGGTTCTC
ACCGTATTGGCAGGTTTACTCATTGGTTTCCCATGTTTAATAAACTTTGGTGTTATACGTCACTGGAATCACAATC
GTGTCACTGCATCATCATGTGGGAATTGTGTAAAAGGTCTTTGTTGTTTTGAGGAGAAACATAAGCCAAGTTTT

GAAGCTATAGGGGGCTTCCGCAGATTTTGACCAGGACTAGTTGGGTGAATGGTAGGTATAATATATGTAAGGG
GTTTTTCTACTAGTTGCAAGACAGCCTCATTCTCATCCACCCGTTACTCTTGTACTAAAATCTCGTCATAACTTTTT
GTTCAGTTGTTGTGTATTTGTGTAAAAGATAAGTCCTAGGACTGAGTGTAATGGTTCAAGATCAGTGTTAAGTA
AATGACGGCAACTCTATTGTTTTAAAGTTGACAGCTTTCTTTATATATTATGGGGTTTGATTCAGAATTTTGTTTT
TAATAAGGAAA

Appendix III: CRISPR guide sequences

Name	Locus	Sequence	Location	Construct
RVE3_G19	AT1G01520	CCGGTATCGTTGTTGCCGTG	1st exon	8X_RVE
RVE3_G20	AT1G01520	ATGCACTAATCCATGCTTAC	4th exon	8X_RVE
RVE4_G21	AT5G02840	GGTCGCCGAAGTAATACCGG	1st exon	8X_RVE
RVE4_G22	AT5G02840	CCTGCCTGGATATACTCCAT	4th exon	8X_RVE
RVE6_G23	AT5G52660	GGTATGACTGTTCCTGGTCT	1st exon	8X_RVE
RVE6_G24	AT5G52660	AAGGTACAAAAGAGTGGGAC	3rd exon	8X_RVE
RVE8_G25	AT3G09600	GGAGGTGCTTCGGCGTTCGT	1st exon	8X_RVE
RVE8_G26	AT3G09600	TCGCGTAGTAGTAAAAGACG	4th exon	8X_RVE
RVE3_G31	AT1G01520	GGTATCGTTGTTGCCGTGTG	1st exon	6X_RVE
RVE3_G32	AT1G01520	CAAATCTAGAGAGAACTGGA	1st exon	6X_RVE
RVE3_G33	AT1G01520	TTACGGGTGGTGCTAATCAC	4th exon	6X_RVE
RVE5_G34	AT4G01280	GGCCACGGGACGGACCAGTA	1st exon	6X_RVE
RVE5_G35	AT4G01280	GCTTTCCTCTTAGGTCGAGG	3rd exon	6X_RVE
RVE5_G36	AT4G01280	ACGGTAATGTACTCGAAGAC	4th exon	6X_RVE

Appendix IV: Plasmid and Glycerol Stocks

Plasmid Stocks

Box	Location	Name	Selection	Notes
1	A1 – A4	pC2LUC7A	Spec	CCR2::LUC+ vector used to make pC2L2
1	A5 – A7	pGL4.10	Amp/Carb	LUC2 used to make pC2L2
1	B1 – B6	pC2L2	Spec	CCR2::LUC2 vector
1	B7 – B9	pEn-Chimera	Amp/Carb	entry vector that guides were cloned into
1	C1 – C3	pMR-300	Spec, Basta	RPS5A promoter, destination vector for use with pEn-Chimera
1	C4	pMR-333	Spec, Basta	RPS5A promoter, destination vector for use with pEn-Chimera, contains GFP
1	C5 – C7	10X RVE pUC57	Kan	from Genewiz; 10X guides targeting RVE3, RVE4, RVE5, RVE6, RVE8
1	D1 – D3	10X RVE pMR-300	Spec, Basta	10X guides + Cas9
1	D4 – D8	10X RVE pMR-333	Spec, Basta	10X guides + Cas9
1	E1 – E4	10X RVE pEn-Chimera	Amp/Carb	10X guide entry vector
1	F1 – F2	8X RVE pUC57	Kan	8X guides targeting RVE3, RVE4, RVE6, RVE8
1	F3 – F6	8X RVE pEn-Chimera	Amp/Carb	8X guide entry vector
1	F7 – F9	8X RVE pMR-300	Spec, Basta	8X guides + Cas9
1	G1 – G3	8X RVE pMR-300	Spec, Basta	8X guides + Cas9
1	G4 – G7	8X RVE pMR-333	Spec, Basta	8X guides + Cas9
1	H1	10X RVE pUC57	Kan	Genewiz order
1	H2	8X RVE pUC57	Kan	Genewiz order
1	H3	6X RVE pUC-GW	Kan	Genewiz order
1	H4	4X RVE pUC57	Kan	Genewiz order
2	A1 – A3	4X pUC57	Kan	4X guides targeting RVE5
2	A4 – A7	4X pEn-Chimera	Amp/Carb	4X guide entry vector
2	B1 – B6	4X pMR-333	Spec, Basta	4X guides + Cas9
2	C1	6X pUC57	Kan	6X guides targeting RVE3 and RVE5
2	C2 – C8	6X pEn-Chimera	Amp/Carb	6X guide entry vector
2	D1 – D6	6X pMR-333	Spec, Basta	6X guides + Cas9

Glycerol Stocks

Box	Location	Name	Host	Selection	Notes
1	A1 – A3	pC2LUC7A	DH5α	Spec	CCR2::LUC+ vector used to make pC2L2
1	A4 – A6	pGL4.10	DH5α	Amp/Carb	LUC2 used to make pC2L2
1	A7	pC2L2	DH5α	Spec	CCR2::LUC2 vector
1	A8	pC2L2	GV3101	Spec	CCR2::LUC2 vector
1	B1 – B2	pMR-292	DH5α	Spec, Basta	Arabidopsis GEX1 promoter, Cas9 with Basta resistance
1	B3 – B4	pMR-293	DH5α	Spec, Hyg	Arabidopsis GEX1 promoter, Cas9 with Hyg resistance
1	B5 – B6	pMR-294	DH5α	Spec, Kan	Arabidopsis GEX1 promoter, Cas9 with Kan resistance
1	C1 – C3	pEn-Chimera	DH5α	Amp/Carb	entry vector that guides were cloned into
1	C4 – C6	pMR-300	DH5α	Spec, Basta	RPS5A promoter, destination vector for use with pEn-Chimera
1	C7	pMR-333	DH5α	Spec, Basta	RPS5A promoter, destination vector for use with pEn-Chimera, contains GFP
1	D1 – D3	10X RVE pUC57	DH5α	Kan	from Genewiz; 10X guides targeting RVE3, RVE4, RVE5, RVE6, RVE8
1	D4 – D7	10X RVE pEn-Chimera	DH5α	Amp/Carb	10X guide entry vector
1	E1 – E3	10X RVE pMR-300	DH5α	Spec, Basta	10X guides + Cas9
1	E4	10X RVE pMR-300	GV3101	Spec, Basta	10X guides + Cas9
1	E5 – E7	10X RVE pMR-333	DH5α	Spec, Basta	10X guides + Cas9
1	E8	10X RVE pMR-333	GV3101	Spec, Basta	10X guides + Cas9
1	F1 – F2	8X RVE pMR-333	DH5α	Spec, Basta	8X guides + Cas9
1	F3 – F4	8X RVE pMR-333	GV3101	Spec, Basta	8X guides + Cas9
1	F5 – F6	6X pEn-Chimera	DH5α	Amp/Carb	6X guide entry vector
1	F7	6X pMR-333	GV3101	Spec, Basta	6X guides + Cas9
1	G1 – G3	4X RVE pUC57	DH5α	Kan	4X guides targeting RVE5
1	G4 – G7	4X RVE pEn-Chimera	DH5α	Amp/Carb	4X guide entry vector
1	H1 – H6	4X RVE pMR-333	DH5α	Spec, Basta	4X guides + Cas9

Appendix V: Primer Stocks

Box	Location	Name	Sequence (5'-3')	Purpose	Reference
1	B4	ztl-103_CAPS_F	TGGTGCTAAAAGACTCGGTTG	Genotyping	2007 Martin-Tryon et al[58]
1	B5	ztl-103_CAPS_R	CAACCAGATTGGAGCCATTT	Genotyping	2007 Martin-Tryon et al[58]
1	B10	35S_F	AAACCTCCTCGGATTCCATT	Genotyping	
1	C1	RVE8-HA_F	ACCAGTTCAGGCTTCTTGCA	Genotyping	
1	C2	HA_R	GCGTAATCTGGAACATCGTATGG	Genotyping	
1	C3	RVE8-HA_e6_F	TGGGAGTGTCTTTGATCCTGA	Genotyping	
1	C4	HA_new_R	TCAAGCGTAATCTGGAACA	Genotyping	
1	C5	RVE8-HA_e5_F	TGCTTCACGGTAACCATCTG	Genotyping	
1	C6	RVE8-HA_R	CAAGCGTAATCTGGAACATCG	Genotyping	
1	E1	pMR_colony_1	GCTCCCTAGGCCTGTTATCC	Genotyping	
1	E2	pMR_colony_2	GTGGTGATTCAAGGGCTGAT	Genotyping	
1	E4	CCR2_LUC2_F	CTTTTCTCGCATCGTCGTCTTT	Genotyping	
1	E5	CCR2_LUC2_R	GAAACGACAATCTGATCCAAGCTC	Genotyping	
1	E6	pGL_LUC2_F	CTAACTGGCCGGTACCTGAG	Genotyping	
1	E7	pGL_LUC2_R_PstI	AAGAGCGCTGCAGGCACC	Genotyping	
1	E9	pMR-300_F	CTCACAGCTCGGTGGTGATT	Genotyping	
1	I1	RVE3_upstream_F	TTTTAGTCGAACCAGGCCCC	Sequencing	
1	I2	RVE3_e5_R	AGTGCTGCAACAGTTCTCTGA	Sequencing	
1	I3	RVE4_upstream_F	GGCCTGAAATTGCAAGCGAA	Sequencing	
1	I7	RVE6_upstream_F	GCCGACCTCAAAAACGATCAC	Sequencing	
1	I8	RVE6_e5_R	TTCCATGGTCTCTTGCGTCC	Sequencing	
1	I9	RVE8_upstream_F	GATGGCCACAAACTCGCAAG	Sequencing	
1	I10	RVE8_e5_R	CTTGAGCTTCCCATGCCAGA	Sequencing	
1	J6	RVE4_i5_R	CAACAGCGTCCACCACAAAA	Sequencing	
2	A1	G21_ind_F	GAGAAAAATGGATGGCCTGA	Genotyping	
2	A2	G21_ind_R	GCAGAAACCAGATGCCAAGT	Genotyping	
2	A3	G22_52_F	CCTCAAAAGGCATCGAAAAA	Genotyping	
2	A4	G22_52_R	CGCCAGTCTCAAACCCTTAG	Genotyping	
2	A5	G24_ind_F	CACATGCGTTTGTCGCTTAT	Genotyping	
2	A6	G24_ind_R	GCGAAGTCATCAGCATTGAA	Genotyping	
2	A7	G26_ind_F	TGGTCGCAGTTACTTTGTGG	Genotyping	
2	A8	G26_ind_R	AGCACTGGAGGCTGTTTAGC	Genotyping	
2	C3	8X_G19_F	GTATCGTTGTTGCCGTGGTT	Genotyping	
2	C4	pMR-300_R	GCTGGATCGGAATTATCGAA	Genotyping	
2	D1	HY5_5'UTR	ATTCCTTCCCAAAATGTCTCG	Genotyping	
2	D2	HY5_intron3	AGAATATGCGAGTGAATGACCA	Genotyping	
		LB b1.3	ATTTTGCCGATTTCGGAAC	Genotyping	
2	D3	lhy-100_F	CTTATGCGAGTGTCGGGAAT	Genotyping	2007 Martin-Tryon et al[58]

2	D4	lhy-100_R	TGGAGTTGGAACTGCAACAG	Genotyping	2007 Martin-Tryon et al[58]
2	D5	CCA1_mut_F	GATGCACTCGAAATCAGCCAATTTTAGAC	Genotyping	
2	D6	CCA1_F	TGAGATTTCTCCATTTCCGTAGCT	Genotyping	
2	D7	CCA1_R	TCAGGCTTTGATTGTTGTCG	Genotyping	
2	E2	PP2A_qPCR_F	TAACGTGGCCAAAATGATGC	qPCR	2005 Czechowski et al[125]
2	E3	PP2A_qPCR_R	GTTCTCCACAACCGATTGGT	qPCR	2005 Czechowski et al[125]
2	E4	IPP2_qPCR_F	GTATGAGTTGCTTCTCCAGCAAAG	qPCR	2005 Hazen et al[31]
2	E5	IPP2_qPCR_R	GAGGATGGCTGCAACAAGTGT	qPCR	2005 Hazen et al[31]
2	E6	RVE4_qPCR_F	GTGGTCGCCGAAGTAATACC	qPCR	2013 Hsu et al[24]
2	E7	RVE4_qPCR_R	TCTGGTGGAATAACCCCACTT	qPCR	2013 Hsu et al[24]
2	E8	RVE6_qPCR_F	ACGGAGCCTGAGCATGATAAATTCC	qPCR	2013 Hsu et al[24]
2	E9	RVE6_qPCR_R	TGAATGACCCTGGTACTTGCAGTTG	qPCR	2013 Hsu et al[24]
2	F1	RVE8_qPCR_F	GGGAAGCTCAAGCCGAACAGTATC	qPCR	2013 Hsu et al[24]
2	F2	RVE8_qPCR_R	GGCCTCTCGTTTCAGGATCAAAGA	qPCR	2013 Hsu et al[24]
2	F3	RVE4_qPCR2_F	AAACCCTGACTTTGAACCTACTTC	qPCR	
2	F4	RVE4_qPCR2_R	TCCTCTTGTTTGTGACGACGA	qPCR	
2	F5	RVE4_qPCR3_F	ACCCTGACTTTGAACCTACTTCT	qPCR	
2	F6	RVE4_qPCR3_R	TCACACGACTGGTTCTGACC	qPCR	
2	F9	APRR5_F_qPCR	ATTCCGAATGAAGCGAAAGGA	qPCR	2004 Mockler et al[126]
2	G1	APRR5_R_qPCR	TCGTAACGAACCTTTTTCTCATAACAT	qPCR	2004 Mockler et al[126]
2	G2	ELF4_qPCR_F	CAAAGCAACGTTCTTCGACA	qPCR	2008 Martin-Tryon and Harmer[127]
2	G3	ELF4_qPCR_R	CGACAATCACCAATCGAGAA	qPCR	2008 Martin-Tryon and Harmer[127]

2	G4	LUX_qPCR_F	CGGATTCGAAGAAGCAAAAG	qPCR	2008 Martin-Tryon and Harmer[127]
2	G5	LUX_qPCR_R	TCATCTCCATCACCGTTTGA	qPCR	2008 Martin-Tryon and Harmer[127]
2	G6	TOC1_qPCR_F	AATAGTAATCCAGCGCAATTTTCTTC	qPCR	2004 Mockler et al[126]
2	G7	TOC1_qPCR_R	CTTCAATCTACTTTTCTTCGGTGCT	qPCR	2004 Mockler et al[126]
2	G8	CCA1_qPCR_F	CAGCTCCAATATAACCGATCCAT	qPCR	2004 Mockler et al[126]
2	G9	CCA1_qPCR_R	CAATTCGACCCTCGTCAGACA	qPCR	2004 Mockler et al[126]
2	H1	BOA_qPCR_F	ACATATCCTTCTGTTGGTGGT	qPCR	2018 Hajdu et al[112]
2	H2	BOA_qPCR_R	CATAAGCCAAGAACCAGTATCTC	qPCR	2018 Hajdu et al[112]
2	H5	PIF4_qPCR_F	GTTGTTGACTTTGCTGTCCCGC	qPCR	2011 Nusinow et al[40]
2	H6	PIF4_qPCR_R	CGACTCAGCCGATGGAGATGTT	qPCR	2011 Nusinow et al[40]
2	H7	PIF5_qPCR_F	CGCCGGAGATCCAAATCCCAACAT	qPCR	2011 Nusinow et al[40]
2	H8	PIF5_qPCR_R	GCGGGAAATCAGACCGTGCAACAA	qPCR	2011 Nusinow et al[40]
2	I2	TAA1_qPCR_F	CCCTGCGTTTGCGTGGCTAGGGA	qPCR	2012 Sun et al[47]
2	I3	TAA1_qPCR_R	GAGCTTCATGTTGGCGAGTCTCT	qPCR	2012 Sun et al[47]
2	I4	IAA29_qPCR_F	ATCACCATCATTGCCCGTAT	qPCR	2011 Kunihiro et al[46]
2	I5	IAA29_qPCR_R	ATTGCCACACCATCCATCTT	qPCR	2011 Kunihiro et al[46]

2	I6	ATHB2_qPCR_F	GAGGTAGACTGCGAGTTCTTACG	qPCR	2011 Kunihiro et al[46]
2	I7	ATHB2_qPCR_R	GCATGTAGAACTGAGGAGAGAGC	qPCR	2011 Kunihiro et al[46]
		YUC8_qPCR2_F	TGTATGCGGTTGGGTTTACGAGG A	qPCR	2012 Sun et al[47]
		YUC8_qPCR2_R	CCTTGAGCGTTTCGTGGGTTGTTT	qPCR	2012 Sun et al[47]

Appendix VI: Seed Stocks

ID	Genotype	Reporter	Notes
Homozygous lines with *CCR2::LUC2*			
A1	Col	*CCR2::LUC2*	from 102.05; used for phenotyping
A2	Col	*CCR2::LUC2*	
A3	*rve4-11*	*CCR2::LUC2*	Dull584 #102; used for phenotyping
A4	*rve4-11*	*CCR2::LUC2*	Dull584 #318
A5	*rve6-11*	*CCR2::LUC2*	Dull584 #73; used for phenotyping
A6	*rve6-11*	*CCR2::LUC2*	Dull584 #57
A7	*rve8-11*	*CCR2::LUC2*	Dull584 #194; used for phenotyping
A8	*rve8-11*	*CCR2::LUC2*	Dull584 #205
A9	*rve4-11; rve6-11*	*CCR2::LUC2*	Dull584 #124; used for phenotyping
A10	*rve4-11; rve6-11*	*CCR2::LUC2*	Dull584 #376
A11	*rve4-11; rve8-11*	*CCR2::LUC2*	Dull584 #154; used for phenotyping
A12	*rve4-11; rve8-11*	*CCR2::LUC2*	Dull584 #135
A13	*rve6-11; rve8-11*	*CCR2::LUC2*	Dull584 #293; used for phenotyping
A14 – A17	*rve6-11; rve8-11*	*CCR2::LUC2*	
A18	*rve4-11; rve6-11; rve8-11*	*CCR2::LUC2*	Dull584 #251; used for phenotyping
A19	*rve4-11; rve6-11; rve8-11*	*CCR2::LUC2*	Dull584 #430
A20	*cca1-1; lhy-100; rve4-12; rve6-12; rve8-12*	*CCR2::LUC2*	Kirk124 #412; used for phenotyping
A21	*cca1-1; lhy-100; rve4-12; rve6-12; rve8-12*	*CCR2::LUC2*	bulk from Kirk124 #412
A22 – A27	*cca1-1; lhy-100; rve4-12; rve6-12; rve8-12*	*CCR2::LUC2*	
A28	*cca1-1; lhy-100*	*CCR2::LUC2*	used for phenotyping
A29 -A34	*cca1-1; lhy-100*	*CCR2::LUC2*	
A35	*rve4-11; rve6-11; rve8-11; hy5*	*CCR2::LUC2*	used for phenotyping
A36 – A47	*rve4-11; rve6-11; rve8-11; hy5*	*CCR2::LUC2*	
A48 – A49	*hy5*	*CCR2::LUC2*	Salk_096651; used for phenotyping
A50 – A70	*hy5*	*CCR2::LUC2*	Salk_096651
Other homozygous lines			
B1 – B7	Col	*CCR2::LUC+*	
B8	Col	*PRR5::LUC+*	
B9	Col	None	From Rod
B10 – B14	*rve4-11; rve6-11; rve8-11*	*CCR2::LUC+*	from 89.17
B15	*rve4-1*	*CCR2::LUC+*	

B16	*rve8-1*	*CCR2::LUC+*	
B17	*rve4-1; rve8-1*	*CCR2::LUC+*	
B18	*rve4-1; rve6-1; rve8-1*	*CCR2::LUC+*	From 2011 packet
B19 – B20	*rve4-1; rve6-1; rve8-1*	*CCR2::LUC+*	From 2013 packet
B21 – B22	*rve4-1; rve6-1; rve8-1*	*CCR2::LUC+*	From 2015 packet
B23	*rve4-1; rve6-1; rve8-1*	*CCR2::LUC+*	
B24	rve3-1; rve4-1; rve5-1; rve6-1; rve8-1	*CCR2::LUC+*	
B25 – B26	*cca1-1; rve3-1; rve4-1; rve5-1; rve6-1; rve8-1*	*CCR2::LUC+*	
B27 – B29	*cca1-1; lhy-20; rve4-1; rve6-1; rve8-1*	*CCR2::LUC+*	
B30 – B31	*cca1-1; lhy-100*	*CCR2::LUC+*	
B32 – B33	*cca1-1; lhy-100*	None	
B34 – B39	*cca1-1; lhy-100; rve5-1*	*CCR2::LUC+*	
B40 – B44	*hy5*	*CCR2::LUC+*	Salk_096651; from 86.17
B45 – B46	*hy5*	*CCR2::LUC+*	Salk_096651; from 86.23
B47	*hy5*	None	Salk_096651 Chen et al PNAS 2008; from Rod
B48	*ztl-103*	*CCR2::LUC+*	
B49	*rve8-1; ztl-103*	*CCR2::LUC+*	
B50	*gi-2*	*CCR2::LUC+*	
B51	*rve8-1; gi-2*	*CCR2::LUC+*	
B52	*prr5*	*CCR2::LUC+*	
Tagged lines			
C1	*RVE4::RVE4-FLAG; rve4-1*		from YA E92-E101
C2	*RVE4::RVE4-FLAG; rve4-1*		
C3	*RVE6::RVE6-FLAG; rve6-1; rve8-1*		from YA F2
C4	*RVE6::RVE6-FLAG; rve6-1; rve8-1*		
C5	*35S::RVE8-HA; rve8-1*		from RR 31-18
C6 – C12	*RVE8::RVE8-HA; rve8-1*		
C13	*RVE8::RVE8-HA; rve8-1; ztl-103*		
C14	*RVE8::RVE8-LUC*		from RR 91-7
C15 – C17	*RVE8::RVE8-GR; rve8-1*		
C18	*RVE8::RVE8-GR; rve8-1*	*CCR2::LUC+*	
C19 – C21	*35S::RVE8-GR; rve8-1*		
C22	*35S::RVE8-GR; rve8-1*	*CCR2::LUC+*	
C23 – C26	*HY5-MYC*		
C27	*GFP-MYC*		
Segregating lines			
D1 – D4	*cca1-1; lhy-100; rve4-12; rve6-12; rve8-12; 6X pMR-333*	*CCR2::LUC2*	T2 generation
D5 – D16	*cca1-1; lhy-100; rve4-12; rve6-12; rve8-12; 6X pMR-333*	*CCR2::LUC2*	T1 generation
D17 – D25	*rve4-11; rve6-11; rve8-11; 6X pMR-333*	*CCR2::LUC2*	T1 generation
D26 – D50	*cca1-1; lhy-100; 8X pMR-333*	*CCR2::LUC2*	T3 generation

D51 – D68	*cca1-1; lhy-100; 8X pMR-333*	*CCR2::LUC2*	T1 generation
D69 – D78	*rve4-11; rve6-11; rve8-11* x *cca1-1; lhy-100; CCR2::LUC2*	*CCR2::LUC2*	F2 generation
D79 – D85	*cca1-1 lhy-100; CCR2:LUC2* x *hy5*	*CCR2::LUC2*	F2 generation
D86 – D89	*cca1-1 lhy-100; CCR2:LUC2* x *hy5*	*CCR2::LUC2*	Genotyped
D90 – D98	from 89.26 (T4 generation)	*CCR2::LUC+*	potential rve3468
D99 – D101	from 89.26	*CCR2::LUC+*	potential rve3468
D102 – D109	from 89.27 (T4 generation)	*CCR2::LUC+*	potential rve3468
D110	from 89.27	*CCR2::LUC+*	potential rve3468
D111 – D113	from 89.17	*CCR2::LUC+*	potential rve468
D114 – D117	from 89.18	*CCR2::LUC+*	potential rve468
D118 – D120	from 89.01	*CCR2::LUC+*	potential rve48
D121 – D124	from 89.13	*CCR2::LUC+*	potential rve48
D125 – D131	*RVE8::RVE8-HA; rve8-1* x *HY5-MYC*		F2 generation
D132 – D138	*RVE8::RVE8-GR; rve8-1* x *Col; PRR5::LUC+*	*PRR5::LUC+*	F2 generation
D139 – D146	*35S::RVE8-GR; rve8-1* x *Col; PRR5::LUC+*	*PRR5::LUC+*	F2 generation
Misc	*RVE6::RVE6-FLAG; rve6-1; rve8-1*		from YA F2; in tube
Misc	*RVE8::RVE8-HA; rve8-1*		from Jen's C1; in tube
Misc	*RVE8::RVE8-LUC*		in tube
Misc	*HY5-MYC*		received packet
Misc	*GFP-MYC*		received packet
Misc	*RVE8-sGFP; rve8*		2021 Kidokoro et al[12]
Misc	*RVE4-sGFP; rve4*		2021 Kidokoro et al[12]
Misc	*RVE8-sGFP OX*		2021 Kidokoro et al[12]
Misc	*RVE4-sGFP OX*		2021 Kidokoro et al[12]